Friedrich-Alexander-Universität
Naturwissenschaftliche Fakultät

Master's Thesis
in Physics

ANALYTICAL MODELS OF RANDOM ORGANIZATION

Mishael Derla

Supervisor: Prof. Dr. Michael Schmiedeberg

Institut für Theoretische Physik I
Friedrich-Alexander-Universität Erlangen-Nürnberg

Submission date: 26.11.2025

Abstract

I present my literature work on and own investigations into the *continuous dynamical phase transition* displayed by *random organization* and other closely related models. These systems are constituted by spatially extended grains initially placed at randomly, uniformly and independently distributed locations; they are then subjected to iterative protocols trying to eliminate overlaps. In random organization, in each iteration, every grain overlapping with other grains is shifted by a small, random step in space. This protocol displays two regimes of behaviour, depending on its *packing density* Φ, separated by a dynamical phase transition at some critical packing density Φ_c: the *absorbing phase* $\Phi < \Phi_c$, where after some finite time the system finds an overlap-free state such that all motion ceases, and an *active phase* $\Phi > \Phi_c$, where the system fails to find overlap-free configurations and grains move around indefinitely. My literature work is on continuous transitions far from equilibrium in general and two universality in particular: *(non-conserved) directed percolation* (DP), which I mostly use to illustrate the concepts and methods in the study of critical dynamical systems, and the *Manna* or *conserved directed percolation* (CDP) class, to which the absorbing state transition in random organization probably belongs. I conclude that analytical studies into the universal critical behaviour of CDP are dominated by field-theories of the associated order parameter, the density $\rho_A(\boldsymbol{r}, t)$ of active grains. This is because large-scale field-theories boast methods geared towards understanding universal behaviour. They are not, however, immediately suitable for finding precise (highly model-dependent) critical densities. The latter task has been left to simulation studies. My own investigations explore and try to assess possible pathways to analytical theories for predicting critical densities. To the end of calculating Φ_c on paper, I suggest a reaction system, whose analysis is ongoing, that respects spatial correlations beyond mean-field by formulating it in the *operator formalism* introduced by Masao Doi in two papers from 1976 that are seminal for theoretical non-equilibrium physics.

Contents

1 Introduction

From the reference frame of Newtonian dynamics, which is deterministic and time-reversible, physics on scales much larger than that of atoms, such as the scale of humans, has peculiar features: apparent randomness and irreversibility. These features, loosely speaking, emerge from the fact that no experimenter could possibly express the motions of, for example, 10^{23} constantly colliding molecules in a glass of water, much less track or predict them - any model of the fluid's behaviour must, by this simple argument, necessarily be ignorant to the vast majority of information about it. Yet, a lot of phenomena still admit useful descriptions, where the ignorance is respected, on some level, by introducing *randomness*, often resulting in *time-irreversibility*.

Explanations for the power of this approach regularly invoke *chaos*, meant in a technical sense, as in behaviours "[...] whose variations *are not random but look random* [...] ones that appear to proceed according to chance even though their behavior [sic] is in fact determined by precise laws" (Lorenz 1995, p. 2). Note that this is unrelated to having many constituent parts, as is made evident by the famous double pendulum (which has only two degrees of freedom) whose long term motion can be drastically different even for barely distinguishable but distinct initial conditions. While detrimental to the ability of finding exact solutions on paper or even numerical ones spanning any substantial amount of time, chaotic systems are not unapproachable. Indeed, aspects of their qualitative behaviour may be captured by random processes.

An example from the theory of gases is the *Stoßzahlansatz*[1] (Ehrenfest and Ehrenfest 1911), which has as a consequence that within any infinitesimally short time period $[t, t + \mathrm{d}t]$ the pair density[2] of colliding molecules $F(\boldsymbol{v}_1, \boldsymbol{v}_2)$ factorizes into the product $f(\boldsymbol{v}_1)f(\boldsymbol{v}_2)$, where $f(\boldsymbol{v})$ is the number of particles per unit volume that have velocity $\boldsymbol{v}$. The latter amounts to assuming, that velocities are both random and uncorrelated[3] (Brown, Myrvold, and Uffink 2009, eq. 1, p. 3). We quantify the degree of ignorance about the exact state of the gas by (information-theoretical) entropy

$$H[f(\boldsymbol{v}, t)] \coloneqq -\int \mathrm{d}^3 v\, f(\boldsymbol{v}, t)\, \log(f(\boldsymbol{v}, t))$$

Famously, when evolving a probability distribution on phase space in classical Hamiltonian mechanics (with the Liouville-equation), H will remain unchanged (no ignorance incurred, reversibility given), while with the Stoßzahlenansatz in place, the

---

[1] found in the (in the past very controversial) discussions on Boltzmann's H-theorem

[2] The number of pairs per unit volume with velocities $\boldsymbol{v}_1$ and $\boldsymbol{v}_2$ respectively that will collide during the time span $[t, t + \mathrm{d}t]$

[3] and also ignores any particle interactions beyond pair collisions, effectively limiting this line of thinking to dilute gases

Boltzmann H-Theorem reveals that H increases over time. So while the closure with $F(\boldsymbol{v}_1, \boldsymbol{v}_2) \approx f(\boldsymbol{v}_1)f(\boldsymbol{v}_2)$ yields a tractable model for something with as many degrees of freedom as a gas, it comes at the cost of reversibility.

Another example is Brownian motion, which refers to jittery movement of very light particles suspended in a fluid, which they are subject to because molecules from the fluid scatter off them. This motion is well described by random, mutually statistically independent paths with independent increments. The concentration profile $\rho(\boldsymbol{r}, t)$ of an entire suspension of such particles evolves according to the diffusion equation

$$\frac{\partial \rho(\boldsymbol{r}, t)}{\partial t} = D\nabla^2 \rho(\boldsymbol{r}, t)$$

where D is called the *diffusion constant* and reflects the jitter motion's magnitude. The independence of particle paths reflects that they do not interact, so the overall concentration profile $\rho(\boldsymbol{r}, t)$ is proportional to the probability density for the location of any given particle $P(\boldsymbol{r}, t) \sim \rho(\boldsymbol{r}, t)$. These dynamics are also irreversible by virtue of any given increment $\boldsymbol{r}(t + \mathrm{d}t) - \boldsymbol{r}(t)$ of any given particle's position $\boldsymbol{r}$ being statistically independent of the history of its previous locations $\{\boldsymbol{r}(t')\}_{t \geq t' \geq 0}$. The irreversibility here also expresses itself in the growth of entropy $H[P(\boldsymbol{r}, t)] = -\int \mathrm{d}^d r \, P(\boldsymbol{r}, t) \, \log(P(\boldsymbol{r}, t))$ over time, since

$$\frac{\partial H}{\partial t} = D \int \mathrm{d}^d r \, \frac{(\nabla P(\boldsymbol{r}, t))^2}{P(\boldsymbol{r}, t)} \quad \overset{\nabla P \not\equiv 0}{>} \quad 0$$

is always increasing[4] (where d is the number of spatial dimensions, that the suspended particles move in).

Tracing the way in which irreversibility manifests on the macroscopic scale is a paradigmatic task to statistical physics. An interesting contribution to this endeavour is being discussed in Pine et al. (2005) who report a system that can, depending on system parameters, display both reversible and irreversible behaviour. The setup is as follows: extended particles (with some *packing density* Φ) are suspended in a very viscous fluid. They have the weight and size necessary for being suspended, but are too heavy to be subject to Brownian motion. To the authors discuss what happens when the suspension is periodically sheared with strain $\gamma(t) = \gamma_0 \sin(\omega t)$ and strain amplitude γ_0 and shearing frequency ω. To accomplish that, the fluid is poured in-between two concentric cylinders that can be rotated against each other (see fig. 1.1), a setup commonly employed in rheology. At low enough Reynolds numbers (basically when the shearing is done slowly enough) the fluid is in *Stokes-flow* (or *creeping flow*), described by the equation[5]

$$\eta \nabla^2 \boldsymbol{u} = \nabla p$$

where ∇p is the gradient of pressure and η is viscosity. Under this regime non-linear flow behaviour like turbulence, caused by the (now neglected) advection-term $(\boldsymbol{u} \cdot \nabla)\boldsymbol{u}$, are absent. Under the no-slip boundary conditions that apply here, right at the

---

[4] unless $P(\boldsymbol{r}, t)$ is perfectly uniformly distributed in space ($\nabla P(\boldsymbol{r}, t) \equiv 0$), in which case there is no concentration imbalance to diffuse anyway

[5] For all intents and purposes, the suspending fluid is incompressible and Newtonian, so neglecting inertia by $\rho(D\boldsymbol{u}/Dt) \approx 0$ indeed reduces to $\eta \nabla^2 \boldsymbol{u} = \nabla p$,

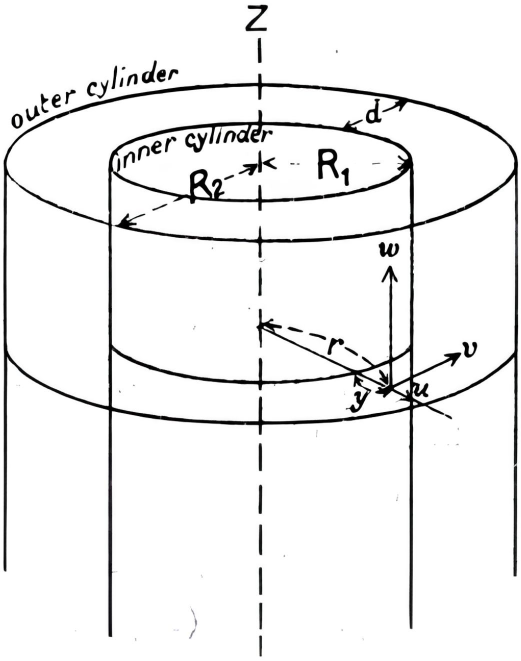

Figure 1.1: Illustration from Taylor (1923) of what is now usually called the *Taylor-Couette geometry*

cylinder wall the fluid velocity $\boldsymbol{u}$ will be exactly the same as cylinder velocity, handing experimenters control over the boundary conditions for $\boldsymbol{u}$. Under these circumstances, the shearing of the fluid is reversible, as in: every fluid element deformed and displaced by rotating the cylinders against each other by an angle θ can be replaced and their shape reverted by rotating back by the angle $-\theta$. This may be demonstrated by suspending dye in such a fluid and shearing, which will apparently mix the colour after some number of rotations; however, turning the cylinder back the exact same number of rotations will reassemble the supposedly scrambled colour droplet.

Mediated by the fluid, the suspended particles can influence each others' velocities (in both direction and magnitude) appreciably if they are sufficiently close. When packing density Φ and strain amplitude γ_0 are low, the particles will, after some number of shear cycles τ, arrange themselves into a configuration in which any given particle will be undisturbed enough to remain on the same spot after each cycle, just like the aforementioned dye droplet can be sheared back into its original shape. However, beyond a (Φ dependent) critical strain amplitude γ_0^{c} particles do not return to their starting points, which the authors attribute to the chaos[6] in three-body or higher interactions. The suspension's behaviour transitions from reversible $\gamma_0 < \gamma_0^{\mathrm{c}}$ to irreversible for $\gamma_0 > \gamma_0^{\mathrm{c}}$.

A simple interpretation of this goes as follows[7]: shearing the suspension will move particles around and hence provoke chaotic interactions that, given both the uncertainty and high sensitivity on initial conditions, will displace them in an effectively

---

[6] Pine et al. (2005) argues away the possibility of inertia, grain roughness and the like playing a role

[7] Taking strong inspiration from the introductory explanations from Corté et al. (2008), which I will lead over to immediately after

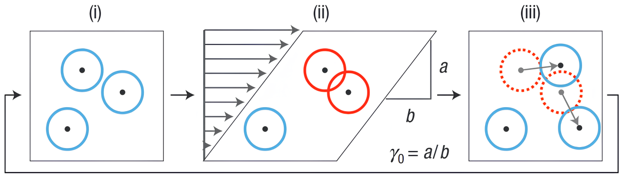

(a) Random organization update rules: spherical particles (depicted as disks) in (i) are sheared with strain amplitude γ_0. Any particles that come in contact in the process (ii) are given random displacements (iii)

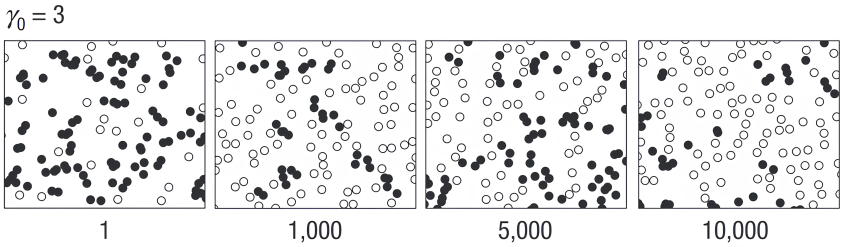

(b) Beneath each frame can be found the number of performed shear cycles. Black disks are active particles, the remaining white ones inactive. One can see that activity decays over time (to some steady-state value)

Figure 1.2: Depictions figures 1 (fig. 1.2a) and 2a (fig. 1.2b) from Corté et al. (2008, fig. 1), illustrating random organization.

random way. However, after a few cycles of provoking collisions, particles already in a spot avoiding all others during the shear cycle stay put, while those who are not will be repeatedly moved by subsequent interactions until they find such a vacant avoidance-spot. That one would see a transition in behaviour depending on γ_0 becomes clear by considering that if the particles are barely moved, they will not even meet, while a very high strain amplitude will provide many chances for encounters. The packing density dependence of γ_0^c is also not surprising: if Φ was very high, it should not be possible to avoid collisions, say if they are spheres and already arranged in a configuration close to an FCC crystal, while at very low densities particles should not even encounter each other, no matter how far the shearing makes them travel. Pine et al. (2005) additionally simulated the system with Stokesian Dynamics[8] and found the same behaviour. They also found that in the regime $\gamma_0 > \gamma_0^c$ where particle displacements never cease, also referred to[9] as the *active regime*, the new positions of displaced particles after every shear cycle perform random walks.

Understanding the most important mechanisms in the transition has been done with a simpler model of this behaviour, called *random organization* (RO), introduced in Corté et al. (2008) and realized as a simulation[10]: starting from randomly and independently placed spheres or disks, every time step the system is periodically sheared with strain amplitude γ_0 at some packing density Φ. Any particles that overlap in

---

[8] Numerically integrating the creeping flow equations, akin to molecular dynamics, where one numerically integrates Newton's equations (Pine et al. 2005)

[9] In the lingo of Corté et al. (2008)

[10] One can find animations of random organization under `https://physics.nyu.edu/pine/random_organization.html` (last visited on 14.11.2025 at 09:41)

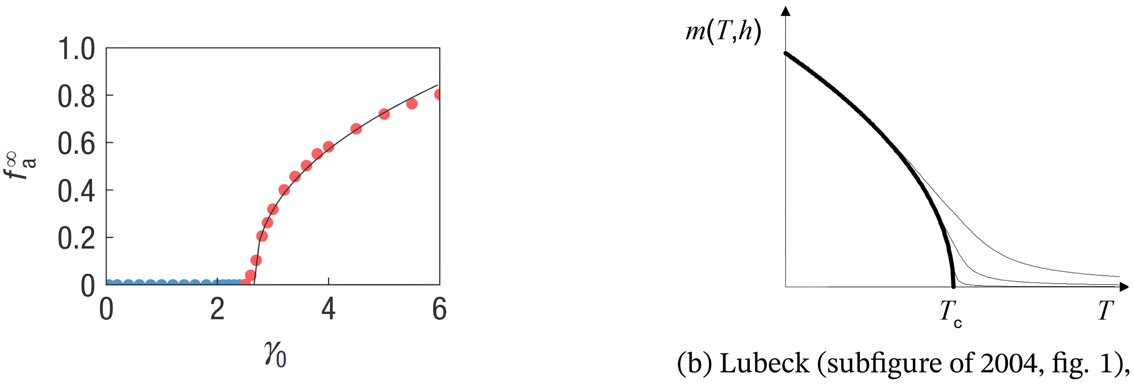

(a) Corté et al. (snapshot from 2008, fig. 2), where the solid line is a fit to the power law $f_a^\infty \sim |\gamma_0 - \gamma_0^c|^\beta$

(b) Lubeck (subfigure of 2004, fig. 1), where the thick line is for zero external field $h = 0$ (and the slight lines for $|h| > 0$)

Figure 1.3: Side by side comparison of the steady-state activity of random organization f_a^∞ as a function of shear amplitude and the magnetization m of a ferromagnet as a function of temperature. The images would be much more similar if m was plotted as a function of inverse temperature $1/T$

the process of this are given small random displacements (see fig. 1.2a), mimicking that the suspended particles from the Taylor-Couette geometry perform random walks beyond the critical packing density (Pine et al. 2005). Particles in motion due to collision are referred to as *active particles*[11], not to be confused with the microscopic constituents of active matter. The observed behaviour is that, indeed, (for any given strain amplitude) there is again a critical $\gamma_0^c(\Phi)$ that separates the system behaviour into two possible regimes: if $\gamma_0 > \gamma_0^c$ particle displacements never cease and the (emsemble-averaged) fraction $f_a(t)$ of particles that are being displaced at any given step t plateaus as $t \to \infty$ to some stationary value $f_a^\infty := \lim_{t\to\infty} f_a(t)$; on the other hand, if $\gamma_0 < \gamma_0^c$ particle overlaps and hence displacements eventually cease (or in other words: $f_a^\infty = 0$), where the characteristic[12] number of steps τ necessary to find the overlap free configuration diverges to ∞ with a power law $\tau \sim |\gamma_0 - \gamma_0^c|^{-\nu}$ as the critical amplitude is approached from below $\gamma \uparrow \gamma_0^c$.

This behaviour is interesting from a statistical physics point of view because it is akin to phase transitions. Note that this is not a phase transition as Maxwell or Ehrenfest would have understood them, with firm roots in the study of thermal equilibrium systems. The just described *reversibility-irreversibility* transition reported by Pine et al. (2005) or the analogous *absorbing-state transition* (AST) of random organization, indeed, do not admit equilibrium descriptions at all (Corté et al. 2008; Chatterjee, Das, and Pradhan 2018). Yet, the similarities to a continuous (second order or higher) phase transition[13], like the transition of e.g. slabs of iron or cobalt from permanent- to para-magnets beyond the curie temperature T_c, are unmistakable: the qualitative

---

[11] or active *grains* in works discussing a class of similar nodels called *stochastic sandpiles*, e.g. Wiese (2016)

[12] The decay of $f_a(t)$ to its plateau value can be successfully fit by $f_a(t) = f_a^\infty + ({e^{-t/\tau}}/{t^\delta})\left(f_a(0) - f_a^\infty\right)$ for some characteristic time τ and exponent δ, a formula that contains the possibility of power-law behaviour in the limit $\tau \to \infty$ (Corté et al. 2008)

[13] See chapter 2 for a brief recapitulation of these concepts

behaviour experiences a change ($f_a^\infty = 0$ to $f_a^\infty > 0$) as some control parameter, the strain amplitude γ_0, crosses some critical threshold γ_0^c. Random organization even displays power law behaviour $f_a^\infty \sim |\gamma_0 - \gamma_0^c|^\beta$ near the transition , which is familiar from the power law behaviour of spontaneous magnetization in the permanent-magnetic (i.e. $T < T_c$) phase $m \sim |T - T_c|^{\beta_m}$ as (all other things being equal) T approaches the Curie temperature T_c (Wilson 1974, sec. 2.1, eq. 2.1). And similarities are far from stopping here: the time τ necessary for a random organization system with some pending collisions to find a configuration free of particle path overlaps is, in a sense, a susceptibility: imagine manually disturbing the random organization model by relocating a particle to a position where it will experience collision in the next shear cycle or inserting a new particle on top of an already existing one; then small τ means the system reverts back to an overlap-free configuration very quickly after being disturbed, while very large τ means that the system retains activity for a substantial duration ; in the first case, the system has low susceptibility to perturbation (quick die-down of inserted activity), while in the second it is highly susceptible (relatively long-lasting activity). This makes the external forcing of an overlap analogous to an external magnetic field H on the aforementioned magnetizable slab, incurring a magnetization response $m = \chi H$ with magnetic susceptibility χ. With the backdrop of this similarity, it is perhaps less surprising than it would be otherwise to realize the likeness between $\tau \sim |\gamma_0 - \gamma_0^c|^{-\nu}$ as measured by Corté et al. (2008) and the much more well known divergence of magnetic susceptibility with the power law $\chi \sim |T - T_c|^{-\gamma}$ as the system approaches the Curie temperature from the paramagnetic side $T > T_c$ (Wilson 1974, sec. 2.1, eq. 2.7).

As I will discuss in chapter 2, the similarities between thermal equilibrium phase transitions and transitions in the dynamical behaviour of, in the present case, random organization do not end even there. Amongst other things, they can be theoretically studied with similar tools. Literature thus confidently refers to such non-equilibrium phenomena as *dynamical phase transitions*. Far from being the only one, the reversibility-irreversibility transition of random organization can be grouped with other continuous dynamical phase transitions into *universality classes*. The latter are classes of transitions that turn out to have a common theoretical description, including the same critical *critical exponents*, which is how literature refers to the exponents from the power law behaviour of various quantities near the transition, such as the just mentioned β and ν.

At the outset of the thesis, I sought to relate random organization to similar models, like instances of *directed percolation* (DP) and the related *Manna* or *conserved directed percolation* (CDP) universality class. The literature work necessary to get a reasonably good impression of what research into the topic has already yielded, however, turned out to be a particularly interesting, non-negligible effort. Hence I will recount parts of my literature research into universality and criticality in chapter 2 and my research into random organization and other related models in chapter 3. These chapters provide further relevant context for the final chapter 4, where I present my attempts at formulating analytical models geared towards determining Φ_c at zero strain amplitude $\gamma_0 = 0$.

2 Continuous Phase Transitions

The purpose of this section is to provide background on the study of phase transitions, such that subsequent sections have less friction while reading: renormalization flow techniques, simulation studies, etc. were not mandatory parts of my physics education, giving me no reason to expect my target group to have any familiarity with them either. Reading into these topics constituted an integral part of my literature work, since the formulation and study of analytical models of dynamical phase transitions are both phrased in this language and take it for granted. The concepts and lingo of dynamical, non-equilibrium phase transitions are based on results secured for systems in thermodynamic equilibrium (Hinrichsen 2000; Ódor 2004, respective introductions), so I deem it helpful to discuss introduced concepts in terms of the latter before delving into the non-equilibrium approaches to dynamical phase transitions found in literature.

2.1 Order Parameters

2.1.1 First- and Second-Order Transitions in Equilibrium Physics

A paradigmatic system for classifying phase transitions of systems in thermodynamic equilibrium is the so called *Ehrenfest scheme*, in which discontinuities in the n-th derivative of Gibbs free energy G are defined as so called *phase transitions of n-th order* (Reichl 2016, ch. 4, sec. 3). In a fluid, Gibbs free energy $G^{(\text{fluid})}$ is given by temperature T, pressure p and molecule number N. First derivatives with respect to any of these renders entropy S, volume V and chemical potential μ

$$S = -\left(\frac{\partial G^{(\text{fluid})}}{\partial T}\right)_{p,N} \qquad V = -\left(\frac{\partial G^{(\text{fluid})}}{\partial p}\right)_{T,N} \qquad \mu = \left(\frac{\partial G^{(\text{fluid})}}{\partial N}\right)_{p,T} \tag{2.1}$$

Second derivatives of thermodynamic potentials are susceptibilities, like (isobaric) heat capacity in fluids

$$\frac{C_p}{T} = \left(\frac{\partial S}{\partial T}\right)_{p,N} = -\left(\frac{\partial^2 G^{(\text{fluid})}}{\partial T^2}\right)_{p,N} \tag{2.2}$$

Now, for example the liquid-vapour transition comes (at fixed N) with a jump in volume (a first derivative of $G^{(\text{fluid})}$) and hence is a *first-order* transition. In the Ising model[1] $G^{(\text{Ising})}$ depends on temperature T, the number of constituents N and the externally applied field H (which plays a role analogous to pressure p in fluids). Magnetization m is given by

$$m = -\left(\frac{\partial G^{(\text{Ising})}}{\partial H}\right)_{T,N} \tag{2.3}$$

Magnetic susceptibility χ is the response of m to a change in the externally applied field H and hence a second derivative of Gibbs free energy

$$\chi = \left(\frac{\partial m}{\partial H}\right)_{T,N} = -\left(\frac{\partial^2 G^{(\text{Ising})}}{\partial H^2}\right)_{T,N} \tag{2.4}$$

Around the Curie point T_c magnetization is continuous (recall fig. 1.3b), but χ is not. Hence in this case the transition is *second-order* in the Ehrenfest scheme. Second order (or higher) transitions are also referred to as *continuous*, as opposed to the *discontinuous* (in first-order quantities) first-order transitions. Ehrenfest originally envisioned these discontinuities to not have any divergences, but discoveries like the theoretically determined divergence (as T approaches T_c) of the heat capacity of the Ising model on a (two-dimensional) square lattice, found by Onsager (1944), necessitated the extension of the scheme or the adaption of different frameworks altogether (Jaeger 1998; Reichl 2016, ch. 4, sec. 3).

The later developed approach of *Landau-Ginzburg theory* seeks to describe the qualitative features of second-order phase transitions by constructing phenomenological, large-scale models in the form of field theories for a quantity in which the phase transition is evident, a so called *order-parameter* (Reichl 2016, ch. 4, sec. 8; Tong 2017, sec. 1.2; Cheung 2023, sec. 2.1). In the context of the order-disorder transition in the Ising model, such a quantity would be $m(\boldsymbol{r})$ (because $m = 0$ above T_c while $m \neq 0$ below T_c), denoting the magnetization $\sum s_i$ around some location $\boldsymbol{r}$ on scales where the sites of individual spins are not resolved and locations on the lattice may be considered effectively continuous. Such a large-scale description is referred to as *coarse-grained*. In the Landau-Ginzburg ansatz the magnitude $|m(\boldsymbol{r})|$ of the order-parameter of choice (as well as the magnitude of any of its physically relevant derivatives, say $|\nabla m(\boldsymbol{r})|$) should be small in the regime of interest (Tong 2017, sec. 1.2), in order to approximate the so called *Landau-Ginzburg free energy E* as a (local[2]) functional expanded in powers of $m(\boldsymbol{r})$, $\nabla m(\boldsymbol{r})$, etc. which obey symmetries

---

[1] A simplified model of magnetic materials, where the magnet is assumed to be made up of spatially separated sites i which can have two states of magnetization, up $s_i = +1$ and down $s_i = -1$, mimicking the two-valuedness of quantum mechanical spin (leading to s_i being referred to as *spins*); note that it has a non-quantum formulation, where energy E is given by a spin-spin-coupling J_{ij}, which may in principle couple any two spins, and an external field H which may in principle vary from site to site. Usually one places the spins on lattices, connects nearest neighbours with some coupling constant $J > 0$ and applies a spatially uniform field, such that $E = -\sum_{\langle i,j\rangle} J s_i s_j + \sum_i H s_i$ where $\sum_{\langle i,j\rangle}$ denotes the sum over unique pairs $\{i, j\}$ of nearest neighbours on the lattice

[2] as in: $E[m(\boldsymbol{r})] = \int \mathrm{d}^d r\, \varphi(m(\boldsymbol{r}), \nabla m(\boldsymbol{r}), (\nabla \otimes \nabla) m(\boldsymbol{r}), \dots))$ for some *free-energy density* φ depending on $m(\boldsymbol{r})$ and its derivatives

that are known to hold[3]

$$E[m(\boldsymbol{r})] = \int \mathrm{d}^d r \left(\frac{c_2(T)}{2}\, m(\boldsymbol{r})^2 + \frac{c_4(T)}{4}\, m(\boldsymbol{r})^4 + \frac{v_2(T)}{2}\, (\nabla m(\boldsymbol{r}))^2 + \cdots \right) \tag{2.5}$$

Landau-Ginzburg free energy relates to the partition function Z by

$$Z = \int \mathcal{D}m \,\exp\!\left(-\frac{E[m(\boldsymbol{r})]}{k_\mathrm{B} T} \right) \tag{2.6}$$

where $\int \mathcal{D}m$ denotes the path-integral over all possible realizations of $m(\boldsymbol{r})$, perhaps familiar from quantum field theory. Note that the Landau-Ginzburg free energy can neither be interpreted as a Hamiltonian as one would be accustomed to from statistical mechanics (because the coefficients have arbitrary temperature dependence instead of just division by $k_\mathrm{B}T$), nor does it play the role of a free energy F in the sense of a thermodynamic potential, which would be given by $F = -k_\mathrm{B}T \log(Z)$. Instead, E should be thought of as reflecting the weight

$$P[m(\boldsymbol{r})] =: \frac{1}{Z} \cdot \exp\!\left(-\frac{E[m(\boldsymbol{r})]}{k_\mathrm{B} T} \right) \tag{2.7}$$

with which the magnetization field $m(\boldsymbol{r})$ configuration should contribute to the path-integrals for the determination of averaged quantities

$$\langle \mathscr{A} \rangle = \int \mathcal{D}m \, \mathscr{A}[m(\boldsymbol{r})]\, P[m(\boldsymbol{r})] \tag{2.8}$$

where one should imagine $P[m(\boldsymbol{r})]$ as arising from a previous coarse-graining of the fully resolved system; in practice the form of E is chosen by phenomenological arguments (compare sec. 1.3 Tong 2017; sec. 2.2 Cheung 2023).

The descriptive power of this approach is easily showcased by invoking the *saddle-point approximation* $Z \approx \int \mathcal{D}m_\mathrm{s} \exp(-E[m_\mathrm{s}(\boldsymbol{r})]/k_\mathrm{B}T)$ where $\int \mathcal{D}m_\mathrm{s}(\cdots)$ is a dramatically restricted path integral including only the minima of $E[m]$. Candidates for the minima are found by checking where Landau-Ginzburg free energy is extremal $\delta E[m_\mathrm{s}] = 0$. The saddle-point approximation is valid whenever the partition function is dominated by contributions of magnetization fields $m(\boldsymbol{r})$ similar to any of the minima $m_\mathrm{s}(\boldsymbol{r})$. The justification for this is that the Boltzmann weights $\exp(-E[m_\mathrm{s}(\boldsymbol{r})]/k_\mathrm{B}T)$ are the largest there (an argument very similar to the typical reasoning for how the classical-mechanical principle of least action can emerge from quantum path-integrals). Keeping only the first two terms

$$E[m(\boldsymbol{r})] = \int \mathrm{d}^d r \left(\frac{c_2}{2}\, m(\boldsymbol{r})^2 + \frac{c_4}{4}\, m(\boldsymbol{r})^4 \right) =: \int \mathrm{d}^d r\, \varepsilon(m(\boldsymbol{r})) \tag{2.9}$$

(where the coefficients have a T dependence, which I drop to reduce visual clutter) and assuming a homogeneous magnetization $m(\boldsymbol{r}) \equiv m$ turns the variation of $E[m(\boldsymbol{r})]$ with respect to $m(\boldsymbol{r})$ into a derivative of $\varepsilon(m)$ with respect to m

$$0 = \frac{\partial \varepsilon(m)}{\partial m} = c_2\, m + c_4\, m^3 = m(c_2 + c_4\, m^2) \tag{2.10}$$

---

[3] such as switching the definition of $s = \pm 1$ leading to $m(\boldsymbol{r}) \longmapsto (-m(\boldsymbol{r}))$ being a symmetry transformation, or isotropy allowing only rotationally invariant expressions in vectorial quantities (or higher rank, tensorial quantities), say dot products like $\nabla m(\boldsymbol{r}) \cdot \nabla m(\boldsymbol{r})$

with solutions $m = 0$ and $m^2 = -c_2/c_4$. Given that the magnetization m is real-valued, the non-zero value for m is only a valid solution if $c_2/c_4 < 0$, in which case we define $-m_0^2 = c_2/c_4$ and see that

$$m = \pm m_0$$

are indeed minima of $\varepsilon(m)$ and global ones at that, as curve sketching[4] quickly demonstrates. Additionally retaining the term $({}^1\!/_2)v_2(\nabla m(\boldsymbol{r}))^2$

$$\varepsilon(m(\boldsymbol{r}), \nabla m(\boldsymbol{r})) = \frac{c_2}{2}\, m(\boldsymbol{r})^2 + \frac{c_4}{4}\, m(\boldsymbol{r})^4 + \frac{v_2}{2}(\nabla m(\boldsymbol{r}))^2 \tag{2.11}$$

after integration by parts in the variation δE results in

$$0 = \frac{\delta E}{\delta m(\boldsymbol{r})} = -v_2 \nabla^2 m(\boldsymbol{r}) + c_2\, m(\boldsymbol{r}) + c_4\, m(\boldsymbol{r})^3 \tag{2.12}$$

which again has trivial solution $m = 0$; furthermore, when $-m_0^2 = c_2/c_4 < 0$ and $-w^2 := 2v_2/c_2 < 0$ then

$$\frac{m(z)}{m_0} = \tanh\left(\frac{z}{w}\right) \tag{2.13}$$

where z is a coordinate along an arbitrarily chosen axis with an arbitrarily chosen origin. The latter solution can be interpreted as a Weiss domain wall (see plot in fig. 2.1), because $\tanh(\xi)$ has the limits $\lim_{\xi\to\pm\infty} \tanh(\xi) = \pm 1$ and the transition around $\xi = 0$ between those two limit values has an extension of characteristic size w (compare Tong 2017, sec 1.2.1 and sec. 1.3.2)[5] . These two calculations show how already at the two lowest orders in m^2 and $(\nabla m)^2$ the behaviour of the model includes a transition from $m = 0$ to spontaneously magnetized $m \neq 0$ and domain walls separating two regions.

Another example application of the Landau-Ginzburg approach is superconductivity (Reichl 2016, sec. 4.8.3.3), which in Bardeen-Cooper-Schrieffer theory occurs due to electrons experiencing a phonon-mediated effective attraction, with respect to which electron-pairs have a ground state in which they propagate jointly as a boson (Bardeen, Cooper, and Schrieffer 1957), nowadays referred to as a *Cooper-pair.* To model this situation in a minimalist fashion a Landau-Ginzburg free-energy is defined, expressed in terms of a complex order parameter $\psi(\boldsymbol{r})$ encoding both the occupation and phase of the ground state. While discussing the form of Landau-Ginzburg free energy density in the same detail as magnetization would bring little benefit to getting an idea of this method, it is helpful to note that it involves only the $U(1)$-invariant canonical momentum $(-i\nabla + q\boldsymbol{A})$, where q is Cooper-pair charge and $\boldsymbol{A}$ is

---

[4] that also reveals we want $c_4 > 0$ lest ε not be bounded from below

[5] and indeed, the domain wall, given it is a valid solution, indeed has lower Landau-Ginzburg free energy: inserting back into ε, we find by $|\nabla m(z)| = m_0({}^1\!/_w)(1 - \tanh^2({}^z\!/_w))$ that $\lim_{z\to\pm\infty}(\nabla m(z))^2 = ({}^{m_0}\!/_w)^2(1 - (\pm 1)^2) = 0$ while on the other hand we find that $m(z)$ plateaus in either direction to $\lim_{z\to\pm\infty} m(z)^2 = m_0^2$ and similarly $\lim_{z\to\pm\infty} m(z)^4 = m_0^4$ such that (omitting the $\nabla m(z)$ dependence that drops out) Landau-Ginzburg free energy density plateaus to $\lim_{z\to\pm\infty} \varepsilon(z) = ({}^{c_2}\!/_2)(-{}^{c_2}\!/_{c_4}) + ({}^{c_4}\!/_4)(-{}^{c_2}\!/_{c_4})^2 = -({}^{c_2^2}\!/_{2c_4}) + ({}^{c_2^2}\!/_{4c_4}) = -({}^{c_2^2}\!/_{4c_4}) := -\varepsilon_\infty$ which is negative because of the condition for the domain wall solution being $c_2/c_4 < 0$ which by $c_4 > 0$ means $c_2 < 2$ and hence $c_2^2/c_4 > 0$; the small region around the domain wall where ε differs from this plateau value is negligible when integrating over the whole system, making $E[m(z)] \approx -\varepsilon_\infty V < 0$ (lower than $E[0] = 0$ of the trivial $m = 0$ solution), where V is the system volume.

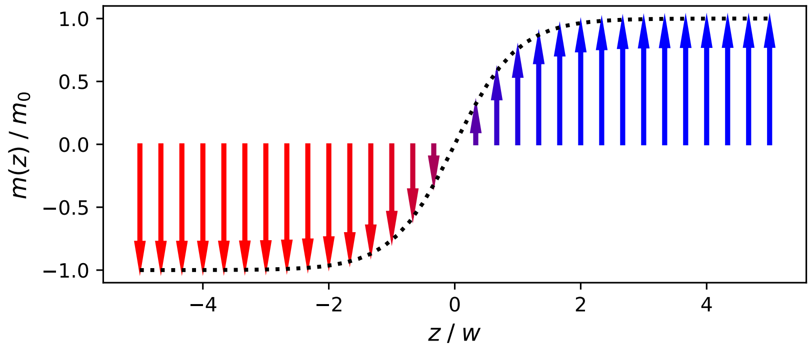

Figure 2.1: Illustration of the saddle-point approximation eq. (2.13) to the Weiss-domain wall. The arrows are supposed to represent magnetization.

the electromagnetic vector potential, and otherwise contains powers of $|\psi(\boldsymbol{r})|^2$ in order to make the model $U(1)$-*gauge-invariant*[6]. Below a critical T_c the system ceases to be gauge-invariant, instead spontaneously taking on one gauge $e^{i\theta^*(\boldsymbol{r})}$ in particular (compare The Royal Swedish Academy of Sciences 2003). This is analogous to the previously described magnet spontaneously preferring one magnetization direction, where in the superconductor case an interpretation is that the system transitions to an overwhelming fraction of electrons occupying the ground state as Cooper-pairs, whose phase is then detectable macroscopically and corresponds precisely to the spontaneously preferred $e^{i\theta^*(\boldsymbol{r})}$.

I should stress that being able to apply concepts from field theory (for example the saddle-point approximation) to the study of phase transitions is a particularly relevant benefit of this coarse-grained statistical field approach. This opens up the possibility of renormalization flow or perturbation theory empowered by diagrammatic techniques. Besides that, the reductionist modelling deliberately ignores details on small scales, which turn out to not be relevant to the qualitative behaviour of the transition. I will substantiate the latter claim in section 2.2 with appropriate references and arguments. I may already foreshadow, that reductionism entails abstractness, such that the same field theory will capture behaviour which a broad class of models have in common. All this also turns out to apply to dynamical phase transitions (see section 2.2).

---

[6] symmetric under redefining phase $\psi(\boldsymbol{r}) \longmapsto \psi(\boldsymbol{r})\, e^{i\theta(\boldsymbol{r})}$ and accordingly vector potential $q\boldsymbol{A} \longmapsto q\boldsymbol{A} - \nabla\theta(\boldsymbol{r})$

2.1.2 Reversibility-Irreversibility and Directed Percolation

As mentioned in the introduction, the transition in random organization cannot be described as a theromdynamic equilibrium model. There I have also already mentioned, that it is also referred to as an absorbing state transition, for the following reason: any system state s of a Markov chain is referred to as *absorbing* if the probability $P(s \to s')$ of transitioning from s to any other system state $s' \neq s$ is zero. Random organization states in which no particle pair will collide in the next shear cycle are absorbing, because they will not be displaced in the next or any subsequent time, remaining put indefinitely. The presence of the absorbing states, in fact, is what rules out the possibility of a (near) equilibrium description of this type of transition, since this bars the system from reaching the detailed balance characteristic of equilibrium (Lubeck 2004, sec. 2.1).

While equilibrium systems are an important reference point, non-equilibrium transitions, like random organization or the reversibility-irreversibility transition from Pine et al. (2005) are fundamentally different in nature: the probability distribution on the states is rarely known a-priori (not even for the long term steady-state, if existent), in contrast to thermal equilibrium, where the probability to be in some state s is governed by some variation (depending on the ensemble) of the Boltzmann-Gibbs-distribution $P(s) \sim \exp(-E(s)/k_{\mathrm{B}}T)$. Instead, these systems are described by a stochastic time-evolution rule (Hinrichsen 2000, introduction), such as stochastic differential equations (see Wiese (2016) for example), update rules for cellular automata (see directed percolation as introduced by Broadbent and Hammersley (1957) or the sandpile lattice model of Manna (1991) for example) or partial differential equations (see Chatterjee, Das, and Pradhan (2018) for example).

For those frameworks, not described by equilibrium concepts such as free energy, Ehrenfest classification (or any of its extensions) cannot apply in its original sense. The idea of order parameters (and with respect to those, the concept of first-order, second-order, etc. transitions), however carries over: in the case of random organization, for example, that would be the steady-state fraction of active grains f_a^∞ (which I will also call *steady-state activity*): in the inactive phase $\gamma_0 < \gamma_0^{\mathrm{c}}$ the steady state activity f_a^∞ is zero with the system eventually falling into one of uncountably many absorbing state configurations, while in the active phase $\gamma_0 > \gamma_0^{\mathrm{c}}$ the steady state activity is positive $f_a^\infty > 0$, as the system establishes a balance between the rate with which grains are inactivating by finding vacant, collision-free spots, and the rate at which the active grains in their random walk find and activate inactive ones. Because there is no jump in f_a^∞ (Corté et al. 2008), the transition can be called continuous or second-order in analogy to equilibrium systems. As hinted at already in section 2.1.1 and further discussed in section 2.2.2, dynamical phase transitions are regularly modelled by field theories of an order-parameter varying both in space *and time* (as opposed to only space, like in equilibrium), which are analysed with tools familiar from Landau-Ginzburg and quantum field theory.

At this point it is obligatory to identify the order parameter in a class of models with many qualitative similarities to random organization: directed percolation[7]. Corté et al. (2008) honour directed percolation as the “Ising model of non-equilibrium phase transitions”, a sentiment echoed in the introduction of Hinrichsen (2000), by

---

[7] lat. *percolare*, engl. to filter, to sift

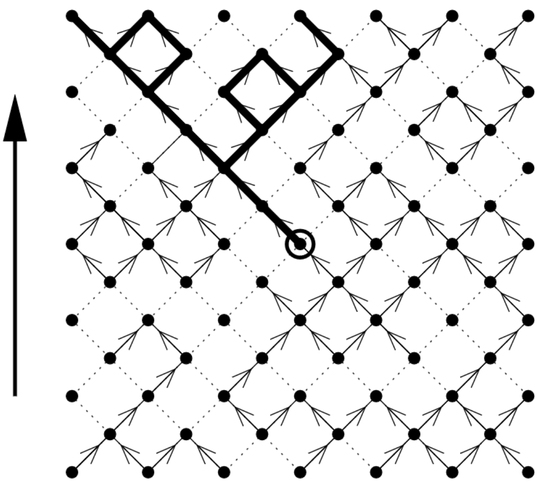

Figure 2.2: Visualization from Hinrichsen (2000, fig. 10) of (1 + 1)-dimensional directed percolation, with every site in any given time-slice being activated by two sites from the previous slice and activating two sites in the subsequent one.

virtue of how broadly studied it is and how it serves as a reference problem for describing and understanding others. Directed percolation is a specific instance of the more general class of *percolation problems* (see Broadbent and Hammersley 1957; Obukhov 1980), who all study under what circumstances local, small-scale random connectivity is likely to make large graphs globally connected. The problem statement reads as follows: Imagine copies of a d-dimensional regular lattice being stacked ad infinitum into parallel *layers* (which I will also call *slices*) in $(d+1)$-dimensional space. We label these layers with some index $t = 0, 1, 2, 3, \dots$ with $t = 0$ being some arbitrary starting layer. Then, proximate sites from subsequent layers t and $t + 1$ shall be connected with *directed bonds* pointing from t to $t + 1$. Next, we randomly and independently make bonds passable with some probability p, which serves as the control parameter of the problem. As an example, see fig. 2.2, which depicts the case when the regular lattice is a line of points, and the connections are with the two nearest neighbours in the subsequent layer. One now asks for the probability P_∞ that, starting from $t = 0$ one can pass arbitrarily far along open bonds. This prescription can be interpreted as a system undergoing stochastic, Markovian, dynamics with the directed dimension playing the role of time (which is why I chose to call the layer-index t, as is customary for times) and the transverse directions the role of space (Cardy and Sugar 1980, introduction), which I choose to index with $\boldsymbol{x}$. Indeed Obukhov (1980) likened directed percolation to the spread of disease or forest fire in space as time passes. With this view in mind, one may write down dynamical equations, say by translating the logic, for whether a bond is connected to the $t = 0$ layer, into an expression

$$\underbrace{1 - \mathscr{W}(\boldsymbol{x}, t+1)}_{\text{“site } \boldsymbol{x} \text{ is not wet”}} = \underbrace{\prod_{\boldsymbol{x}'} (1 - \mathscr{C}(\boldsymbol{x}, \boldsymbol{x}', t)\,\mathscr{W}(\boldsymbol{x}', t))}_{\substack{\text{“all previous sites } \boldsymbol{x}' \text{ with directed bond to } \boldsymbol{x} \\ \text{are not both wet and open ”}}} \tag{2.14}$$

of indicator[8] functions $\mathscr{W}(\boldsymbol{x}, t)$ of the event that site $(\boldsymbol{x}, t)$ is connected to $t = 0$, where for any given $t = 0$ site $\boldsymbol{x}$ we have $\mathscr{W}(\boldsymbol{x}, 0) \in \{0, 1\}$ lest the indicators $\mathscr{W}(\boldsymbol{x}, t)$ in subsequent slices $t > 0$ not take values in $\{0, 1\}$. $\mathscr{C}(\boldsymbol{x}, \boldsymbol{x}', t) = 0$ in case there cannot even in principle be a direct bond $\boldsymbol{x} \rightsquigarrow \boldsymbol{x}'$ and otherwise takes on the value of 1 with probability p and 0 with probability $(1 - p)$, where $\mathscr{C}(\boldsymbol{x}, \boldsymbol{x}', t)$ and $\mathscr{C}(\boldsymbol{y}, \boldsymbol{y}', s)$ are independent

---

[8] Indicators are 0 if the statement they describe is false and 1 otherwise. They are often denoted $\mathbf{1}\{\cdots\}$, so e.g. here $\mathscr{W}(\boldsymbol{x}, t) = \mathbf{1}\{\text{site } (\boldsymbol{x}, t) \text{ is connected to } t = 0\}$

of each other for distinct bonds $(\boldsymbol{x}, \boldsymbol{x}', t) \neq (\boldsymbol{y}, \boldsymbol{y}', s)$. Because directed percolation has also been seen as a model for fluid permeating a porous medium, sites $(\boldsymbol{x}, t)$ with $\mathscr{W}(\boldsymbol{x}, t) = 1$ have been referred to as *wet sites*, while the comparison to the spread of disease has incurred them the name *infected sites* (though I will stick to the name wet sites). One can observe in numerical realizations of directed percolation, that the *fraction of wet sites* $f_w(t)$, given by

$$f_w(t) := \left\langle \frac{\sum_{\boldsymbol{x}} \mathscr{W}(\boldsymbol{x}, t)}{\sum_{\boldsymbol{x}} 1} \right\rangle \tag{2.15}$$

decays, after some characteristic number of layers τ, to a steady-state value

$$f_w^\infty := \lim_{t \to \infty} f_w(t) \tag{2.16}$$

that depends on the bond probability p. At $p = 0$ no bonds are open ($f_w^\infty = 0$), at $p = 1$ every bond is open ($f_w^\infty = 1$). For all p in between we can, at this abstract stage, only say that enlarging p will never reduce the chance for one site wetting another, hence f_w^∞ can, if changed at all, only increase with growing p: $p_1 < p_2 \Rightarrow f_w^\infty(p_1) \leq f_w^\infty(p_2)$ or similarly $P_\infty(p_1) \leq P_\infty(p_2)$. Both f_w^∞ and P_∞ can serve as order parameters, with $f_w^\infty = 0$ meaning that at some time T the system enters the (unique) absorbing state $\mathscr{W}(\boldsymbol{x}, T) \equiv 0$ while $f_w^\infty > 0$ means wet sites propagate indefinitely in time; in the latter phase one calls the system *percolating*. As with the random organization transition (see introduction for more details and references), the order parameter of directed percolation follows a power law (compare Jensen 1999, eq. 3; Adzhemyan et al. 2023, eq. 7)

$$f_w^\infty \sim |p - p_\mathrm{c}|^{\beta_\mathrm{DP}} \tag{2.17}$$

as p approaches the critical bond probability[9] p_c.

2.2 Critical Behaviour and Universality

2.2.1 Phenomenology of Critical Systems

In the introduction and section 2.1.2, I mentioned many instances of power law behaviour near the so called *critical point* (such as critical strain amplitude γ_0^c, Curie temperature T_c or critical bond probability p_c) of a continuous transition: the Curie point with $m \sim |T - T_\mathrm{c}|^{\beta_\mathrm{m}}$ and $\chi \sim |T - T_\mathrm{c}|^{-\gamma}$, the reversibility-irreversibility transition with $f_a^\infty \sim |\gamma_0 - \gamma_0^\mathrm{c}|^{\beta}$ and $\tau \sim |\gamma_0 - \gamma_0^\mathrm{c}|^{-\nu}$, the onset of superconductivity $\psi \sim |T - T_\mathrm{SC}|^{\beta_\mathrm{SC}}$ or the transition in DP from finite penetration depth to percolation in $f_w^\infty \sim |p - p_\mathrm{c}|^{\beta_\mathrm{DP}}$. These are an expression of behaviour that literature refers to as *scaling*.

Correlators Talking about the phenomenology of scaling (and then subsequently characterizing it) requires introducing the concept of *correlators* first, in particular two-point correlators. Generally speaking, one calls an object a correlator if it contains averages of products of a spatially resolved order parameter $f(\boldsymbol{r})$, for example

---

[9] For the $(1+1)$-dimensional lattice depicted in fig. 2.2 and fig. 2.3 $p_\mathrm{c} = 64.4700185(5)\%$ according to numerics presented in Jensen (1999)

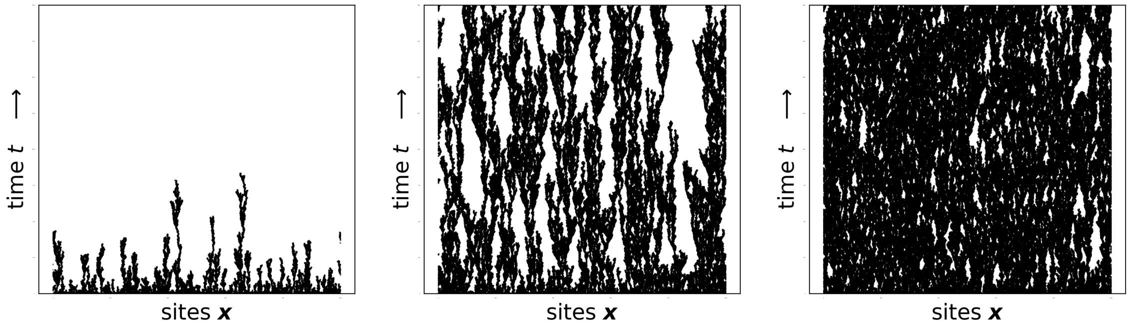

(a) $p = 62\%$ (b) $p = p_\mathrm{c} \approx 64.47\%$ (c) $p = 66\%$

Figure 2.3: Visualization of different regimes of directed percolation, with black representing wet sites. Bonds are open with probability p and the system has periodic boundary conditions, i.e. the last and first site along the $\boldsymbol{x}$-line are considered nearest neighbours.In the *subcritical* $p = 62\%$ (fig. 2.3a) the survival time of wetness experiences exponential dampening, leading to a visible cut-off length. *Critical* directed percolation $p = p_\mathrm{c}$ (fig. 2.3b) has columns of wet sites terminating at all kinds of lengths with the system looking qualitatively the same across scales. At the *supercritical* $p = 66\%$ (fig. 2.3c) columns tend to not terminate at all, instead mostly splitting, proliferating and then combining again with the parent or another column.

$\langle f(\boldsymbol{r}_1)f(\boldsymbol{r}_2)\rangle$ or $\langle f(\boldsymbol{r}_1)f(\boldsymbol{r}_2)f(\boldsymbol{r}_3)\rangle$. Correlators quantify how related, alike or statistically dependent (in short: correlated) the behaviour of $f(\boldsymbol{r})$ is to itself at two different locations. A certain correlator is especially suited to this task: to get it, one mean-centres $(f(\boldsymbol{r}) - \langle f(\boldsymbol{r})\rangle)$ the order parameter at distinct locations $\boldsymbol{r}_1$ and $\boldsymbol{r}_2$. One then computes the ensemble-average of the product of these two deviations from mean to get the *(connected) two-point correlation function* or *two-point cumulant*

$$\begin{aligned}\langle f(\boldsymbol{r}_1)\, f(\boldsymbol{r}_2)\rangle_\mathrm{c} &:= \big\langle\, \big(f(\boldsymbol{r}_1) - \langle f(\boldsymbol{r}_1)\rangle\big) \cdot \big(f(\boldsymbol{r}_2) - \langle f(\boldsymbol{r}_2)\rangle\big)\,\big\rangle \\ &= \langle f(\boldsymbol{r}_1)\, f(\boldsymbol{r}_2)\rangle - \langle f(\boldsymbol{r}_1)\rangle \langle f(\boldsymbol{r}_2)\rangle\end{aligned} \tag{2.18}$$

For dynamical transitions, where the order parameter $f(\boldsymbol{r}, t)$ is also resolved in time, events $(\boldsymbol{r}, t)$ take the role of mere positions.

In thermal equilibrium, correlators are related to thermodynamic observables. Take as an example the Landau-Ginzburg theory of the Curie point introduced in section 2.1.1. To state the obvious first, the one-point correlator is mean magnetization at point $\boldsymbol{r}$ and can be generated by variation of free energy with respect to the externally applied magnetic field $H(\boldsymbol{r})$

$$\begin{aligned}\langle m(\boldsymbol{r})\rangle &= \int \mathcal{D}m\, \frac{1}{Z} \exp\left(-\frac{E[m] - \int \mathrm{d}^d r\, H(\boldsymbol{r}) m(\boldsymbol{r})}{k_\mathrm{B}T}\right) \cdot m(\boldsymbol{r}) \\ &= -(-k_\mathrm{B}T) \frac{\delta}{\delta H(\boldsymbol{r})} \log\underbrace{\left(\int \mathcal{D}m\, \exp\left(-\frac{E[m] - \int \mathrm{d}^d r\, H(\boldsymbol{r}) m(\boldsymbol{r})}{k_\mathrm{B}T}\right)\right)}_{=Z} \\ &= -\frac{\delta F}{\delta H(\boldsymbol{r})}\end{aligned} \tag{2.19}$$

More interestingly, magnetic susceptibility, ordinarily defined by the derivative $\chi = {}^{\partial m}\!/_{\partial H}$ to a change to the externally applied magnetic field, has two position dependences when working with a spatially resolved magnetization

$$\begin{aligned}\chi(\boldsymbol{r}_1,\boldsymbol{r}_2) &= -\frac{\delta m(\boldsymbol{r}_1)}{\delta H(\boldsymbol{r}_2)} = \frac{\delta^2 F}{\delta H(\boldsymbol{r}_1)\,\delta H(\boldsymbol{r}_2)} \\ &= k_{\mathrm{B}}T\frac{\delta^2 \log(Z)}{\delta H(\boldsymbol{r}_1)\,\delta H(\boldsymbol{r}_2)} \\ &= k_{\mathrm{B}}T\left(\frac{1}{Z}\frac{\delta^2 Z}{\delta H(\boldsymbol{r}_1)\,\delta H(\boldsymbol{r}_2)} - \frac{1}{Z^2}\frac{\delta Z}{\delta H(\boldsymbol{r}_1)}\frac{\delta Z}{\delta H(\boldsymbol{r}_2)}\right) \\ &= \frac{1}{k_{\mathrm{B}}T}\cdot\big(\langle m(\boldsymbol{r}_1)\,m(\boldsymbol{r}_2)\rangle - \langle m(\boldsymbol{r}_1)\rangle\langle m(\boldsymbol{r}_2)\rangle\big)\end{aligned} \tag{2.20}$$

where it was inserted, that

$$\begin{aligned}&\frac{1}{Z}\frac{\delta^n Z}{\delta H(\boldsymbol{r}_1)\cdots\delta H(\boldsymbol{r}_n)} \\ &\quad= \frac{1}{Z}\frac{\delta^n}{\delta H(\boldsymbol{r}_1)\cdots\delta H(\boldsymbol{r}_n)}\int \mathcal{D}m\,\exp\left(-\frac{E[m] - \int \mathrm{d}^d r\, H(\boldsymbol{r})m(\boldsymbol{r})}{k_{\mathrm{B}}T}\right) \\ &\quad= \left(\frac{1}{k_{\mathrm{B}}T}\right)^n \int \mathcal{D}m\,\frac{1}{Z}\exp\left(-\frac{E[m] + \int \mathrm{d}^d r\, H(\boldsymbol{r})m(\boldsymbol{r})}{k_{\mathrm{B}}T}\right)\cdot m(\boldsymbol{r}_1)\cdots m(\boldsymbol{r}_n) \\ &\quad= \left(\frac{1}{k_{\mathrm{B}}T}\right)^n \cdot\langle m(\boldsymbol{r}_1)\cdots m(\boldsymbol{r}_n)\rangle\end{aligned} \tag{2.21}$$

On the very right hand side of eq. (2.20) one can recognize the two-point correlator of magnetization, rendering

$$k_{\mathrm{B}}T\,\chi(\boldsymbol{r}_1,\boldsymbol{r}_2) = \langle m(\boldsymbol{r}_1)m(\boldsymbol{r}_2)\rangle_{\mathrm{c}} \tag{2.22}$$

Generally, susceptibilities associated with an order parameter reflect its two-point correlations (Tong 2017, sec. 2.2). This state of affairs does not change in dynamical phase transitions, except that the presence of time makes these theories richer, involving additional features like causality. The characteristic time for random organization to reach a steady- or absorbing state, for example is related amongst other things to $\langle f_a(t')f_a(t)\rangle_{\mathrm{c}}$ where the angled brackets average over the ensemble of all possible realizations of the time evolution of $f_a(t)$.

Critical Scale Invariance In the *disordered phase*[10] of a continuous transition, where the order parameter vanishes $f = 0$, qualitatively speaking the correlation functions $\langle f(\boldsymbol{r})f(\boldsymbol{r}')\rangle_{\mathrm{c}}$ decay with growing $|\boldsymbol{r}' - \boldsymbol{r}|$ with some characteristic length scale ξ, the so

---

[10] The names *ordered* and *disordered* comes from the observation that continuous phase transitions often come with *spontaneous symmetry breaking*, referring to the possibility that a microscopically respected symmetry may not apply to the macroscopic state of the system. Examples: the invariance of the Ising model to replacing $m \to -m$ is broken by the spontaneous choice of either of the magnetizations $\pm m_0$ below T_{c}. Similarly, in the Landau-Ginzburg theory of superconductivity the order parameter $\psi(\boldsymbol{r})$ spontaneously chooses a gauge $e^{i\theta_*}$ in the superconducting phase, despite the corresponding free energy being gauge-invariant

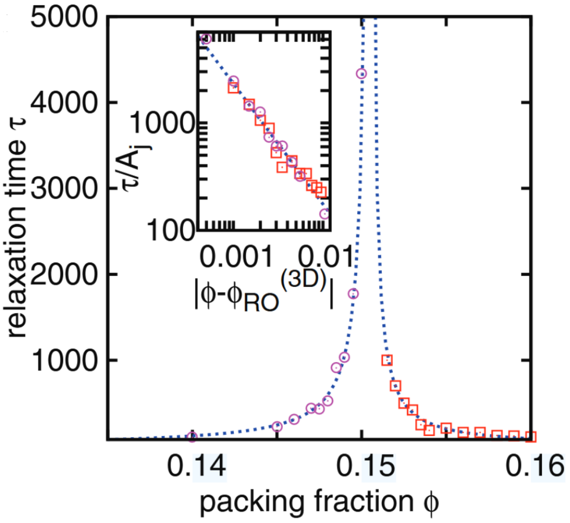

Figure 2.4: Plot from Milz and Schmiedeberg 2013, fig. 3 of diverging relaxation times τ (which strictly grows with the correlation time $\xi_{\|}$) as the critical packing density $\Phi^{(3D)}_{\mathrm{RO}}$ is approached in $\gamma_0 = 0$ three-dimensional random organization

called *correlation length*. Again, this transfers to the far-from-equilibrium case, where additionally to the correlation length $\xi_{\perp}$, there is also a fall-off in time with a characteristic *correlation-time* $\xi_{\|}$ (Cheung 2023, sec. B); note the subscripts differentiating the two. Back in equilibrium, ξ is the characteristic size over which the order parameter $f(\boldsymbol{r})$ varies. Importantly, the behaviour of the system, while affected quantitatively, is not qualitatively affected by processes on length scales much shorter than the correlation length (Lubeck 2004, sec 1.1, Tong 2017, sec. 2.2.3), basically by definition. Far from equilibrium, the correlation-time $\xi_{\|}$ in addition analogously marks the smallest timescale over which qualitatively important processes happen.

Continuous phase transitions are characterized by the divergence of correlation lengths (and, in dynamical transitions, the correlation times, see for example random organization in fig. 2.4) as the critical point is approached from the disordered phase. To make more tangible what this means, take as a first example the Ising model: above the Curie point $T > T_{\mathrm{c}}$ the system is in a disordered phase, where the magnetization $m(\boldsymbol{r})$ and $m(\boldsymbol{r}')$ of near-by sites $|\boldsymbol{r}' - \boldsymbol{r}| \ll \xi$ will reliably be aligned, while distant sites $|\boldsymbol{r}' - \boldsymbol{r}| \gg \xi$ will have no correlation $\langle m(\boldsymbol{r})m(\boldsymbol{r}')\rangle_{\mathrm{c}} = 0$. In this sense, the correlation length quantifies the characteristic size of patches of similar magnetization. As the system is cooled towards T_{c} (making the lower energy of aligned spins ever more dominant over the entropy of thermal noise), there will be increasingly larger patches that overwhelmingly have the same magnetization. In the magnetized phase $T < T_{\mathrm{c}}$ the entire material has the same magnetization, which one may read as the size of patches having diverged $\xi \to \infty$ (Tong 2017, sec. 2.2.3).

As an example for far-from equilibrium, take directed percolation problems as introduced in section 2.1.2: the critical point $p = p_{\mathrm{c}}$ divides their behaviour into a phase where an externally forced, isolated wet site would eventually die out (fig. 2.5a) and a phase where wetness propagates indefinitely (fig. 2.5c). In the dying out phase, the correlator $\langle w(\boldsymbol{r}', t')w(\boldsymbol{r}, t)\rangle_{\mathrm{c}}$ of the (coarse-grained) density of wet sites $w(\boldsymbol{r}, t)$ decays exponentially fast with both $|t' - t|$ and $|\boldsymbol{r}' - \boldsymbol{r}|$. In the subcritical absorbing phase

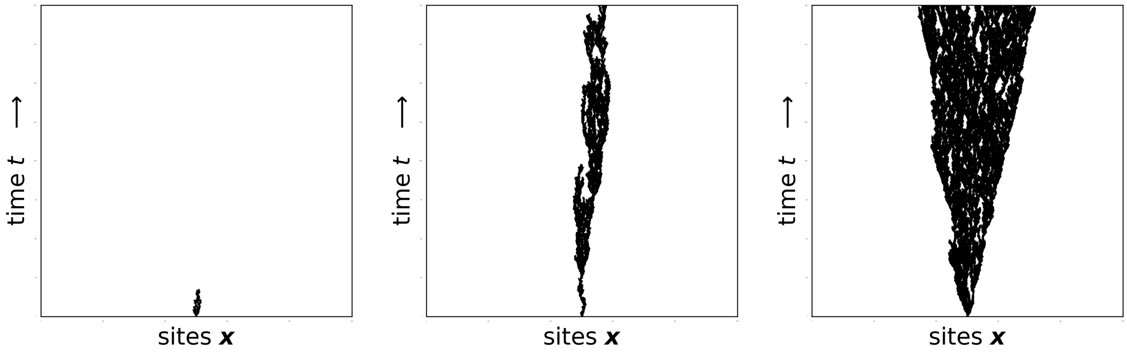

(a) $p = 62\%$ (b) $p = p_\mathrm{c} \approx 64.47\%$ (c) $p = 66\%$

Figure 2.5: Directed percolation (bonds are open with probability p) in different phases with a single wet site at $t = 0$, in order to visualize how far in time and space a single externally forced wet site can influence system behaviour, as quantified by the correlation time $\xi_{\|}$ and correlation length $\xi_\perp$ (grey or black representing wet sites): below the critical bond probability (fig. 2.5a) the reach of the original wet site's influence is finite. At $p = p_\mathrm{c}$ (fig. 2.5b) the correlation length is infinite, but the wet sites barely manage to proliferate. At $p > p_\mathrm{c}$ (fig. 2.5c) the $t = 0$ wet site's influence has arbitrarily far reach in both time and space, spreading in a causal-cone whose opening angle, quantifying the speed at which influence propagates in space, is given by the ratio of $\xi_\perp$ and $\xi_{\|}$ (Lubeck 2004, sec. 3.3)

$p < p_\mathrm{c}$, the reach in time of a cone of wet sites, initiated by an isolated wet site, is finite (see fig. 2.5a), with $\xi_\perp$ being its characteristic length by definition; this is analogous to patches of magnetization having finite characteristic extension. In the supercritical phase $p > p_\mathrm{c}$ in contrast, wetness persists indefinitely. As the critical bond probability is approached, the characteristic reach of wet sites will grow, as depicted in fig. 2.6, and eventually diverge $\xi_{\|} \to \infty$ as $p \uparrow p_\mathrm{c}$. (Hinrichsen 2000, introduction, Lubeck 2004, sec. 1.1).

That the correlation lengths diverge at criticality has a very important consequence: right at the critical point, the system has no characteristic scale (which would have been given by ξ or $\xi_\perp$ and $\xi_{\|}$). This manifests itself with *scale-invariance* (also referred to as *conformal symmetry*). More concretely: let α (for the scope of this paragraph) denote the distance of the control parameter to its critical point, for example $\alpha = |p - p_\mathrm{c}|$ for DP. Then, beyond a certain length scale that is much larger than the characteristic scale of microscopic interaction, rescaling

- the difference of the control parameter to its critical value by $\alpha \to \lambda\alpha$
- all times with $t \to \lambda^{-\nu_{\|}} t$
- all lengths by $r \to \lambda^{-\nu_\perp} r$
- and the order parameter with $f \to \lambda^{\beta} f$

where $\lambda > 1$ is a scaling factor, leaves the physics unchanged (see fig. 2.9). Note that this is not strictly speaking a symmetry (like translational-, rotational- or guage-symmetry are) as one cannot zoom-in all the way to the microscopic scale while keeping the qualitative behaviour. Hence (under the appropriate precise definition of what

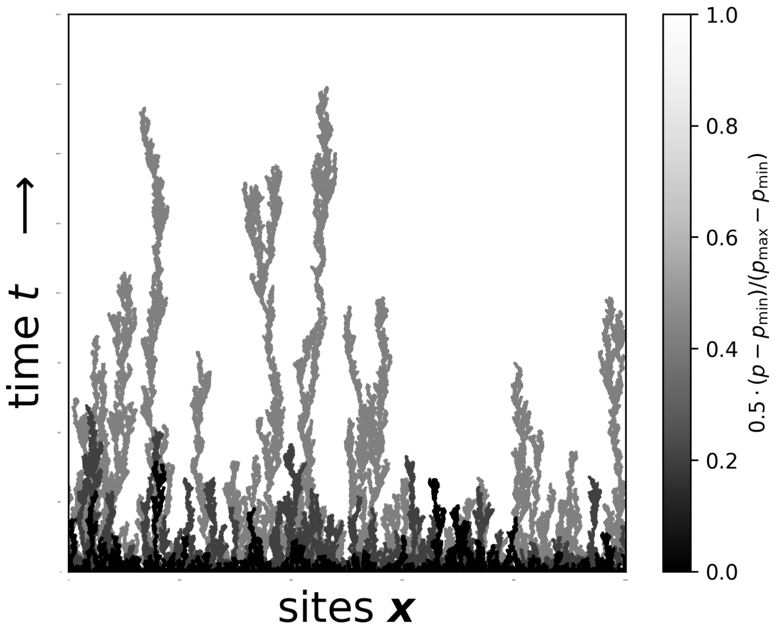

Figure 2.6: Depiction of a few (1+1)-dimensional DP realizations, showing the growth of the reach of wetness in subcritical DP as $p \uparrow p_c$: the lighter the shading, the closer p is to p_c.

it means for the physics to be qualitatively the same) these rescaling operations, while not constituting a group, are a *semi-group*, thanks to factoring

$$(\lambda_1 \lambda_2)^{(\cdots)} = \lambda_1^{(\cdots)} \lambda_2^{(\cdots)} \tag{2.23}$$

of power laws. $\nu_\parallel$, $\nu_\perp$ and β are not by accident named like the exponents of the power laws listed at the beginning of section 2.2.1; they are the same quantities and referred to as *critical exponents* (Janssen and Täuber 2005, sec. 2.3).

At criticality, not only the fundamental dimensions of time and space or control- and order-parameter, but all kinds observables scale. Their exponents can, by dimensional-analysis-like arguments, be linked to a set of fundamental exponents; thermal equilibrium transitions, for example, come with only two independent exponents β and ν (Cheung 2023, sec. 3.1) and absorbing state transitions, for example, only come with four independent exponents β, β', $\nu_\perp$, and $\nu_\parallel$ (Lubeck 2004, A.2 Scaling); β' has not appeared in this text before: it is associated with the *causal* response of the critical absorbing state system to perturbation (like manually provoking overlaps in random organization or artificially placing a wet site in directed percolation).

Any list of examples I could give would not do the ubiquity of critical behaviour justice. Percolation foreshadows the relevance of this body of theory to various phenomena involving large networks (Coupette 2023). Directed percolation is built on a directed network; to give at least one example for percolation on an undirected network, I want to mention *isotropic percolation* (IP). While I am more frequently referencing directed percolation (because of its similarities to random organization) IP is actually the typical example for a percolation problem on a lattice. As the name suggests, bonds have no directedness in IP. Bonds to nearest neighbours are randomly and independently passable (and hence connected) or impassable with some probability p. The challenge now consists of working out for what probabilities p there will be a large-scale (infinitely extended) connected component and how the system behaves. While this formulation of the problem does not immediately reveal this connection, isotropic percolation can be mapped to a limit of an equilibrium system, the so called Potts-model, that generalizes Ising model (Obukhov 1980), though this is of no further importance here besides clarifying that this problem is approachable with equilibrium physics, in contrast to directed percolation (Jensen 1999). Some aspects of its behaviour are quickly deduced, very similarly to directed percolation: it is clear, that at $p = 0$ there will not even be a local connection, while at $p = 1$ all bonds are open, making the system one single connected component. It is also clear that increasing p will only open up more bonds on average and hence can only increase the probability P_∞ for one infinitely extended connected component. The system is also trivially solved in a one-dimensional lattice (i.e. a line), because, starting from any arbitrary origin, the probability for connection to a site that is n bonds away is just p^n, which vanishes for all $p < 1$ as we go to infinite extension $n \to \infty$, making the behaviour uninterestingly $P_\infty = 0$ for $p < 1$ and $P_\infty = 1$ for $p = 1$. Dimension $d = 2$ is the first interesting d for isotropic percolation on a square/(hyper-)cubic lattice $\mathbb{Z}^d$ where, in contrast to $d = 1$, there are arbitrarily many paths connecting any two lattice sites, with paths partly coinciding and paths of size n being passable with probability p^n (exponentially less likely to be open the longer the path); this interplay between dampening of path probability with length and the ubiquity of paths results in a non-trivial critical bond probability $0 < p_\mathrm{c} < 1$ below which $P_\infty = 0$ and above which $P_\infty > 0$, monotonically increasing with p. The probability P_∞ serves as the order-parameter of the IP transition and goes to zero as $p \downarrow p_\mathrm{c}$ with a power law $P_\infty \sim |p - p_\mathrm{c}|^{\beta_\mathrm{IP}}$. Furthermore, the expected diameter of connected patches of the lattice serves as a correlation length and diverges with a power law $\xi \sim |p - p_\mathrm{c}|^\nu$ towards the critical point, beyond which one may reasonably expect infinitely large connected components (see fig. 2.7), leaving the system scale-invariant at the critical point $p = p_\mathrm{c}$ (a familiar sounding motif at this point in the text).

Universality Classes Scale invariance has a dramatic consequence for systems displaying these transitions: the microscopic details of the dynamics/energetics, which happen on scales far below the (diverging) correlation lengths, are not relevant to the qualitative behaviour of the system. Instead, very unspecific properties of the physical problems in question, like the existence of absorbing states in directed percolation problems and random organization or the symmetries of the problem in question, play a role. With this little dependence on microscopic details, problems fall into only a handful of classes, the so called *universality-classes*, which unify into a common theory at the critical point. Thanks to the description by a free energy function(al), thermal equilibrium systems can, in principle, be analysed with generally applicable, established theoretical methods (Hinrichsen 2000, introduction) and one can satisfactorily define what constitutes “the same qualitative behaviour” and hence unambiguously discern what universality class a system belongs to: at criticality, free energy is

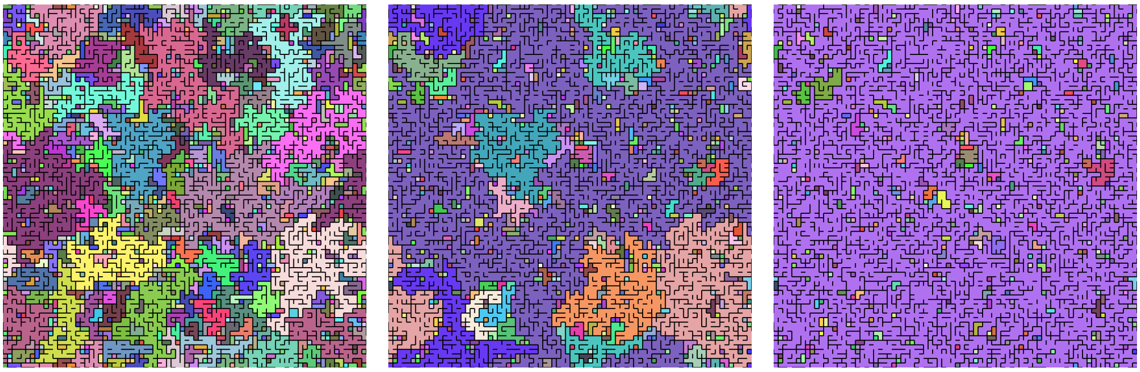

(a) $p = 45\%$ (b) $p = 50\%$ (c) $p = 55\%$

Figure 2.7: Visualization of different regimes of isotropic percolation on a square lattice $\mathbb{Z}^2$. Bonds are open with probability p. Open walls correspond to open bonds, closed walls to closed bonds and connected components have the same colour. $p = 45\%$ and $p = 55\%$ have a characteristic size (related to the correlation length ξ) for connected regions and disconnected regions respectively, while $p = 50\%$ is critical and hence scale invariant; the system will (on larger scales) have no characteristic lengthscale, making it look qualitatively the same across scales, with connected components of all sizes appearing with reasonable likelihood. Visualizations are courtesy of Chandan Relekar, created with their online tool found under `https://visualize-it.github.io/bernoulli_percolation/simulation.html` (last visited on 01.11.2025 at 21:16)

dominated by a singular, homogeneous[11] contribution, which, by the circumstance of how little freedom this leaves to the closed form of the contribution, is (up to rescaling of physical quantities) universal to the entire universality class. Derivatives of homogeneous functions are again homogeneous and also (up to rescaling of quantities) universal, aptly called *universal scaling functions* (Lubeck 2004, sec. 1.2); fig. 2.8 depicts two examples for those.

Far-from-equilibrium problems do not have such a general framework. And indeed, what does or does not constitute a universality class far from equilibrium is not yet established (Lubeck 2004, introduction, Hinrichsen 2000, introduction). Authors judge mainly by the critical exponents. Field theorists in particular tend to also go by symmetry arguments and methods like the analysis of fixed points of *renormalization-flow* also known as the *renormalization (semi)-group procedure* (which I briefly sketch in section 2.2.4), however also often to the end of computing critical exponents. Interestingly, the scale invariance of far-from-equilibrium continuous transitions also appears to lead to the existence of universal scaling functions; Lubeck (2004) calls for the determination and comparison of these when trying to determine a transition's universality class. Hence, it is, pedantically speaking, still questionable whether far-from-equilibrium phenomena should group into universality classes.

In percolation on directed lattices, random organization and many other systems,

---

[11] A function $f(x_1, \dots, x_n)$ is called homogeneous, if for any $\lambda > 0$ scaling it has the effect of scaling all arguments by some power of λ, mathematically expressed by $\lambda \cdot f(x_1, \dots, x_n) = f(\lambda^{p_1} x_1, \dots, \lambda^{p_n} x_n)$ (compare Lubeck 2004, eq. 1.12). Simple example are multinomials like $f(x, y, z) = x^2 y z^4$ or more generally power-laws, say $f(x, y, z) = x^{-1.23} y^{3.44} z^{-4.52}$

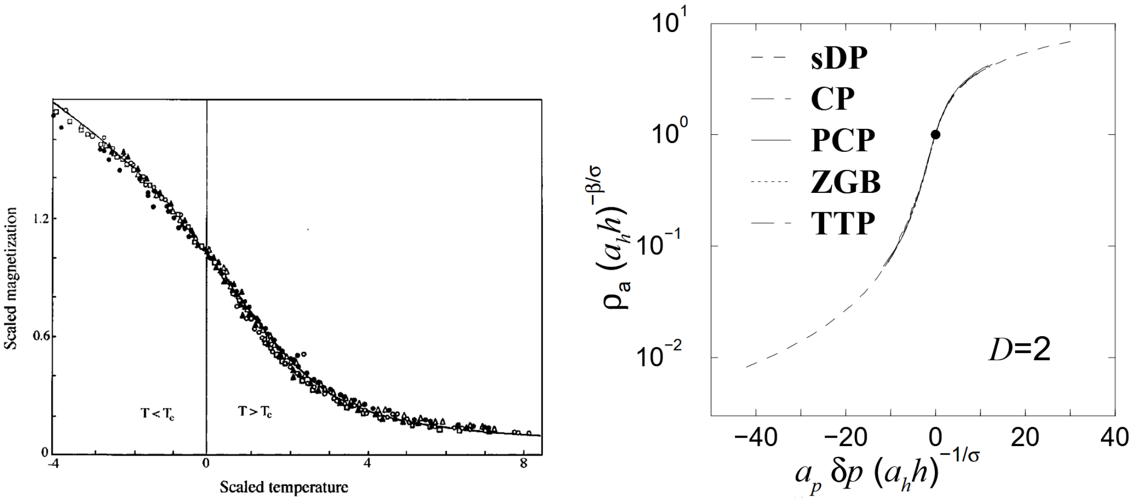

(a) Plot from Lubeck (2004, fig. 4) depicting the dependence of magnetization on temperature for various magnetic materials of the "three-dimensional Heisenberg" universality class)

(b) Plot from Lubeck (2004, fig. 24) depicting the dependence of the (steady-state) order parameter on the control parameter of various dynamical phase transitions in the DP universality class (*D* denoting dimensionality)

Figure 2.8: Example depictions of universal scaling functions, both in (fig. 2.8a) and far from equilibrium (fig. 2.8b)

however, literature is satisfied with the assumption that scaling applies (which is then referred to as *assuming scaling* or the *scaling hypothesis*) and for good reason: both empirical evidence and successful theoretical frameworks point towards the applicability of the concept and both critical exponents and universal scaling functions (fig. 2.8b shows as an example from the *universality class DP*, into which percolation on directed lattices falls). They have been determined for many far from equilibrium transitions by assuming the scaling hypothesis holds.

As a closing remark: universality classes can group together models with wildly different physical backgrounds. For example, directed percolation problems can be found in same universality class as a certain pre-quark-model theory for the scattering of hadrons (Reggeon field theory) at high-energy and low-momentum-transfer with the (square root of the) total scattering cross section $\sqrt{\sigma_{\text{tot}}}$ as the order parameter and the so called Pomeron intercept α_P (a constant of the theory) as (one possible) control parameter (Grassberger and Sundermeyer 1978; Cardy and Sugar 1980). The DP class also encompasses the onset of turbulence in pipe-flow, where the steady-state density of turbulent puffs ρ_∞ is the order-parameter and Reynolds-number Re the control parameter. Although the list of DP transitions is long, it is believed that the phase transition in random organization is not amongst them (see section 3.2.2 for the likely reasons and references).

2.2.2 Large-Scale Field Theories for Dynamical Transitions

As explained in section 2.1.1, Landau-Ginzburg Theory is an important means by which critical behaviour is studied without troubling oneself with the very intricate details of any given system displaying the transition under study. It relies on defining

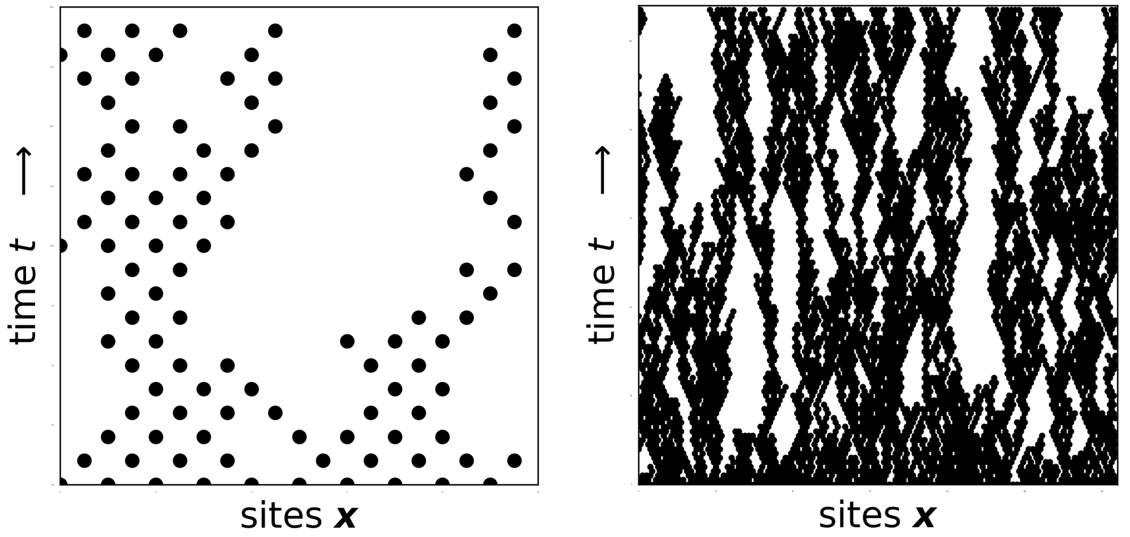

(a) 10 spatial sites (b) about 100 spatial sites

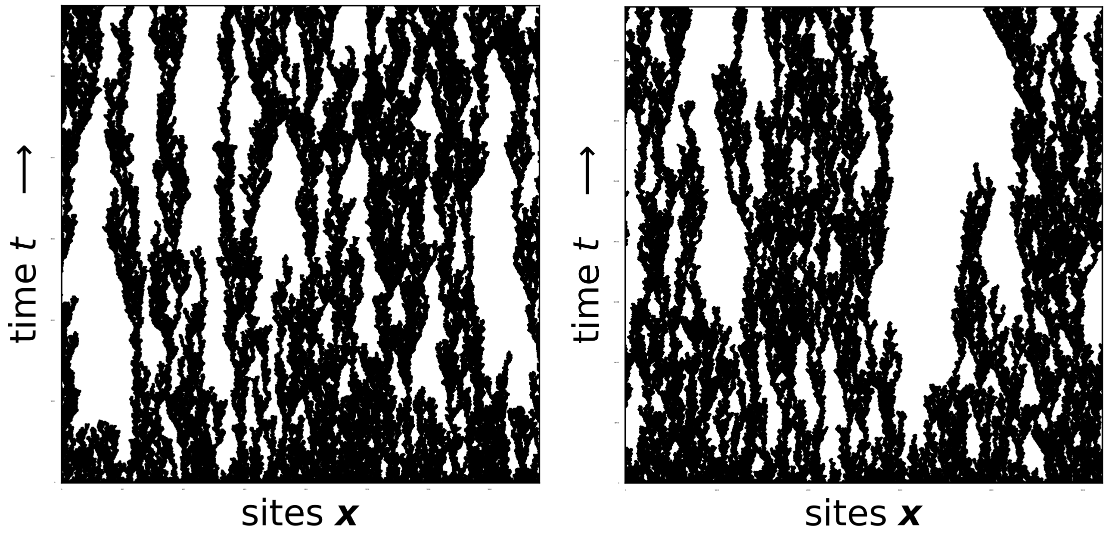

(c) about 1000 spatial sites (d) about 5000 spatial sites

Figure 2.9: Snapshots of critical directed percolation across scales. Except for the full microscopic zoom-in fig. 2.9a, they are hard to even tell apart (probably only with the hint that these are different scales). The largest-scale snapshots fig. 2.9c and fig. 2.9d make it challenging to tell that there are lattice sites at all: the boundaries of the spreading wetness, while looking rough, seem to be fractal curves in continuous space and time.

a suitable Landau-Ginzburg free energy functional of the order parameter and understanding its singular, scale-invariant contribution at the critical point (Lubeck 2004, sec. 1.2)

One may now ask, whether a similar approach is available for random organization, percolation on directed lattices and other systems with dynamical phase transitions. After all, the idea of focusing only on large-scale processes could reasonably be expected to apply to them too, as they evidently also experience scaling, including the divergence in correlation lengths/times. As mentioned in section 2.1.2, systems far from equilibrium are not describable by Boltzmann-Gibbs distributions. However, it does not sound far-fetched to claim, that one can in principle consider the ensemble of all possible realizations $\{R(t)\}$ of, say, a random organization or directed percolation problem, approximate the weight $P[R(t)]$ with which any given realization $R(t)$ contributes (say, by counting all micro-scale time-evolutions giving rise to $R(t)$) and then normalizing by something not unlike a partition function $Z = \int \mathcal{D}R\, P[R(t)]$ to compute averages $\langle \mathscr{A} \rangle = (1/z) \int \mathcal{D}R\, \mathscr{A}[R(t)]\, P[R(t)]$.

The problem with this idea is, that we have no immediate means like the Gibbs-distribution and Ginzbuzrg-Landau free energy at hand. It is easy to find systems displaying a dynamical transition with hardly any rigorous treatments available, let alone a comprehensive solution, directed percolation and random organization being amongst them.

Recall however (section 2.2.1) that around the critical point a lot of smaller scale detail can be safely ignored in understanding the essential, universal physics of the transition. In fact, it turns out that literature has been proposing (nominally) coarse-grained stochastic continuum theories of the order-parameters of various transitions and has been successfully subjecting them to the same sort of treatment as Landau-Ginzburg- or quantum field theories, drawing from expertise in both fields of study (Hinrichsen 2000; Lubeck 2004; Ódor 2004; Janssen and Täuber 2005).

Coarse-Graining Example To make understandable at least one way that one may arrive at such a continuum theory before presenting random-organization-adjacent theories in chapter 3, I want to present a line of thought heavily leaning on Janssen and Täuber (2005, sec. 2.1) on how to arrive at one for DP while only incorporating very general properties of the model; on top of recounting the argument, I try to directly incorporate the spatial dependences, which the source material does not do for simplicity; for a waterproof account, I refer the reader to Janssen and Täuber (2005, sec. 2.1).

As noted in section 2.1.2, directed percolation can be understood as a Markov chain, where $\mathscr{W}(\boldsymbol{r}, t + \mathrm{d}t)$ (see eq. (2.14)) one time-step $\mathrm{d}t$ into the future are determined by an equation of the form

$$\mathscr{W}(\boldsymbol{r}, t + \mathrm{d}t) - \mathscr{W}(\boldsymbol{r}, t) = \mathscr{V}[\mathscr{W}(\boldsymbol{x}, t)](\boldsymbol{r})\, \mathrm{d}t\, \mathrm{d}^d r \tag{2.24}$$

where $\mathrm{d}^d r$ is an arbitrarily chosen but very small volume of a lattice site (needed for the continuum limit later) and where $\mathscr{V}[f(\boldsymbol{x})]$ is a random functional of the spatial dependence of $\mathscr{W}(\boldsymbol{r}, t)$, encoding how the number of wet sites changes from one layer t to the next $(t + \mathrm{d}t)$. The notation here already anticipates a later formal continuum limit $\mathrm{d}t \to 0$ (note that $(t + 1)$ from eq. (2.14) has been replaced by $(t + \mathrm{d}t)$). The distribution of its values is in principle given by the structure of the lattice and the bond probability p via eq. (2.14), but we will never specify its exact form. That $\mathcal{V}$ is a functional of the $\mathcal{W}(\boldsymbol{r},t)$ only and not of the entire spatio-temporal course of $\mathcal{W}(\boldsymbol{r},t)$ is necessary to not violate that percolation on directed lattices can be understood as a Markov chain. We clarify this further in notation by introducing the shorthand

$$\mathcal{V}(\boldsymbol{r},t) := \mathcal{V}[\mathcal{W}(\boldsymbol{x},t)](\boldsymbol{r}) := \mathcal{V}[f(\boldsymbol{x})](\boldsymbol{r})\Big|_{f(\boldsymbol{x})\equiv\mathcal{W}(\boldsymbol{x},t)} \tag{2.25}$$

The Markov chain interpretation also makes it necessary that $\mathcal{V}(\boldsymbol{r},t)$ and $\mathcal{V}(\boldsymbol{r}',t')$ must be statistically independent if $t \neq t'$. We now seek to neglect a lot of detail about $\mathcal{V}[\mathcal{W}(\boldsymbol{x},t)]$ that is not essential to the critical behaviour of the model[12].

Imagine now an ensemble of all mathematically possible values $W(\boldsymbol{r},t)$ for the random variable $\mathcal{W}(\boldsymbol{r},t)$, in the sense of all possible combinations of declaring the sites $(\boldsymbol{r},t)$ wet and not wet, no matter whether it constitutes a valid evolution of percolation on a directed lattice as dictated by eq. (2.14). The weight with which any of these realizations $W(\boldsymbol{r},t)$ contributes to the ensemble of realizations is obtained by turning eq. (2.24) into a constraint

$$P[W(\boldsymbol{r},t)] \sim \prod_{\boldsymbol{r},t}\sum_{V_t}\delta\Big(W(\boldsymbol{r},t+\mathrm{d}t) - W(\boldsymbol{r},t) - V_t[W(\boldsymbol{x},t)](\boldsymbol{r})\,\mathrm{d}t\,\mathrm{d}^d r\Big) \tag{2.26}$$

where a variable V_t has taken the role of the previous random variable $\mathcal{V}$ and, for every time t, runs over all possible combinations of open and closed bonds. It should be read as counting, by means of a product of Dirac-deltas, all realization of V_t in which eq. (2.24) holds true for $W(\boldsymbol{r},t)$. To get this in a form resembling the expression for the weight of a Landau-Ginzburg order parameter (see eq. (2.7)), we use the Fourier-transform a identity

$$\delta(x) = \int_{-\infty}^{+\infty}\mathrm{d}f\, e^{2\pi i f x} = \int_{-i\,\infty}^{+i\,\infty}\frac{\mathrm{d}s}{2\pi i}\exp(sx) \tag{2.27}$$

replacing every factor in the product over all $(\boldsymbol{r},t)$ by such a Fourier integral

$$\begin{aligned}
&P[W(\boldsymbol{r},t)]\\
&\sim \prod_{\boldsymbol{r},t}\sum_{V_t}\int_{-i\,\infty}^{+i\,\infty}\frac{\mathrm{d}\tilde{w}(\boldsymbol{r},t)}{2\pi i}\exp\Big(\tilde{w}(\boldsymbol{r},t)\left(W(\boldsymbol{r},t+\mathrm{d}t) - W(\boldsymbol{r},t) - V_t[W(\boldsymbol{x},t)](\boldsymbol{r})\,\mathrm{d}t\,\mathrm{d}^d r\right)\Big)\\
&= \int \mathcal{D}\tilde{w}\,\mathcal{D}V\,\exp\Big(-\sum_{\boldsymbol{r},t}\tilde{w}(\boldsymbol{r},t)\,V_t[W(\boldsymbol{x},t)](\boldsymbol{r})\,\mathrm{d}t\,\mathrm{d}^d r\Big)\\
&\qquad\qquad\times\exp\Big(\sum_{\boldsymbol{r},t}\tilde{w}(\boldsymbol{r},t)\big(W(\boldsymbol{r},t+\mathrm{d}t) - W(\boldsymbol{r},t)\big)\Big)
\end{aligned} \tag{2.28}$$

where $\tilde{w}(\boldsymbol{r},t)$ labels all the integration dummy variables from inserting eq. (2.26) and the notation $\int\mathcal{D}V$ stands for

$$\int \mathcal{D}V\,(\cdots) = \prod_t\sum_{V_t}(\cdots) \tag{2.29}$$

---

[12] I will briefly mention how one could judge the relevance of terms to critical behaviour in section 2.2.4, but these reasons are of no importance to getting accustomed to the idea of using field-theory to model stochastic processes in space and time

and

$$\int \mathcal{D}\tilde{w}\;(\cdots) = \prod_{\boldsymbol{r},t} \int_{-i\,\infty}^{+i\,\infty} \frac{\mathrm{d}\tilde{w}(\boldsymbol{r},t)}{2\pi i}\;(\cdots) \tag{2.30}$$

Literature refers to the $\tilde{w}(\boldsymbol{r},t)$ as *response fields*. Because their introduction is attributed to Martin, Siggia, and Rose (1973), they are regularly called *MSR response fields*. We now average out the rapid degrees of freedom by (1) implicitly choosing a continuum-coarse graining $w(\boldsymbol{r},t)\,\mathrm{d}^d r$ for $W(\boldsymbol{r},t)$ and (2) integrating out V_t. We obtain a weight for the coarse-grained wet-site field $w(\boldsymbol{r},t)$

$$\begin{aligned}
&P[w(\boldsymbol{r},t)]\\
&\quad= \langle P[W(\boldsymbol{r},t)]\rangle_{\text{rapid}}\\
&\quad\sim \int \mathcal{D}\tilde{w}\,\Big\langle \exp\Big(-\sum_{\boldsymbol{r},t} \tilde{w}(\boldsymbol{r},t)\cdot V_t[W(\boldsymbol{x},t)](\boldsymbol{r})\,\mathrm{d}t\,\mathrm{d}^d r\Big)\\
&\qquad\qquad\qquad \times \exp\Big(\sum_{\boldsymbol{r},t} \tilde{w}(\boldsymbol{r},t)\big(W(\boldsymbol{r},t+\mathrm{d}t) - W(\boldsymbol{r},t)\big)\Big)\Big\rangle_{\text{rapid}}\\
&\quad= \int \mathcal{D}\tilde{w}\,\prod_{\boldsymbol{r},t}\Big\langle \exp\Big(-\tilde{w}(\boldsymbol{r},t)\cdot V_t[W(\boldsymbol{x},t)](\boldsymbol{r})\,\mathrm{d}t\,\mathrm{d}^d r\Big)\Big\rangle_{\text{rapid}}\\
&\qquad\qquad \times \Big\langle \exp\Big(\sum_{\boldsymbol{r},t} \tilde{w}(\boldsymbol{r},t)\big(W(\boldsymbol{r},t+\mathrm{d}t) - W(\boldsymbol{r},t)\big)\Big)\Big\rangle_{\text{rapid}}
\end{aligned} \tag{2.31}$$

where the last two equal signs implicitly *defines* how the coarse-graining of $W(\boldsymbol{r},t)$ to $w(\boldsymbol{r},t)\,\mathrm{d}^d r$ works *exactly*, that is, conveniently so that we could (a) factorize the rapid-degree-of-freedom average $\langle\cdots\rangle_{\text{rapid}}$ as seen in eq. (2.31) and (b) replace $W(\boldsymbol{r},t)$ by $w(\boldsymbol{r},t)\,\mathrm{d}^d r$ in the exponentials, amounting to

$$\begin{aligned}
&\exp\Big(\sum_{\boldsymbol{r},t} \mathrm{d}^d r\;\tilde{w}(\boldsymbol{r},t)\big(w(\boldsymbol{r},t+\mathrm{d}t) - w(\boldsymbol{r},t)\big)\Big)\\
&\qquad\qquad \overset{!}{:=} \Big\langle \exp\Big(\sum_{\boldsymbol{r},t} \tilde{w}(\boldsymbol{r},t)\big(W(\boldsymbol{r},t+\mathrm{d}t) - W(\boldsymbol{r},t)\big)\Big)\Big\rangle_{\text{rapid}}
\end{aligned} \tag{2.32}$$

We make use of the concept of a *cumulant distribution function*[13]

$$\begin{aligned}
&\exp\Big(-\sum_{n=1}^{\infty} \frac{1}{n!} K_n[w(\boldsymbol{x},t)]\,\mathrm{d}t\cdot\tilde{w}(\boldsymbol{r},t)^n\Big)\\
&\qquad\qquad \overset{!}{:=} \Big\langle \exp\Big(-\tilde{w}(\boldsymbol{r},t)\cdot V_t[W(\boldsymbol{x},t)](\boldsymbol{r})\,\mathrm{d}t\,\mathrm{d}^d r\Big)\Big\rangle_{\text{rapid}}
\end{aligned} \tag{2.33}$$

where $K_n[w(\boldsymbol{x},t)]$ are the cumulants of $V_t[W(\boldsymbol{x},\boldsymbol{t})]$ with respect to the rapid degrees of freedom (still depending on the large-scale degrees of freedom $w(\boldsymbol{x},t)$), now resulting

---

[13] Reminder from statistics: the cumulants K_n of a random variable $\mathcal{X}$ are related to its moments $\langle\mathcal{X}^n\rangle$: the first cumulant is the mean $K_1 = \langle\mathcal{X}\rangle$ while the second cumulant is the variance $K_2 = \langle(\mathcal{X} - \langle\mathcal{X}\rangle)^2\rangle$; all higher cumulants are comprised of factors of centred moments $(\mathcal{X} - \langle\mathcal{X}\rangle)^k$. They are generated by $\log\langle\exp(s\mathcal{X})\rangle$ in the sense that they are its Taylor-coefficients $\log\langle\exp(s\mathcal{X})\rangle = \sum_{n=1}^{\infty} ({}^{K_n}\!/_{n!})\, s^n$

in

$$P[w(\boldsymbol{r},t)] \sim \int \mathcal{D}\tilde{w}\ \exp\Big(\sum_{\boldsymbol{r},t} \mathrm{d}^d r\, \tilde{w}(\boldsymbol{r},t) \Big(w(\boldsymbol{r},t+\mathrm{d}t) - w(\boldsymbol{r},t) - \sum_{n=1}^{\infty} \frac{1}{n!} K_n[w(\boldsymbol{x},t)]\, \mathrm{d}t\ \tilde{w}(\boldsymbol{r},t)^n\Big) \tag{2.34}$$

Next, $\mathrm{d}^d r$ and $\mathrm{d}t$ are very small compared to physically relevant scales at criticality, justifying the continuum limits

$$\begin{aligned} w(\boldsymbol{r},t+\mathrm{d}t) - w(\boldsymbol{r},t) &\approx \frac{\partial w(\boldsymbol{r},t)}{\partial t}\,\mathrm{d}t \\ \sum_{\boldsymbol{r},t} \mathrm{d}^d r\,\mathrm{d}t\,(\cdots) &\approx \int \mathrm{d}^d r\,\mathrm{d}t\,(\cdots) \end{aligned} \tag{2.35}$$

This leads to an expression of the weight of $w(\boldsymbol{r},t)$, now understood as an order parameter depending continuously on space and time

$$P[w(\boldsymbol{r},t)] \sim \int \mathcal{D}\tilde{w}\ \exp\left(\int \mathrm{d}^d r\,\mathrm{d}t \left(\tilde{w}(\boldsymbol{r},t)\frac{\partial}{\partial t} w(\boldsymbol{r},t) - \sum_{n=1}^{\infty} \frac{1}{n!} K_n[w(\boldsymbol{x},t)] \cdot \tilde{w}(\boldsymbol{r},t)^n \right)\right) \tag{2.36}$$

where $\int \mathcal{D}\tilde{w}$ is now to be understood as the path integral over all possible spatio-temporal evolutions of the response field. We may invoke the locality of interactions at criticality again to assume that the cumulants are local functionals $K_n[w(\boldsymbol{x},t)] = \int \mathrm{d}^d x\, \kappa_n(w(\boldsymbol{x},t), \nabla w(\boldsymbol{x},t), \dots)$. Since DP is a continuous transition, towards criticality (from above $p \downarrow p_\mathrm{c}$) the values taken up by the order parameter $w(\boldsymbol{r},t)$ are very small and one may expand in it. This expansion is informed by the fact that DP has an absorbing state: at $w(\boldsymbol{r}) \equiv 0$, all cumulants need to vanish $K_n[0] = 0$, since non-vanishing cumulants means non-vanishing fluctuations, which would cause w fluctuate out of $w \equiv 0$ and thus contradict the assertion that $w \equiv 0$ is absorbing; hence $K_n[w] = \mathcal{O}(w)$. Neglecting *irrelevant* (in a renormalization-flow sense, see section 2.2.4 for an explanation of the term) higher order terms leaves

$$P[w(\boldsymbol{r},t)] = \frac{1}{Z} \int \mathcal{D}\tilde{w}\ \exp\big(S[w,\tilde{w}]\big) \tag{2.37}$$

with

$$Z = \int \mathcal{D}w\,\mathcal{D}\tilde{w}\ \exp\big(S[w,\tilde{w}]\big) \tag{2.38}$$

and

$$S[w,\tilde{w}] = \int \mathrm{d}^d r\,\mathrm{d}t \left(\underbrace{\tilde{w}\left(\frac{\partial}{\partial t} - D\nabla^2 - \alpha\right) w}_{\text{propagation and multiplication of wet sites}} + \underbrace{\frac{1}{2} g \left(\tilde{w}^2 w + \tilde{w} w^2\right)}_{\text{reduction of sites by dead-ends and merging}} \right) \tag{2.39}$$

(for this form, compare not only Janssen and Täuber (2005, sec 2.1), but also the earlier Janssen, Kutbay, and Oerding (1999) and Adzhemyan et al. (2023)).

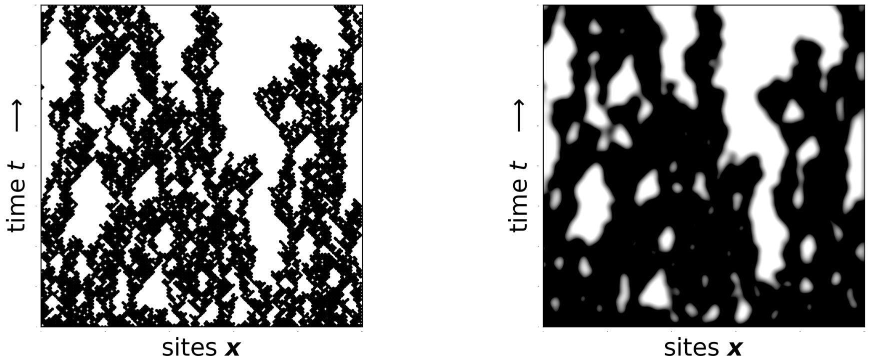

(a) microscopically resolved wet sites $W(\boldsymbol{x}, t)$

(b) coarse grained continuous field $w(\boldsymbol{x}, t)$

Figure 2.10: Conceptual depiction of coarse graining of a discrete set of wet sites, as indicated by $W(\boldsymbol{x}, t)$, to a continuous field $w(\boldsymbol{x}, t)$, loosely quantifying the density of wet sites

Meaning of Response Fields The response field $\tilde{w}(\boldsymbol{r}, t)$, while being introduced as an auxiliary variable to rewrite the product of Dirac-deltas in eq. (2.26), can be involved in correlators to produce very meaningful physical quantities. One differentiates between the two-point function of the order parameter $\langle w(\boldsymbol{r}, t) w(\boldsymbol{r}', t')\rangle_{\mathrm{c}}$ already familiar from Landau-Ginzburg theory and the *response function* or *propagator* $\langle w(\boldsymbol{r}, t)\tilde{w}(\boldsymbol{r}', t')\rangle_{\mathrm{c}}$. In equilibrium, the information contained in correlators of the order parameter does not differentiate between cause and effect. Behaviour at $\boldsymbol{r}_1$ does not "cause" behaviour at $\boldsymbol{r}_2$ et vice versa, they are just correlated. When time gets involved, however, there is causality: the wet sites further down a cone of propagation in DP (see fig. 2.6) are conditioned on the existence of the wet site that seeded it, but not the other way around (compare Wiese 2020, sec. 3.4 MSR formalism).

Brief Summary A brief summary is in order: starting out from stochastic dynamics for percolation on directed lattices (which one may replace with other Markovian dynamics, such as random organization) one can motivate a time- and space-continuous theory of the behaviour around the critical point. This theory is given by a dynamic functional that plays a role analogous to action in quantum field theory and Landau-Ginzburg free energy. Novel compared to the latter is the introduction of response fields, correlators of which encode the causal response of the system to perturbations; in particular, the two-point correlator $\langle w(\boldsymbol{r}, t)\tilde{w}(\boldsymbol{r}', t')\rangle_{\mathrm{c}}$ is analogous to the propagator of a quantum field.

2.2.3 Mean Field Theory

Depending on what exactly one seeks to understand about a phase transition, it is not always necessary to face the full complexity of a model. Take as an example the saddle-point approximation of the Landau-Ginzburg theory of the Ising magnet presented in section 2.1.1, that could be analysed in barely a page of computation and still displayed both a phase transition from vanishing to spontaneous magnetization and even less obvious phenomena like domain walls. It turns out that there is a system to establishing such approximations.

To arrive at this system, it is best to revisit the interpretation of the saddle-point approximation: given a Landau-Ginzuburg free energy $E[f]$ of some order parameter $f(\boldsymbol{r})$ and the associated partition function $Z = \int \mathcal{D}f \, \exp(-E[f]/k_\mathrm{B}T)$, the realizations $f_\mathrm{s}(\boldsymbol{r})$ minimizing E are referred to as the saddle-points of the functional. When one can assume that $E[f_\mathrm{s}(\boldsymbol{r})]$ is so much lower than dissimilar configurations $f(\boldsymbol{r})$ that other contributions can be neglected the saddle-point approximation is valid. An important consequence of only looking at saddle-points is that one *neglects all fluctuations*, since the noise around saddle-point behaviour f_s comes precisely from the variation of $f(\boldsymbol{r})$ in the realizations close to the f_s which get neglected.

In field-theory, the saddle-point approximation, is used synonymously with the term *mean-field theory* (Tong 2017, sec. 2.2), where the latter is usually characterized as an approximation where fluctuations in the order parameter can be neglected. Whether or not fluctuations play a role at a macroscopic scale depends on dimensionality d of the system experiencing the phase transition in question, since volumes will scale with L^d (where L the characteristic extension of a volume) while fluctuations around the average value of the order parameter in said volume may very well grow slower than that. This is loosely speaking the reason why transitions have a so called *upper critical dimension* d_c, above which fluctuations $\langle f^2 \rangle \ll \langle f \rangle^2$ are negligible on large scales and the mean-field theory of the transition yields correct critical behaviour (Cheung 2023, sec. 2.8; Tong 2017, sec. 2.2.4). The existence of upper critical dimensions also paves the way for a method of obtaining mean-field theories that may otherwise seem like a very exotic trick: taking the dimensionality of a model to infinity $d \to \infty$ and expanding in $(1/d)$ as a small parameter.

For completeness it should be mentioned that transitions can also exhibit *lower critical dimensions* d_l below which fluctuations destroy any long-range order. This is for example the case when free energy has (sufficiently) short ranged interactions and the order parameter has a continuous symmetry, that is when the transformations that one may apply to f (and still leave the physics unchanged) form a continuous group (for example orthogonal transformations $O(d)$). These fall into the scope of the famous *Mermin-Wagner theorem*, which rules out the existence of long-range order for these theories in dimensions $d \leq 2$ (Tong 2017, sec. 4.2.1).

Mean Field DP To get back on track with absorbing state transitions, consider the saddle-point approximation of DP by only considering the contribution of the saddle-points $w_\mathrm{s}(\boldsymbol{r}, t), \tilde{w}_\mathrm{s}(\boldsymbol{r}, t)$ to eq. (2.38). We determine $w_\mathrm{s}(\boldsymbol{r}, t)$ by the variation $\delta S[w, \tilde{w}]$ with respect to variations of the order parameter $\delta w(\boldsymbol{r}, t)$ and the response field $\delta \tilde{w}(\boldsymbol{r}, t)$; those will only have a solution that is stable, spatially homogeneous and stationary if the saddle-point response field vanishes $\tilde{w} \equiv 0$ (compare Janssen and Täuber 2005, eqs. 22a and 22b), at which point one gets

$$\frac{\partial w(\boldsymbol{r}, t)}{\partial t} = D\nabla^2 w(\boldsymbol{r}, t) + \alpha \, w(\boldsymbol{r}, t) - \frac{1}{2} g \, w(\boldsymbol{r}, t)^2 \tag{2.40}$$

(compare Adzhemyan et al. 2023, eq. 9), where one may refer to $w(\boldsymbol{r}, t)$ as the mean-field approximation to the density of wet sites. One can see that three crucial effects are being respected: the diffusion of wetness in space over time with $D\nabla^2 w$, as well

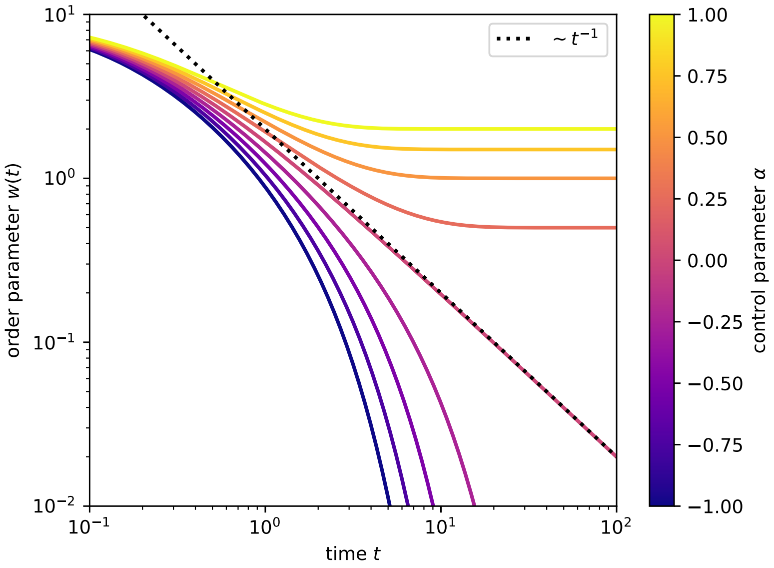

Figure 2.11: Plot of the time evolution eq. (2.43) of the order parameter of the spatially homogeneous mean-field theory of DP, as defined by eq. (2.40) with $\nabla w \equiv 0$, for various values of the control parameter α. At $\alpha = 0$ the system is critical and asymptotically follows the power law $w(t) \sim t^{-1}$, while plateauing to some $w_\infty > 0$ at $\alpha > 0$ and decaying to zero for $\alpha < 0$

as the proliferation $+\alpha w$ and decay $-(1/2)gw^2$ of wetness over time[14].

To demonstrate the value of mean-field theory for understanding DP transitions[15] I want to briefly elaborate the case of a spatially homogeneous system $\nabla w \equiv 0$. In this case, eq. (2.40) simplifies to the ordinary differential equation

$$\frac{\partial w(t)}{\partial t} = \alpha w(t) - \frac{1}{2} g\, w(t)^2 \tag{2.41}$$

which is trivially solved by separation of variables

$$\begin{aligned} \int_{w(0)}^{w(t)} \frac{\mathrm{d}w}{\alpha\, w - (1/2 g\, w^2)} &= \int_0^t \mathrm{d}t' \\ \overset{u:=w-(g/\alpha)}{\Longleftrightarrow} \int_{w(0)-(\alpha/g)}^{w(t)-(\alpha/g)} \frac{\mathrm{d}u}{(\alpha/g)^2 - u^2} &= \frac{g}{2} t \\ \Longleftrightarrow \int_{w(0)-(\alpha/g)}^{w(t)-(\alpha/g)} \left(\frac{\mathrm{d}u}{1 + (g/\alpha)u} + \frac{\mathrm{d}u}{1 - (g/\alpha)u} \right) &= \alpha t \end{aligned} \tag{2.42}$$

which reveals that already at this level of approximation, the model reflects all expected regimes of behaviour:

---

[14] One may wonder why the decay is not modelled with just another linear term $-gw$. A good reason is that this that squaring w tempers the otherwise exponential growth that the linear term would yield; this also necessitates $g > 0$

[15] Recall that the saddle-point approximation (which can be used synonymously with mean-field approximation) eq. (2.10) or eq. (2.12) for the previously mentioned Landau-Ginzburg theories of the Curie point captured a wealth of qualitative features. This is also the case for DP.

1. When $\alpha \neq 0$ we may look to the integration by parts form (last line) of the right hand side of the equations in eq. (2.42), execute the integral and rearrange into

$$w(t) = \left(\frac{2\alpha}{g}\right) \cdot \frac{1}{1 - \left|\frac{w(0)-(2\alpha/g)}{w(0)}\right| \cdot \exp\left(-\alpha t\right)} \tag{2.43}$$

   The expression is plotted for various α in fig. 2.11. Depending the sign of α there are two distinct qualitative behaviours that this expression can have, which reflect the two phases of DP.

   (a) When $\alpha > 0$, the exponential in the denominator converges to 0, such that $w(t)$ overall decays to the positive steady state value $w_\infty = ({}^{2\alpha}/{}_{g})$. Interpreted in terms of percolation on directed lattices, this is the percolating phase. Note that eq. (2.43) is the steady state value multiplied by $(1-z)^{-1} = 1 + z + \mathcal{O}(z^2)$ with $z \sim e^{-\alpha t}$. At sufficiently large times $e^{-\alpha t}$ will be arbitrarily small, such that we may terminate the geometric series at first order. Hence, asymptotically speaking, the density of wet sites exponentially decays into the steady state $w(t) \approx w_\infty(1 + e^{-\alpha t})$ with characteristic time $\tau \sim \alpha^{-1}$

   (b) When $\alpha < 0$, the exponential in the denominator diverges to $+\infty$, making $w(t)$ decay to zero. This is the absorbing phase. At long times $e^{-\alpha t} \gg 1$, such that asymptotically the decay is exponential $w(t) \sim \exp(-|\alpha| t)$ with characteristic time $\tau = |\alpha|^{-1}$. Note that this characteristic time diverges as the critical point $\alpha = 0$ is approached, just as in the full DP theory (beyond the mean-field approximation)

2. Since at $\alpha > 0$ the mean-field theory is percolating ($p > p_c$), and for $\alpha < 0$ it is absorbing ($p < p_c$), the point $\alpha = 0$ can be identified as the critical point ($p = p_c$). In this case the he indefinite integrals on the right hand sides of eq. (2.42) evaluate to ${}^{1}/{}_{w(t)} - {}^{1}/{}_{w(0)}$ such that

$$w(t) = \left(\frac{1}{w(0)} + \frac{g}{2} t\right)^{-1} \tag{2.44}$$

   making $w(t) \sim t^{-1}$ asymptotically as $t \to \infty$ compared to $(g\, w(0)\,)^{-1}$. This power law is reminiscent of the expected universal behaviour $w(t) \sim t^{-\nu_\parallel}$

So, to recapitulate the results up to this point: the spatially homogeneous solution to the mean-field theory eq. (2.40) reproduces the phase transition from percolating to absorbing, the transient behaviour of the system as it relaxes to its steady state and the scaling of the relaxation time $\tau \sim |\alpha|^{-1}$ and the order parameter $w_\infty \sim |\alpha|^{+1}$ (albeit with inaccurate exponents)

In the following I am temporarily dropping the subscripts $(\cdots)_{\mathrm{DP}}$ for the critical exponents of DP, which until now were used to avoid leaving the impression that these were the same across universality classes. Invoking scale invariance at criticality, more specifically $\alpha > 0$ close to $\alpha = 0$, one may find values and relations between exponents by rescaling α by some factor $\lambda > 0$, in response to which lengths x, times

t and the order parameter w will be rescaled by

$$\begin{aligned} \alpha &\to \lambda\alpha \\ x &\to \lambda^{-\nu_\perp} x \\ t &\to \lambda^{-\nu_\parallel} t \\ w &\to \lambda^{\beta} w \end{aligned} \tag{2.45}$$

with critical exponents $\nu_\perp$, $\nu_\parallel$ and β (with minus signs being conventions, that make the exponent values positive). Inserting into eq. (2.40) leads to

$$\lambda^{\nu_\parallel+\beta} \cdot \frac{\partial w(\boldsymbol{r},t)}{\partial t} = \lambda^{2\nu_\perp+\beta} \cdot D\nabla^2 w(\boldsymbol{r},t) + \lambda^{1+\beta} \cdot \alpha\, w(\boldsymbol{r},t) - \lambda^{2\beta} \cdot \frac{1}{2} g\, w(\boldsymbol{r},t)^2 \tag{2.46}$$

To keep its form (and hence be invariant under scaling the order parameter), it is necessary that all the powers of λ are the same. This is most easily seen by dividing by $\lambda^{\nu_\parallel+\beta}$ on both sides, which makes obvious that

$$0 = 2\nu_\perp - \nu_\parallel \qquad 0 = 1 - \nu_\parallel \qquad 0 = \beta - \nu_\parallel \tag{2.47}$$

which may be resolved to find the DP *mean-field exponents* (compare Adzhemyan et al. 2023, eq. 10)

$$\beta^{(\mathrm{MF})} = 1 \qquad \nu_\parallel^{(\mathrm{MF})} = 1 \qquad \nu_\perp^{(\mathrm{MF})} = 1/2 \tag{2.48}$$

which are accurate[16] at and above the critical dimension $d_\mathrm{c} = 4$. For comparison for the interested, in table 2.1 are empirically determined exponents. $d = 3$, while undoubtedly different, is not dramatically far off from mean-field.

d	β	$\nu_\perp$	$\nu_\parallel$
1	0.276486(8)	1.096854(4)	1.733847(6)
2	0.5834 ± 0.0030	0.7333 ± 0.0075	1.2950 ± 0.0060
3	0.813 ± 0.009	0.584 ± 0.005	1.110 ± 0.010
mean field	1	$1/2$	1

Table 2.1: Critical exponents of the DP universality class as found in (Hinrichsen 2000, app. A.3.1, tab. 1)

Phenomenological Mean-Field Theories Plus Noise It is appropriate at this point to mention a common way in which the universal behaviour of theories is written down: first, a mean-field equation like eq. (2.40) is motivated on phenomenological grounds and then turning it into a stochastic partial differential equation by extending it with a noise term

$$\left(\frac{\partial}{\partial t} - D\nabla^2\right) w(\boldsymbol{r},t) = +\alpha\, w(\boldsymbol{r},t) - \frac{1}{2} g\, w(\boldsymbol{r},t)^2 + \underbrace{\kappa\sqrt{w(\boldsymbol{r},t)}\,\zeta(\boldsymbol{r},t)}_{\text{noise term}} \tag{2.49}$$

---

[16] Note that $\beta = \beta'$ in DP (Hinrichsen 2000, app. A.3)

where κ matches up the dimensions with the other terms and $\zeta(\boldsymbol{r},t)$ is a random field with Gaussian white noise statistics

$$\begin{aligned}\big\langle\zeta(\boldsymbol{r},t)\big\rangle_{\text{noise}} &= 0\\ \big\langle\zeta(\boldsymbol{r},t)\zeta(\boldsymbol{r}',t')\big\rangle_{\text{noise}} &= \delta(\boldsymbol{r}'-\boldsymbol{r})\,\delta(t'-t)\end{aligned} \tag{2.50}$$

with all higher cumulants vanishing and $\langle\cdots\rangle_{\text{noise}}$ denoting the average with respect to the noise degrees-of-freedom only. The prefactor of $w(\boldsymbol{r},t)^{1/2}$ has the effect that the noise, as it couples into the equation, vanishes when $w(\boldsymbol{r},t)\equiv 0$; if that was not the case, the system could fluctuate out of the supposed absorbing state $w(\boldsymbol{r},t)\equiv 0$, which would rob the absorbing state transitions in DP of their defining feature (compare Janssen, Kutbay, and Oerding 1999, eqs. 2 - 4). Choosing $w(\boldsymbol{r},t)^{1/2}$ instead of any other strictly monotone positive function of w furthermore gives the influence noise's influence a semblance of Poissonian statistics, where the variance in the stochastic field $w(\boldsymbol{r},t)$ due to noise is equal to the mean

$$\left\langle\sqrt{w(\boldsymbol{r},t)}\zeta(\boldsymbol{r},t)\cdot\sqrt{w(\boldsymbol{r}',t')}\zeta(\boldsymbol{r}',t')\right\rangle_{\text{noise}} = w(\boldsymbol{r},t)\cdot\delta(\boldsymbol{r}'-\boldsymbol{r})\,\delta(t'-t) \tag{2.51}$$

When describing percolation on directed lattices, this may be taken as reflecting that the states are discrete (wet or not wet). The same is done for theories of the universality class of random organization (compare with reasoning in Wiese 2016, sec. VI). Equations with a noise term like eq. (2.49) are also referred to as *Langevin-Equations* (Hinrichsen 2000; Lubeck 2004; Janssen and Täuber 2005).

This noise term models fluctuations stemming from the smaller-scale degrees of freedom, that are not relevant to the study of the critical point. It adds so much richness that the mean-field behaviour is broken and the model gets the correct universal properties, from critical exponents to upper critical dimension. In fact, the Langevin-equation eq. (2.49) can be mapped to a field theory with a similar procedure as the derivation in section 2.2.2. It can be found in Hinrichsen (2000, app. B), which I will try to outline briefly:

$$\begin{aligned}P[w(\boldsymbol{r},t)] &\sim \int\mathcal{D}\zeta\,P[\zeta]\prod_{\boldsymbol{r},t}\delta\Big((\text{mean-field})-\kappa\sqrt{w}\cdot\zeta(\boldsymbol{r},t)\Big)\\ &= \int\mathcal{D}\tilde{w}\int\mathcal{D}\zeta\,P[\zeta]\,\exp\Big(\int\mathrm{d}^d r\,\mathrm{d}t\,\Big(\tilde{w}\cdot(\text{mean-field})-\tilde{w}\cdot\kappa\sqrt{w}\cdot\zeta\Big)\Big)\\ &= \int\mathcal{D}\tilde{w}\,\exp\Big(\int\mathrm{d}^d r\,\mathrm{d}t\,\tilde{w}\cdot(\text{mean-field})\Big)\\ &\qquad\qquad\times\int\mathcal{D}\zeta\,P[\zeta]\,\exp\Big(-\int\mathrm{d}^d r\,\mathrm{d}t\,\tilde{w}\cdot\kappa\sqrt{w}\cdot\zeta\Big)\end{aligned} \tag{2.52}$$

with $\int\mathcal{D}\tilde{w}$ again given by eq. (2.30). Gaussian white noise now has a weight that makes apparent why it contains the name "Gaussian"

$$\begin{aligned}P[\sqrt{\tilde{w}^2\kappa\,w}\zeta] &\sim \exp\left(-\frac{1}{2}\int\mathrm{d}^d r\,\mathrm{d}t\,\frac{\zeta(\boldsymbol{r},t)^2}{\tilde{w}^2\kappa w(\boldsymbol{r},t)}\right)\\ &\sim \exp\Big(-\frac{\kappa}{2}\int\mathrm{d}^d r\,\mathrm{d}t\,w\,\tilde{w}^2\Big)\end{aligned} \tag{2.53}$$

such that

$$P[w(\boldsymbol{r},t)] \sim \int \mathcal{D}\tilde{w}\, J[w,\tilde{w}]\, \exp\left(\int \mathrm{d}^d r\, \mathrm{d}t \left(\tilde{w}\left(\frac{\partial}{\partial t} - D\nabla^2 + \alpha\right) w - \frac{g}{2}\tilde{w}w^2 - \frac{\kappa}{2} w\tilde{w}^2\right)\right) \tag{2.54}$$

where $J[w, \tilde{w}]$ emerged from the replacement $\zeta \to \sqrt{\tilde{w}^2\kappa\, w\zeta}$ and is a path integral object corresponds to a Jacobian in integrals over finitely many degrees of freedom. Rescaling (without loss of generality) w, $\tilde{w}$ and κ can bring the exponent in eq. (2.54) into the form eq. (2.39) derived earlier.

Brief Summary When neglecting fluctuations in the order-parameter of a continuous transition one arrives at the mean-field theory, which is a perfectly valid physical description of the system's critical behaviour above the upper critical dimension d_c. It is synonymous with the saddle-point approximation in the context of field theory and can be solved analytically for DP by simple means. Mean-field behaviour reflects many essential features of the transition: an absorbing and a percolating phase, scaling (albeit very primitive, only with mean-field exponents). Adding a properly engineered noise term onto the mean-field equation retrieves an accurate field theory of the transition again.

2.2.4 Sketch of Renormalization Flow Analysis

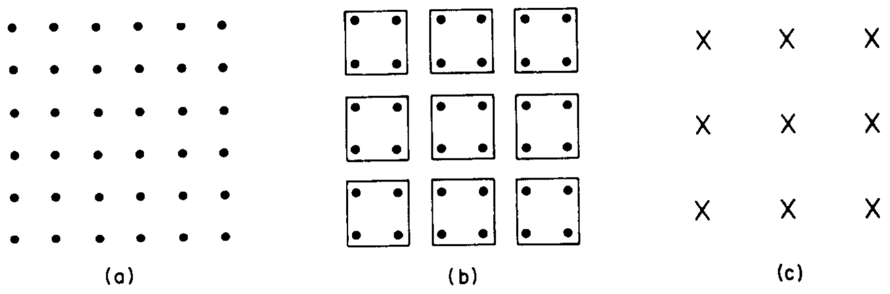

Figure 2.12: Depiction from Wilson (1974, fig. 2.7) of one coarse graining step in the Kadanoff approach to renormalization analysis of the Ising model: in (a) one can see a square lattice of Ising spins. (b) depicts their grouping into blocks, about which we assume that they have only two magnetization states ±m. In (c) the blocks are replaced by crosses, symbolizing the new sites, interacting by new couplings

Thus far, I have not mentioned any methods of understanding statistical field theories of phase transitions beyond looking at the saddle-point approximation. It is not obvious how to improve on the mean-field prediction for critical behaviour. As mentioned numerous times already, an important tool, both for equilibrium and far-from-equilibrium continuous transitions, is *renormalization flow*, also known as the *renormalization technique*, *renormalization group procedure*, *renormalization (semi-)group* (RG) and other remixes of these names.

Its basic idea is to make the ignoring of small-scale detail very literal (and more well-defined) and observing how the theory of the problem changes as a consequence. The ignoring-procedure must, for this approach to be fruitful, yield a theory of the same form as the original one, just with changed coupling constant, since otherwise there is no way to iterate the procedure, which is necessary to formalize the large-scale limit. The simplest first example for this is again the Ising model, whose energy is given by

$$E[\{s_i\}] = -J\sum_{\langle i,j\rangle} s_i s_j + H\sum_i s_i \tag{2.55}$$

with $J > 0$, H an externally applied magnetic field and $\langle i,j\rangle$ denoting the sum over nearest-neighbours on the underlying lattice. As pioneered by Kadanoff (1966), we want to take the diverging correlation lengths at criticality as justification to assume that one may as well understand patches of commonly magnetized spins as being one variable s'_i, where i enumerates patches of (roughly) common magnetization. It is furthermore assumed, that it is a fair approximation that these s'_i can be modelled as a grouping of blocks of spins as depicted in fig. 2.12. To also retain the theory's form (in order to iterate) we seek a reduced set of degrees of freedom $\{s'_k\}$ (taking the same values as the $\{s_i\}$) and modified J' and H' such that one can reasonably assume that for any pair of $\{s_i\}$ and their coarse-grained counterpart $\{s'_k\}$ the free energy is the same. Note that for the s'_k to also take values -1 and 1, we need to (1) assume that the overall magnetization m_k of aligned patches takes only one of two values $\{-m_0, +m_0\}$ (2) assume that the patches interact with each other predominantly via an effective patch-patch coupling constant (3) rescale $s'_k = m_k/m_0$ by absorbing a factor of m_0^2 into said effective coupling constant, resulting in J' (Wilson 1971a).

Suspending disbelief for the time being, it is plausible that this leads to a description of the critical point: given that our procedure is well defined, the determination of J' and H' is a map

$$(J', H') =: C(J, H) \tag{2.56}$$

from the two-dimensional space of theory parameters to itself. We will refer to C as *coarse-graining* of the model. Now crucially, the critical system (J_*, H_*), invariant across scales, should be unaffected by the change of scales $\{s_i\} \to \{s'_k\}$ and hence be a fixed point

$$(J_*, H_*) = C(J_*, H_*) \tag{2.57}$$

The central insight is that it there is a good chance that this fixed point can be obtained by direct iteration[17] of the coarse-graining, i.e. that it is a limit

$$(J_*, H_*) \overset{?}{=} \underbrace{\lim_{n\to\infty} \underbrace{C(C(\cdots C}_{n \text{ applications}}(J, H)))}_{=:(J^{(n)}, H^{(n)})} \tag{2.58}$$

Hence, if one can get a handle on the flow of parameters

$$(J^{(0)}, H^{(0)}) \to (J^{(1)}, H^{(1)}) \to (J^{(2)}, H^{(2)}) \to (J^{(3)}, H^{(3)}) \to \cdots \tag{2.59}$$

then one has established a process that tunes itself to the critical point of the Ising-model and might understand it without having to solve the full model.

---

[17] For example: when a function $f(x)$ from some space to itself is continuous and n-times application $f(f(\cdots f(x))) =: f^{(n)}(x)$ limits in some x_*, then observe that one may do a change of index and pull in the limit to the effect $x_* = \lim_{n\to\infty} f^{(n)}(x) = \lim_{n\to\infty} f^{(n+1)}(x) = f(\lim_{n\to\infty} f^n(x)) = f(x_*)$, i.e. x_* must be a fixed point of f.

There are issues with this picture however: assumptions (1) and (2) are on shaky grounds, as Kadanoff (1966) address themselves and Wilson (1971a) emphasizes. This can be remedied with a more careful approach presented in Wilson (1971a) and Wilson (1974), switching to the Landau-Ginzburg point-of-view. In path integral expressions like $\int \mathcal{D}f$ it is not specified what kinds realizations of the order parameter $f(\boldsymbol{r})$ (or $f(\boldsymbol{r}, t)$ in dynamical transitions) are included: boundary conditions, regularity, etc. are not specified. Importantly for the present discussion: since both thermodynamical Landau-Ginzburg free energy and field theories of stochastic processes are large-scale descriptions, the included realizations should not have arbitrarily fine detail (which would also be self-defeating). Instead, there is a *cutoff-wavenumber* or *UV-cutoff* Λ, where the latter name comes from quantum field theory and has diffused into statistical field theory literature. It defines the length-scales Λ^{-1} (and in dynamical transitions also time-scales) below which the field theory does not resolve the system.

Wilson Renormalization The following ideas can be found in very similar form in Wilson (1974, sec. 3 - 5)[18]. A more recent presentation can be found in Tong (2017, sec. 3). I am sticking to equilibrium because these references do. The ideas carry over with more clutter but with the same principles to non-equilibrium (Janssen 1976; Wijland, Oerding, and Hilhorst 1998). Let $E[f]$ be a local Landau-Ginzburg free energy functional and absorb the $(1/k_\mathrm{B}T)$ into the coupling constants. The partition function then reads

$$Z = \int \mathcal{D}f \, e^{-E[f]} \tag{2.60}$$

The goal is the same as in the Kadanoff approach: backed by the justification of diverging correlation lengths towards criticality we want to ignore smaller lengthscales in a way that gives us a new theory of the same form as $E[f]$ but with different coupling constants as before. Their flow under an iterative application of this scheme is then analysed for fixed points, which are scale-invariant descriptions by definition. These then must correspond to different critical point behaviours, i.e. to different universality classes (Lubeck 2004, sec. 1.4)

For this we pick a new lengthscale $(\Lambda')^{-1} > \Lambda^{-1}$ (or, in terms of wave-numbers, a lower cutuff $\Lambda' < \Lambda$) and attempt to integrate out smaller wavelength detail and hence instate Λ' as the new cutoff. Let the ratio of cutoffs be

$$\zeta = \frac{\Lambda}{\Lambda'} \tag{2.61}$$

where $\zeta > 1$ because the new high wavenumber cutoff is naturally smaller than the old one. Concretely we do this in the following way: $E[f]$ can in principle be written as a functional of the Fourier-transform of the order parameter by expanding

$$f(\boldsymbol{r}) = \int \frac{\mathrm{d}^d k}{(2\pi)^d} \, \tilde{f}(\boldsymbol{k}) \, e^{i\boldsymbol{k}\boldsymbol{r}} \tag{2.62}$$

and inserting that into the functional[19]. We can now split the Fourier-transforms $\tilde{f}(\boldsymbol{k})$

---

[18] In honour of Wilson, the procedure described in the following is known as *Wilson renormalization*

[19] To give an idea of how this changes the expressions of a local functional, consider a f^4-theory $E[f] = \int \mathrm{d}^d r \, ((\nabla f)^2 + af^2 + bf^4)$ which by the identity $(2\pi)^d \delta(\boldsymbol{k}) = \int \mathrm{d}^d r \, e^{i\boldsymbol{k}\boldsymbol{r}}$ becomes $E[\tilde{f}] = \int \mathrm{d}^d k \, ((\boldsymbol{k}^2 + a)\tilde{f}(\boldsymbol{k})\tilde{f}(-\boldsymbol{k})) + b \int \mathrm{d}^d k_1 \int \mathrm{d}^d k_2 \, \mathrm{d}^d k_3 \, \mathrm{d}^d k_4 \, \delta(\boldsymbol{k}_1 + \boldsymbol{k}_2 + \boldsymbol{k}_3 + \boldsymbol{k}_4) \, \tilde{f}(\boldsymbol{k}_1)\tilde{f}(\boldsymbol{k}_2)\tilde{f}(\boldsymbol{k}_3)\tilde{f}(\boldsymbol{k}_4)$

along the new cutoff

$$\tilde{f}(\boldsymbol{k}) = \tilde{f}_-(\boldsymbol{k}) + \tilde{f}_+(\boldsymbol{k}) \tag{2.63}$$

where $\tilde{f}_-(\boldsymbol{k})$ are the large-scale modes (small wavenumber) and $\tilde{f}_+(\boldsymbol{k})$ the small-scale ones (large wavenumber)

$$\begin{aligned} \tilde{f}_-(\boldsymbol{k}) &= \tilde{f}(\boldsymbol{k})\,\Theta(\Lambda' - |\boldsymbol{k}|) \\ \tilde{f}_+(\boldsymbol{k}) &= \tilde{f}(\boldsymbol{k})\,\Theta(|\boldsymbol{k}| - \Lambda') \end{aligned} \tag{2.64}$$

with $\Theta(x)$ being the Heaviside step function. Notice that $\tilde{f}_-(\boldsymbol{k})\tilde{f}_+(\boldsymbol{k}) \equiv 0$ because they vanish respectively on the other's support. Not only that, but because the cutoff is radially symmetric, orthogonally transforming the arguments of $\tilde{f}_-$ and $\tilde{f}_+$ will not get their supports to overlap, such that $\tilde{f}_-(\boldsymbol{k})\tilde{f}_+(R\boldsymbol{k}) \equiv 0$ for any $R \in O(d)$. Very importantly, this includes mirroring $R = -1$ to the effect $\tilde{f}_-(\boldsymbol{k})\tilde{f}_+(-\boldsymbol{k}) \equiv 0$; for this reason, the lowest orders of the field theory (whatever its form beyond that it may have) separate cleanly into an $\tilde{f}_-(\boldsymbol{k})$ and an

$$\begin{aligned} E[f] &= \int \mathrm{d}^d r\,((\nabla f)^2 + a f^2 + \cdots) \\ &= \underbrace{\int \mathrm{d}^d k\,((\boldsymbol{k}^2 + a)\tilde{f}(\boldsymbol{k})\tilde{f}(-\boldsymbol{k}))}_{=:E_0[\tilde{f}]} + \int \mathrm{d}^d k_1 \int \mathrm{d}^d k_2\,(\cdots) + \cdots \\ &= \int \mathrm{d}^d k\,((\boldsymbol{k}^2 + a)\underbrace{(\tilde{f}_+(\boldsymbol{k}) + \tilde{f}_-(\boldsymbol{k}))(\tilde{f}_+(-\boldsymbol{k}) + \tilde{f}_-(-\boldsymbol{k})))}_{=\tilde{f}_+(\boldsymbol{k})\tilde{f}_+(-\boldsymbol{k})+\tilde{f}_-(\boldsymbol{k})\tilde{f}_-(-\boldsymbol{k})} \underbrace{+\cdots}_{=:V[\tilde{f}_+,\tilde{f}_-]} \\ &= E_0[\tilde{f}_+] + E_0[\tilde{f}_-] + V[\tilde{f}_+, \tilde{f}_-] \end{aligned} \tag{2.65}$$

Furthermore, in any discretization of the path integral all the $\tilde{f}(\boldsymbol{k})$ values are varied independently, such that it splits without issues into

$$\underbrace{\prod_{\boldsymbol{k}} \int \mathrm{d}\tilde{f}(\boldsymbol{k})\,(\cdots)}_{\int \mathcal{D}\tilde{f}} = \underbrace{\prod_{|\boldsymbol{k}|<\Lambda'} \int \mathrm{d}\tilde{f}(\boldsymbol{k})}_{\int \mathcal{D}\tilde{f}_-} \underbrace{\prod_{|\boldsymbol{k}|>\Lambda'} \int \mathrm{d}\tilde{f}(\boldsymbol{k})\,(\cdots)}_{\int \mathcal{D}\tilde{f}_+} \tag{2.66}$$

We can hence rewrite the partition function as

$$Z = \int \mathcal{D}\tilde{f}_- e^{-E_0[\tilde{f}_-]} \int \mathcal{D}\tilde{f}_+ e^{-E_0[\tilde{f}_+]}\, e^{-V[\tilde{f}_+,\tilde{f}_-]} \tag{2.67}$$

The inner path integral $\int \mathcal{D}\tilde{f}_+$ now is precisely the sought integration over small scale detail (high wavenumbers). $E_0[\tilde{f}_-]$ is already in the same functional form as $E_0[f]$ (just with a lower cutoff wavenumber), so what remains is finding a functional $V'[\tilde{f}_-]$ fulfilling

$$e^{-V'[\tilde{f}_-]} = \int \mathcal{D}\tilde{f}_+ e^{-E_0[\tilde{f}_+]}\, e^{-V[\tilde{f}_+,\tilde{f}_-]} \tag{2.68}$$

hopefully also of the same functional form. After taking the logarithm on both sides, we get

$$\begin{aligned} V'[\tilde{f}_-] &= -\log\Bigg(\underbrace{\int \mathcal{D}\tilde{f}_+ e^{-E_0[\tilde{f}_+]}\, e^{-V[\tilde{f}_+,\tilde{f}_-]}}_{=Z_+\cdot\frac{1}{Z_+}\int\mathcal{D}\tilde{f}_+(\cdots)}\Bigg) \\ &= -\log\left\langle \exp\left(-V[\tilde{f}_+,\tilde{f}_-]\right)\right\rangle_+ + \log(Z_+) \end{aligned} \tag{2.69}$$

where $Z_+ = \int \mathcal{D}\tilde{f}_+\, e^{-E_0[\tilde{f}_+]}$ and accordingly $\langle\cdot\rangle_+$ denotes the average with respect to the small scale modes. $\log(Z_+)$ is just a constant shift to E and would drop out in all averages. It might as well be dropped now. One can recognize $\log\left\langle\exp\left(-V[\tilde{f}_+,\tilde{f}_-]\right)\right\rangle_+$ as the cumulant generating function of $V[\tilde{f}_+,\tilde{f}_-]$ with respect to the high wavenumber modes

$$\log\left\langle\exp\left(-V[\tilde{f}_+,\tilde{f}_-]\right)\right\rangle_+ = \sum_{n=1}^{\infty}\frac{(-1)^n}{n!}\left\langle V[\tilde{f}_+,\tilde{f}_-]^n\right\rangle_{\mathrm{c}}^{+} \tag{2.70}$$

where $\left\langle V[\tilde{f}_+,\tilde{f}_-]^n\right\rangle_{\mathrm{c}}^{+}$ is the n-th cumulant. For all but the free theory ($V = 0$) the exact solution is out of reach. But cutting off eq. (2.70) at some order and determining all of the included terms (by taming the resulting combinatorics with Wick's theorem and diagrammatic methods, as may be familiar from perturbative calculations in quantum field theory) yields an approximate, perturbative expression that is generally of the same functional form as the starting point $E[f]$. More precisely, every coupling constant in $E[f]$ has a pendant in the new $E'[f_-] = E_0[\tilde{f}_-] + V'[\tilde{f}_-]$, where one should consider couplings that were not present in $E[f]$ has being zero at the outset. All that is left to retain full comparability between $E'[f_-]$ and $E[f]$ are two steps: (1) rescaling lengths in the system by replacing $\boldsymbol{k} = \zeta\boldsymbol{k}'$ such that in these new units the UV-cutoff Λ' has the same value as Λ and (2) rescale the order parameter f_- (and calling the result f') such that the $(\nabla f')^2$ term has the same prefactor as $(\nabla f)^2$ before integrating out the small scale modes. Cruically, all the new couplings are functions of the old values, the old cutoff Λ and of ζ. Detail on scales between Λ^{-1} and Λ'^{-1} has been successfully eliminated.

Performing this procedure twice, respectively with scaling factors ζ_1 and ζ_2, will have the same result as performing it once with scaling factor $\zeta_1\cdot\zeta_2$. This property has incurred this set of operations the name *renormalization (semi-)group*. Since coupling constants of the same term at different ζ can be compared, one may think of the coupling constants as being a function of ζ, flowing through the space of possible combinations of values for the couplings. This picture is where the name *renormalization flow* comes from. To recapitulate: the procedure consists of

1. Choosing a new wave-number cutoff Λ' for a theory $E[f]$ with $\zeta = \Lambda/\Lambda'$

2. Integrating out the high wave number modes from $E[f]$ (the hard part)

3. Rescaling all lengths, such that in the new units Λ' has the same numerical value that Λ had, and hence finally have a theory $E'[f']$ of the same functional form as $E[f]$

Fixed points and couplings Now assume a fixed point E_* in renormalization flow, given by the list of values for all the coupling constants $(c_1^*, c_2^*, c_3^*, \dots)$. Renormalization with rescaling factor ζ, which I will denote by $\mathfrak{R}_\zeta[E]$ or $\mathfrak{R}_\zeta(c_1, c_2, c_3, \dots)$ or $\mathfrak{R}_\zeta[\{c_k\}]$, can be thought of as a flow field in coupling constant space. In the vicinity of a fixed point $E_* + \delta E \simeq (c_1^* + \delta c_1, c_2^* + \delta c_2, c_3^* + \delta c_3, \dots)$, this flow field causes three broad categories of behaviour (see fig. 2.13):

1. *Irrelevant*: Renormalization flow fixed points have a *basin of attraction*, that is directions $\delta E \simeq (\delta c_1, \delta c_2, \delta c_3, \dots)$ in which the flow leads right back to E_*. Recall that these "directions" correspond to terms in the Landau-Ginzburg free energy, so such terms neither cause new critical behaviour, nor do they survive RG flow; hence they are called irrelevant.

2. *Relevant*: When the direction $\delta E \simeq (\delta c_1, \delta c_2, \delta c_3, \dots)$ in coupling constant space puts $E_* + \delta E$ into a region that leads away from E_* under the action of $\mathfrak{R}_\zeta[E]$, then a different fixed point (different universal behaviour) is approached; these terms are hence called relevant.

3. *Marginal*: When renormalization flow neither moves $E_* + \delta E$ away from E_* nor back to it (such that $E_* + \delta E$ stays put), then E_* is just one fixed point on an entire (higher-dimensional) ridge and δE was a step along the ridge. Such perturbations of the coupling constants are called marginal.

Most couplings are irrelevant (Tong 2017, sec. 3.1.1), which is an important source of validity for Landau-Ginzburg theory and stochastic field theories like eq. (2.39), which try to cut off the expansions in the order parameter and its derivatives. It is however necessary to watch out: some couplings can be irrelevant, but still be important for the perturbation theory for relevant couplings; just ignoring these outright can lead to wrong results. Such terms are hence called *dangerously irrelevant*.

Scaling Analysis Arguments An argument akin to dimensional analysis starts becoming a very helpful tool. $E[f]$ is dimensionless. Without loss of generality (by rescaling the order-parameter) one may choose that the first coupling $(\nabla f)^2$ has a prefactor of 1, such that from $E[f] = \int \mathrm{d}^d r \, ((\nabla f)^2 + \cdots)$ one may read off that the units of the (conveniently rescaled) order parameter are given by $1 = L^d L^{-2} [f]^2$ where L is a lengthscale. Rearranging the units gives $[f] = L^{(2-d)/2}$. Very close to the fixed point, theories are already very close to being scale-invariant and correlators may be assumed to take power law form (in a homogeneous system)

$$\langle f(\boldsymbol{r}_1) f(\boldsymbol{r}_2) \rangle_\mathrm{c} \sim |\boldsymbol{r}_2 - \boldsymbol{r}_1|^p \tag{2.71}$$

because power laws Ar^p have the convenient property that they can keep their functional form under rescaling of their argument *by just rescaling constants*

$$Ar^p = A\zeta^{-p}(r/\zeta)^p = A' r'^p \tag{2.72}$$

with new, rescaled constant $A' = A\zeta^p$ and the argument given in the new scale as $r' = r/\zeta$. Applying the RG procedure to $E[f]$ up to the second step leaves the coupling $(\nabla f_-)^2$ with a coupling constant c, whose dimensions may be different and which

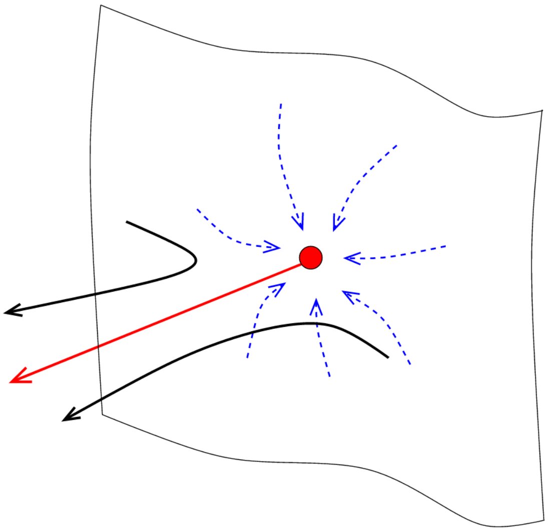

Figure 2.13: Visualization from Tong (2017, fig. 23) of the possible coupling behaviours: under renormalization flow: the red point symbolizes is the fixed point, corresponding to the transition of interest. The red line symbolizes the trajectory of a relevant coupling flowing to a different fixed point. The dotted blue lines are the trajectories of irrelevant couplings, flowing back to the fixed point

can depend in an arbitrarily complicated manner on ζ. Absorbing $f' = \sqrt{c} f_{-}$ will ensure $[f'] = L^{(2-d)/2} = [f]$. However, as a consequence f does not scale under the renormalization step, as could be naively assumed, by $f \sim (L/\zeta)^{(2-d)/2} \sim \zeta^{(d-2)/2}$ but instead with a more general, *non-integer* exponent $f \sim \zeta^{d_f}$ called the *scaling-dimension* d_f. Under rescaling with ζ, we now expect the power law of the correlator to change on either side with

$$\zeta^{2d_f} \langle f(\boldsymbol{r}) f(0) \rangle_{\mathrm{c}} \sim \zeta^{-p} r^p \tag{2.73}$$

such that $-p = 2d_f$ is necessary for scale-invariance. p is typically written as $p = 2 - d - \eta$, such that η is the deviation from the exponent naively expected from $[f]^2 = L^{2-d}$. The exponent η can for example be measured by determining the power law eq. (2.71) in experiment and simulation for a model assumed to be in the studied universality class. One finds

$$d_f = \frac{d - 2 + \eta}{2} \tag{2.74}$$

i.e. an expression for d_f in terms of η. This discussion is supposed to highlight two things about the renormalization flow method: (1) critical exponents come from the scaling dimension of quantities under renormalization and (2) dimensional analysis akin arguments, such as the just presented, allow relating the various critical exponents of power-law exhibiting quantities, *leaving only a handful of independent exponents*. To give two more very relevant examples: the correlation length, as a length-scale, experiences the simplest possible rescaling $\xi' = \xi/\zeta$ under renormalization flow, and is related to the distance α of the control parameter from its critical value by a power law $\xi \sim \alpha^{-\nu}$ (to clarify: α could mean $(T - T_{\mathrm{c}})$ or $\alpha = (p - p_{\mathrm{c}})$ for example). The rescaling dimension d_α of the control parameter is not trivial. Yet the law should be scale invariant, such that $\zeta^{-1}\xi = \xi' \sim {\alpha'}^{-\nu} = (\zeta^{\Delta_\alpha}\alpha)^{-\nu} = \alpha^{-\nu}\zeta^{-\nu\Delta_\alpha}$ which requires

$$\Delta_\alpha = \frac{1}{\nu} \tag{2.75}$$

The expectation value of the order parameter also follows a power law $\langle f \rangle \sim \alpha^{\beta}$. Because, as now established, either of them rescale under an RG procedure like $\zeta^{d_f}\langle f \rangle \sim (\alpha\zeta^{d_\alpha})^{\beta} = \alpha^{\beta}\zeta^{\beta d_\alpha}$, scale invariance demands $d_f = \beta d_\alpha$ and hence

$$\nu \cdot \frac{d-2+\eta}{2} \overset{\text{eq. (2.74)}}{=} \nu d_f \overset{\text{eq. (2.75)}}{=} \frac{d_f}{d_\alpha} = \beta \tag{2.76}$$

Measuring β and ν for example hence already determines the value of η.

3 Random Organization Adjacent Literature

This section discusses some models related to the study of random organization that I encountered in my literature research. The purpose of presenting them is to detail this relevant part of my literature work and to provide the context I am working with in chapter 3.

3.1 Simulations

The *overlap reducing protocol* of Corté et al. (2008) understands itself as shearing the suspension with some strain amplitude γ_0. As noted in Milz and Schmiedeberg (2013) however, replacing particles depending on whether they would meet any others in the process of shearing has the same effect as just elongating them along the shearing axis and, without shearing, replacing them if they overlap. With this argument they eliminate the need for specifying a shear-amplitude γ_0 and replace it with the, much more general, idea of performing $\gamma_0 = 0$ random organization with particless of different shapes. This leaves packing density Φ as the only control parameter. With active particle fraction f_a^∞ kept as the order parameter, Milz and Schmiedeberg (2013) proceed to do a very similar[1] simulation study as Corté et al. (2008) and determine the *critical packing density* Φ_c for a handful of dimensions and particle shapes and also fit the critical exponents to the power-laws displayed by f_a^∞ and the relaxation time τ.

Milz and Schmiedeberg (2013) also point out parallels between random organization and protocols for generating so called *athermally jammed* configurations. This is a very noteworthy observation, but requires giving a very short exposition of *jamming*: a large, composite system is characterized by O'Hern et al. (2003) as *jammed* if they are disordered (for example not crystalline) and the characteristic time over which they relax stresses is effectively infinite on experimental time scales. Amongst the examples given by the authors is granular matter (like sand) funnelled into a hopper, but where at the constriction the grains have such difficulties finding ways past each other that they get stuck. In that example the system is under stress due to gravity and relaxation would consist in the mutual blockades of grains being resolved such that the system can start to flow. But since the grains are stuck, without outside influence like shaking there will be no spontaneous flow for the foreseeable future (effectively

---

[1] Their random organization protocol resolves overlaps by separating the particles, along a random direction, until they just barely touch, as opposed to completely independent random displacements like in Corté et al. (2008)

infinite relaxation time). Note that this behaviour is in stark contrast to equilibrium physics, where characteristic time for the relaxation of stresses (in the form of a slight perturbation out of equilibrium) are very short on experimental time scales, arguably by definition.

O'Hern et al. (2003) suggest understanding this phenomenon with simulations of particles with soft[2] finite range interactions $u(r)$ (where that range is interpreted as the particles' extension σ), at some packing density Φ, subject to a shear stress Σ and a "temperature" T; the latter cannot always be identified with thermodynamic temperature and instead more generally quantifies the ability of the system to overcome energy barriers. They focus on the case $T = 0$ (athermal jamming) by means of the following protocol: first they disperse particles with centres $\{\boldsymbol{x}_k\}$ randomly, independently and uniformly in their simulation box. Since this placing has no respect for the potential energy $V = \sum_{j<k} u(|\boldsymbol{x}_k - \boldsymbol{x}_j|)$ they describe this ensemble to be at $T = \infty$. To get to $T = 0$, they then take a conjugate gradient descent to minimize energy (which will not cross potential energy barriers). In effect, this leads to a repulsion of overlapping particles while particles without overlaps stay in place. Depending on packing density, they observe one of two behaviours: in lower density systems the energy minimization protocol resolves all overlaps and potential energy drops all the way to $V = 0$. In higher density systems some overlaps remain indefinitely unresolved and $V > 0$; in that case the system is considered *jammed*. The authors run this protocol out for various particle numbers N and packing densities Φ and observe how the fraction f_j of initial states that lead to jamming changes with these two parameters. They find that f_j as a function of density Φ develops a sharper and sharper threshold the larger the system size N is (fig. 3.1). For systems of three-dimensional spheres, they extrapolate the thermodynamic limit $N \to \infty$ of this threshold value and find $\Phi_J = 63.9\% \pm 0.1\%$.

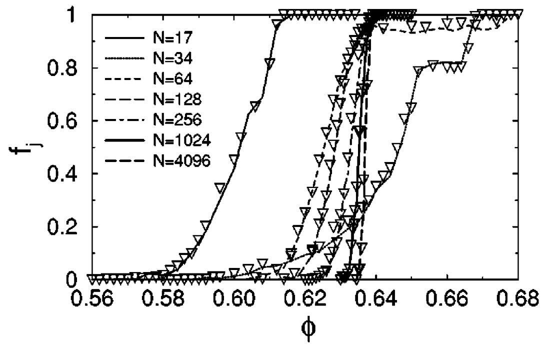

Figure 3.1: O'Hern et al. (2003, fig. 5b), depicting the dependence of the fraction f_j of initial $T = \infty$ particle configurations that jam under their relaxation protocol to $T = 0$.

With view to the energy minimization steps, the similarity to random organization cannot be overlooked. Milz and Schmiedeberg (2013) compare the two protocols by having two variants of their overlap reducing protocol: the earlier described one, where displacements of overlapping particles have random directions, and another protocol, representing athermal jamming, where overlapping particles are moved away from each other along the line connecting their centres. The latter *deterministic-displacement* version of random organization brings the critical packing density way up to $\Phi_c^{(\mathrm{det})} = 62.76\% \pm 0.05\%$ (very close to the athermal jamming density $\Phi_J =$

---

[2] as in: two particles can occupy the same position in space with only a finite amount of work necessary. Contrast this with interactions that have (effective) hard cores like the Lennard-Jones potential $u(r) = 4\varepsilon((\sigma/r)^{12} - (\sigma/r)^6)$

63.9% ± 0.1%. That the critical packing density is that high happens because consciously moving away from any overlap partners lets particles search much more effectively for vacant areas.

Milz and Schmiedeberg (2013) characterized random organization and athermal jamming as two ends in a possible spectrum of overlap reducing protocols. Wilken et al. (2021) and Wilken et al. (2023) followed up on this idea with a protocol they named *biased random organization* (BRO): they interpolate overlap reducing protocols with fully deterministic and fully random directions. They do so with some parameter $0 < \delta < 1$, with $\delta = 1$ being the fully repulsive and $\delta = 0$ entirely random displacements. The length of their particle jumps is chosen uniformly at random from $[0, \varepsilon]$; ε hence can be thought of as the jump size or alternatively as quantifying how close to continuous time the protocol is (since smaller steps correspond to more continuous motion). For all δ they find a Manna class dynamical phase transition (fig. 3.2a). Wilken et al. (2021) observe what happens in the $\varepsilon \to 0$ limit (small steps / time-continuous): at $d = 3$ spatial dimensions, exactly at $\delta = 0$ (fully random displacements) the critical BRO packing density converges to about ≈ 20%, a value close to the critical density of the random organization model of Milz and Schmiedeberg (2013), which lies at ≈ 15% (where the difference is likely due to differences in the exact protocol). For *all* $\delta > 0$ however, Φ_c converges to a value extremely close to the athermal jamming density $\Phi_J \approx 64\%$ (fig. 3.2b) and the absorbing phase configurations near the critical point boast properties commonly associated with random close packing of spheres[3].

Note that this kind of link to jamming is the main motivation for my exploration of analytical random organization descriptions in chapter 4, where, with view to the $\varepsilon \to 0$ limit in Wilken et al. (2021) and Wilken et al. (2023), I try to write down time-continuous dynamical equations. If these methods turn out fruitful, links to jamming physics could be made by introducing the bias; the investigation into this is ongoing.

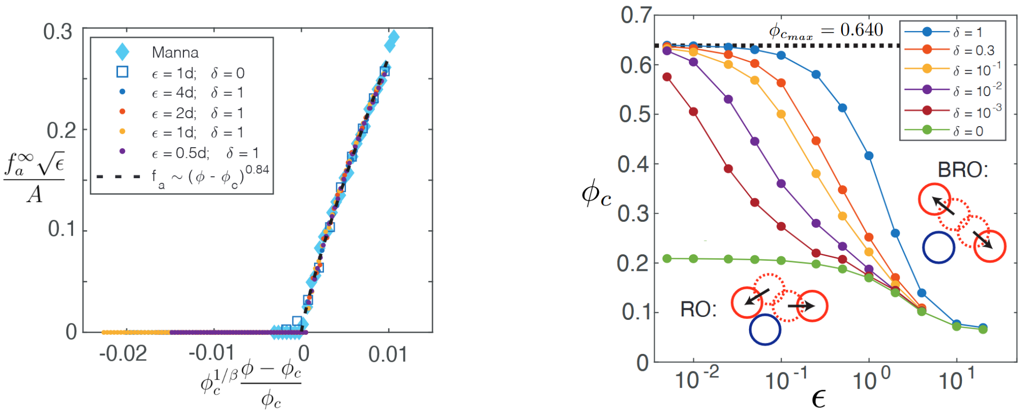

(a) Measured universal scaling near transition

(b) Small jump size limit of the critical density Φ_c

Figure 3.2: Fig. 2a (left) and fig. 1 (right) from Wilken et al. (2021)

---

[3] A not very well defined state of a system of spheres, supposed to be as dense as possible while still being randomly arranged (Bernal and Mason 1960), as opposed to crystalline or otherwise regular. Experiments and protocols claiming to produce and study such packings tend to find them at $\Phi \approx 64\%$ (Wilken et al. 2021)

3.2 Theory of Manna Class Critical Behaviour

3.2.1 Phenomenological Field Equations

Simulation studies like Corté et al. (2008) and Wilken et al. (2021) usually come with more intentions than just studying the critical behaviour of any given universality class. The former, as presented in the introduction, models the physics of sheared colloid suspensions, while the latter, as just discussed, intends to link such models to the physics of jamming. In contrast, the study of the universal behaviour can be comparatively simplified, since it suffices to study the most approachable representative of any given universality class.

Lattice Models According to Wiese (2016, sec. IV) the following model, referred to as a *stochastic sandpile*, is a representative of the Manna universality class: distribute grains at a given density ρ on some lattice. This grain distribution is changed in discrete time steps according to the following protocol: if any given site is occupied by more than one grain, these grains will be randomly redistributed to neighbouring sites[4]. Such sandpiles have been the subject of simulation studies into Manna class behaviour (for example Dantas et al. 2006) and analytical theories that write down Master-equations for the probability distribution of the grain configurations (for example Wijland, Oerding, and Hilhorst 1998).

The analogy to random organization is self-evident and unsurprisingly, the grain-density ρ serves as the control parameter in a dynamical phase transition, that has the active grain density ρ_A as an order parameter: below some critical grain density ρ_c all grains eventually find a lattice site on which they are alone, while above the critical density grains move around indefinitely (see fig. 3.3). The two phases are separated by a continuous transition, towards which the time τ it takes to find the absorbing configuration diverges, all with exponents in line with the Manna universality class.

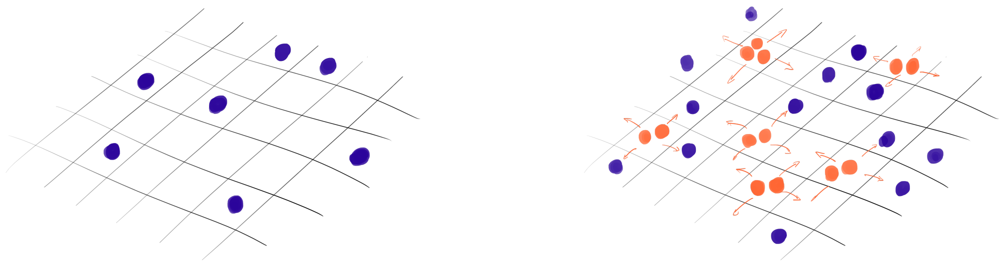
(a) absorbing phase (b) active phase

Figure 3.3: Visualization of the Stochastic sandpile, depicting a snapshot of the steady-state of the system in either phase

---

[4] a very similar model was introduced in Manna (1991) for the related purpose of studying the paradigm of self-organized criticality; I mention this because the author donated their name to the universality class, but self-organized criticality publication is of no further relevance here

Wiese (2016, sec. VI) obtains a mean-field theory for the stochastic sandpile by considering the $d \to \infty$ limit, that is in the approximation that all sites have an immediate connection. This allows ignoring the spatial dependencies and focusing entirely on the balance of the rate of activation of inactive grains $A+I \to 2A$ an the decay of active grains to inactivity $A \to I$ by landing on empty lattice sites. The result are reaction equations of the form

$$\frac{\partial \rho_A(t)}{\partial t} = -\underbrace{\mu\rho_A(t)}_{\substack{\text{deacti-}\\ \text{vation}}} + \underbrace{\lambda\,\rho_A(t)\,(\rho - \rho_A(t))}_{\substack{\text{activation of}\\ \text{inactive grains}}} \tag{3.1}$$

where the coefficients of the various terms vary from author to author (see for example Pastor-Satorras and Vespignani 2000; Wijland 2002), because, as explained in next in section 3.2.1, these reaction-equations are extended to stochastic field theories. To get spatial dependence back into the picture, the $d \to \infty$ behaviour is assumed to hold locally, while grain density ρ and the density $\rho_A(t)$ of active grains can still vary in space; this is similar to the adiabatic approximation in hydrodynamics, that allows talking about local thermal equilibrium and spatially varying temperature or pressure. Since the replacement of the active grains is uniformly random in the simplified $d \to \infty$ treatment, the statistics of motion after giving ρ_A and ρ an additional spatial dependence are argued to be that of random walks. Hence

$$\frac{\partial \rho_A(\boldsymbol{r},t)}{\partial t} = D\nabla^2\rho_A(\boldsymbol{r},t) - \mu\rho_A + \lambda\,\rho_A(\boldsymbol{r},t)\,(\rho(\boldsymbol{r},t) - \rho_A(\boldsymbol{r},t)) \tag{3.2}$$

Furthermore, local particle conservation is respected by making the grain density ρ evolve according to

$$\frac{\partial \rho(\boldsymbol{r},t)}{\partial t} = D\nabla^2\rho_A \tag{3.3}$$

The latter equation also entails, that inactive grains do not diffuse, since matter transport apparently is given entirely by active grain diffusion.

Very similar and, also reportedly in the conserved directed percolation class, is the *conserved lattice gas* studied numerically by Rossi, Pastor-Satorras, and Vespignani (2000): initially, grains are randomly distributed on a lattice with no double-occupancy. If all grains who have neighbours are then considered active and get, if possible, moved randomly to any neighbouring empty site; control- and order-parameter are respectively grain density ρ and active grain density ρ_A, just as in the stochastic sandpile.

Compared to simulations of grains with continuous positions, the lattice models are benign (in terms of memory and compute) and simplistic, making them excellent vehicles for understanding the universality class their dynamical transition belongs to. The conserved lattice gas, for example, lead the authors to conjecture

> "[...] in the absence of additional symmetries, absorbing phase transitions in systems with stochastic dynamics in which the order parameter is locally coupled to a static conserved field define a single and new universality class" (Rossi, Pastor-Satorras, and Vespignani 2000, concolusion)

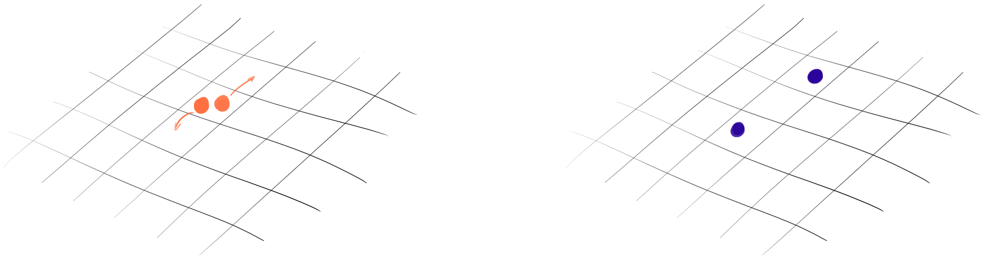

(a) deactivation $A \to I$

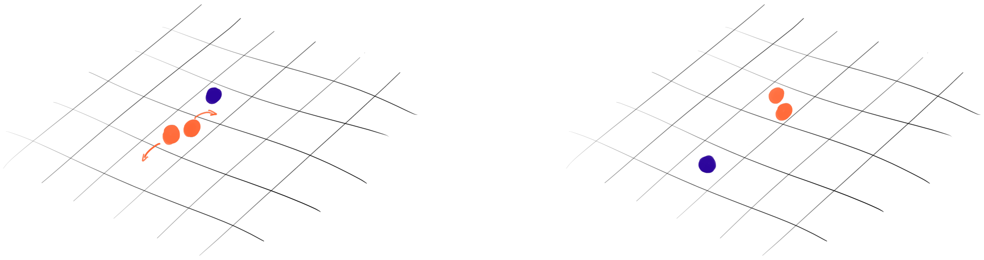

(b) activation $A + I \to 2A$

Figure 3.4: Visualization of the competing processes in the stochastic sandpile; time runs from left to right in either subfigure.

where *absorbing phase transition* is a synonym for absorbing state transition. The universality class they are referring to is CDP. This conjecture echoes a similar one attributed to Janssen and Grassberger, that any continuous absorbing state transition (with a scalar, real, non-negative order-parameter) emerging from short-ranged interactions with a *unique* absorbing state and no further features (like additional symmetries) lie in the DP universality class (Janssen 1981; Grassberger 1982; Hinrichsen 2000). It remains to be seen if they hold true in this form.

Stochastic Field Theories for the Manna Class The purely analytical study of the Manna transition is dominated by stochastic field theories and their analysis with the renormalization flow method. As explained in section 2.2.3, one of the central differences between regimes in which mean-field theory is very accurate and regimes where it fails (notably by predicting inaccurate critical exponents) is whether fluctuations can be neglected on large scales or not. In transitions where they can be ignored, mean-field behaviour delivers a very complete picture of the transition's physics. As further discussed in section 2.2.3, given a mean-field theory, a properly chosen noise can be added to obtain a theory, in form of a Langevin equation, that is accurate even below the upper critical dimension. Doing so for the mean-field equation of the stochastic sandpile eq. (3.2) would yield such a description.

As explained in section 2.2.4, when the goal is to understand the critical behaviour of a system with the renormalization semigroup, the presence of a coupling is more essential than the values of the coupling constants. Their exact value is subject change under the rescaling operations leading to the critical point. When the goal is to capture more than just critical behaviour, of course, one may set the constants to more specific values or otherwise constrain them and include couplings that are irrelevant in the RG sense. Langevin equations for the Manna class tend to be given in a form similar to this (and hence feature the relevant couplings leading to the Manna fixed point):

$$\begin{aligned}\frac{\partial \rho_A}{\partial t} &= D\nabla^2\rho_A - \mu_1\rho_A - \mu_2\rho_A^2 + \lambda\rho_A\rho + \kappa\sqrt{\rho_A}\zeta \\ \frac{\partial \rho}{\partial t} &= D\nabla^2\rho_A\end{aligned} \tag{3.4}$$

(compare Doussal and Wiese 2015, eqs. 4 and 5; Janssen and Stenull 2016, eqs. 2.8) where $\zeta(\boldsymbol{r}, t)$ is spatio-temporal Gaussian white noise from eq. (2.50); it read

$$\begin{aligned}\big\langle\zeta(\boldsymbol{r},t)\big\rangle_{\text{noise}} &= 0 \\ \big\langle\zeta(\boldsymbol{r},t)\zeta(\boldsymbol{r}',t')\big\rangle_{\text{noise}} &= \delta(\boldsymbol{r}'-\boldsymbol{r})\,\delta(t'-t)\end{aligned}$$

with $\langle\cdots\rangle_{\text{noise}}$ denoting the average with respect to the noise degrees-of-freedom only. Mapping to a field-theory with the recipe described at the end of section 2.2.3 and treating it to the renormalization flow fixed point analysis sketched in section 2.2.4 allows computing the critical exponents of the Manna class (compare Wiese 2024, leadup to eqs. 25 - 28). Given that the involved quantities and constants can have vastly different names depending on the authors, the form of eq. (3.4) has been chosen to keep quantities and equations recognizable and comparable across this text.

Adding an appropriate noise term on a mean-field theory to obtain a Langevin description valid below the upper critical dimension caters well to the intuitions surrounding the role of fluctuations in the applicability of mean-field treatments (see section 2.2.3). It should be noted however, that it is not the only (and in fact no the first) way in which people have arrived at a field theory description of conserved directed percolation. In Wijland, Oerding, and Hilhorst (1998), whose work is linked to conserved directed percolation by Pastor-Satorras and Vespignani (2000), the starting point and reference frame is a reaction-diffusion system involving two species of reagents A and I (that I have suggestively renamed here relative to the source material in order to avoid confusion with related results). They each diffuse with constants D_A and D_I respectively and are involved in two reactions: spontaneous decay $A \to I$ and proliferation $A+I \to 2A$ of A-reagents. The concentrations of either reagent will relax to a steady-state given by the balance of the two reactions. The steady state concentration of A-reagents serves as the order parameter of an absorbing state transition, that has the ratio of the reaction rates as its control parameter: in one phase $A \to I$ dominates $A + I \to 2A$ and the A species dies out, while in the other $A + I \to 2A$ out-runs decays $A \to I$, leading to a finite steady state concentration (which serves as the order parameter). Writing down the reaction-diffusion equations of this problem would be a mean-field theory, since such equations do not model noise in any way. To get beyond mean-field Wijland, Oerding, and Hilhorst (1998) formulate a lattice model of the reaction-diffusion system: reagent particles take positions on the lattice sites and perform random walks at rates proportional to D_I and D_A respectively. Sites can be occupied by arbitrarily many particles and reactions only occur between particles on the same site. They derive the master equation for the model by understanding the probability distribution as a state-vector $|P\rangle$ on which an operator acts, that generates the sought reactions and diffusion. Thanks to the analogy of this approach to quantum systems, they can derive an associated "action $S[A, A^*, I, I^*]$" in terms of "classical fields $A(\boldsymbol{r}, t)$, $A^*(\boldsymbol{r}, t)$, $I(\boldsymbol{r}, t)$ and $I^*(\boldsymbol{r}, t)$" (leaning heavily into quantum lingo). In terms of the concepts introduced in section 2.2.2, S is[5] the exponent of the weight $\exp(S)$ with A and I as order-parameter candidates. A^* and I^* are the corresponding response fields. The second set of fields I and I^* are the bookkeeping device with which the authors implement reagent-number conservation (i.e. the coupling to a *conserved field*): they are a limited resource for A-proliferation $A + I \to 2A$ that can only be replenished by the decay $A \to I$.

Remark on the Ambiguity of Coupling Constants Not only the values, but the precise interpretation and derivation of any given term in these models can vary wildly. This is not necessarily a weakness, but a feature of the field theory approach: it reflects that the many different models of a given universality class all behave in the same way towards the critical point. Hence, this kind of ansatz is similar in spirit and method to Landau-Ginzburg theory in its purposeful ignorance. None of the terms specify what, on a small scale, the activation process looks like, whether the grains scatter or not while getting close enough to react, in what configuration *exactly* particles have to be to react (imagine penetrable eccentric ellipses versus penetrable spheres, penetrable cubes, etc.); such variance could never be captured in the few free parameters in eq. (3.4).

---

[5] With the subtle difference that they insert their boundary conditions as terms into the action instead of postponing their insertion to the choice spatio-temporal evolutions to include in the path-integral

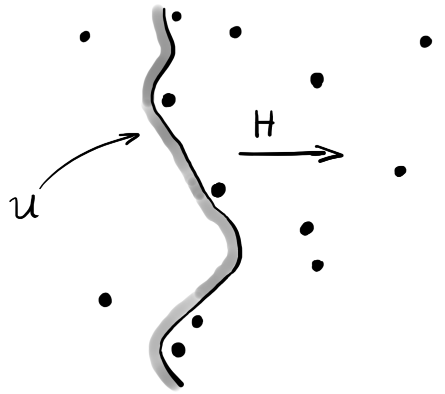

Figure 3.5: Random surface as described by eq. (3.5) with displacement field $u(\boldsymbol{r},t)$ (black line with shade) whose shape is relaxed by $\nabla^2 u(\boldsymbol{r},t)$ but subject to spatially random forcing $f(\boldsymbol{r},u(\boldsymbol{r},t))$ (here in the form of impurities symbolized by the black dots) and an homogeneously applied external forcing field of strength H

A good example for how abstract these models are, is the following entry to Manna-class transitions, identified as such by Doussal and Wiese (2015): the *quenched Edwards-Wilkinson model*, a simplified description of random surfaces under (spatially) random forcing:

$$\frac{\partial u(\boldsymbol{r},t)}{\partial t} = \nabla^2 u(\boldsymbol{r},t) + f(\boldsymbol{r},u(\boldsymbol{r},t)) + H \tag{3.5}$$

Here $u(\boldsymbol{r},t)$ is the displacement field of the surface (a scalar, for simplicity, i.e. displacement is assumed to only happen in one direction) and $f(\boldsymbol{r},u)$ is the random forcing that the surface experiences around $\boldsymbol{r}$ given it is displaced there by u. $\nabla^2 u$ models the relaxation of stress in the surface caused by the displacement field being different at two close-by locations. An example application of the quenched Edwards-Wilkinson model are Weiss-domains in ferromagnets under the pressure of an external magnetic field H, which are pinned in place by crystal impurities (fig. 3.5) below a critical external forcing $H < H_\mathrm{c}$ (analogous to the absorbing phase in random organization) but indefinitely shifting for $H > H_\mathrm{c}$ (analogous to the active phase). At face value, this model seems unrelated to grains on lattices or sheared suspensions. In fact, it does not look like eq. (3.4). It can however be mapped to the Manna class equations in a non-obvious manner.

3.2.2 Relationship to Non-Conserved Directed Percolation

Similarities and Differences in Theory DP and Manna systems are very similar, which still warrants some discussion: both of them are a feature of respective absorbing state transitions. Both of their theories can be understood as driven by the competition between proliferation and decay of a an active physical state in an otherwise passive system. It is, however, widely believed that, despite the similarities, DP and Manna are distinct universality classes (Pastor-Satorras and Vespignani 2000; Hinrichsen 2000; Lubeck 2004; Corté et al. 2008; Doussal and Wiese 2015; Janssen and Stenull 2016; Wilken et al. 2021) though the closeness of many of their critical exponents (Rossi, Pastor-Satorras, and Vespignani 2000; Milz and Schmiedeberg 2013) and the ambiguity of what exactly should constitute a universality class far from equilibrium advise some caution. In what follows I will stick to the understanding found in literature, that DP and Manna are distinct. On this note, a side-by-side comparison of the terms appearing in the Langevin equations eq. (2.54) for DP and eq. (3.4) Manna

class	free propagation	interaction	coupling to conserved field	noise
CDP	$\left({}^{\partial}/_{\partial t} - D\nabla^2 + \mu_1\right)\rho_A$	$-\mu_2\rho_A^2$	$+\lambda\rho_A\rho$	$\kappa\sqrt{\rho_A}\zeta$
DP	$\left({}^{\partial}/_{\partial t} - D\nabla^2 - \alpha\right)w$	$-({}^1/_2)g\,w^2$	n.a.	$\kappa\sqrt{w}\zeta$

show that the only coupling differentiating them is the Manna class coupling to the conserved field ρ (Doussal and Wiese 2015). This is another perspective from which to justify the synonym conserved directed percolation for the Manna class. When neglecting the noise in both models (such that we are dealing with their mean-field theories) and choose the Manna system to be spatially homogenous by making $\rho(\boldsymbol{r}, t)$ a constant ρ, then one can joint the $\lambda\rho \cdot \rho_A$ and $-\mu_1\rho_A$ term into one $(\gamma\rho - \mu_1)\rho_A$. Unsurprisingly, the mean-field exponents are hence also the same (Lubeck 2004, app. A.3).

My Own Thoughts That Manna class models can draw only on a conserved and hence locally limited number of particles (Corté et al. 2008) has an important consequence, that explains why it might make such an important qualitative difference: in directed lattice percolation problems (see fig. 2.2), whether or not the neighbouring sites of a wet site will be wet in the subsequent time step, are statistically independent events. This is not the case in random organization: an active grain that is busy activating one part of its neighbourhood by jumping there cannot at the same time do so in the opposite direction. If one wanted capture such physics faithfully with directed percolation on a lattice, it would be necessary to introduce a book-keeping device into the model that tracks grains and correlates the probability of activations accordingly. This circumstance also makes any map between established DP models and Manna models like the conserved lattice gas or stochastic sandpile (not to speak of space-continuous random organization) necessarily unfaithful.

Put another way: say one attempted a map from a random organization model to a percolation problem on a directed lattice. Nothing stops one from declaring spatial lattice sites in the percolation problem as a tiling of the space that grains from a random organization model can occupy. One may then proceed to declare, that wet sites indicate the presence of active grains (which bears the possibility of activating neighbouring "regions of space" as represented by the percolation problem's lattice sites). One can even suggest an effective bond probability p given some grain density ρ. Though, again, one has to mind, that activations are correlated in random organization but independent in directed percolation on lattices. Furthermore, grains are tracked in random organization, for which there is no analogous device available in the directed lattice percolation problem. This makes it hard to justify assuming, that one timestep in random organization corresponds to one timestep in the other model. A salvaging attempt would be to try and identify one time step in the directed lattice percolation with multiple steps in random organization; the idea behind this is the hope, that, after multiple steps of moving, the correlations between simultaneous close-by activations may be low enough to assume statistical independence. While there is no arguing against this, there clearly is a lot of room for choice and hence ultimately ambiguity in the map.

I do not rule out however that introducing correlation in a well studied DP model may make it resemble the coupling to a conserved quantity. This still leaves the grain tracking question unanswered, however. Hence, to be quantitatively accurate, probably such a model still requires a priori information on how the positions of grains correlate. Ideally, an analytic description of random organization should *predict* these correlations, not require them. This is not to say, that there is no possibility of some processes in random organization, biased random organization, etc. displaying some variant of directed percolation behaviour. However once more, without tracking grains, there is probably no way to make quantitative predictions about anything that involves the correlation of grain positions (like critical density). *Given* a packing structure, however, a DP problem may serve to analyse how activity propagates.

4 Attempts at Critical Packing Density

The aim here is to introduce analytical models which encode the critical packing density of random organization (or overlap reduction protocols more generally). The analytical studies of absorbing state transitions from literature that I presented earlier are not suited for this task: these Landau-Ginzburg-reminiscent large-scale phenomenological field theories are geared towards studying critical behaviour with renormalization flow methods. Details on microscopic length scales become irrelevant as the descriptions for all models of the same universality class unify towards the critical point. The packing density is, however, linked to exactly such small scale details, making, for example, the difference between random organization and biased random organization behaviour (which have different critical packing densities) or the differing densest packings for grains of different shapes (think, for example, of spherical versus very eccentric ellipsoid grains, given that they can rotate). In order to resolve this level of spatial detail, we require a language allows expressing the entire grain shape. In the following I present my attempts at, if one may call it that, first-principles analytical calculations to that end.

In section 4.1 I discuss the simplest possible model I could think of that still produced a critical packing density. That model turned out to not be very extendable, hence in section 4.2 I derive a time-continuous variant of random organization (which can be thought of as the formal $\varepsilon \to 0$ limit of the random organization protocol of Wilken et al. (2021)). Unfortunately, the generator of time evolution in the resulting equation eq. (4.13) contains many higher order terms. Hence my final attempt section 4.3 tries to circumvent these higher order terms by setting up a reaction system with only two-body interaction vertices; this is achieved by making activation and deactivation gradual instead of instantaneous. I am still investigating how fruitful this last approach is, but will present preliminary insights that compel me to continue.

4.1 Structureless Random Replacement

Intentions Recall the mean-field stochastic sandpile from section 3.2.1: grains are assumed to have no spatial correlations and are replaced to *any* location in the system every time step. Given the dramatic simplicity that these assumptions can provide, I decided to investigate, analogously, what happens when I assume that the grains in the overlap reducing protocol are, in analogy to the mean-field sandpile, both (1) replaced with uniform probability density somewhere in the finite but large box while (2) neglecting spatial correlations (see illustrating fig. 4.2).

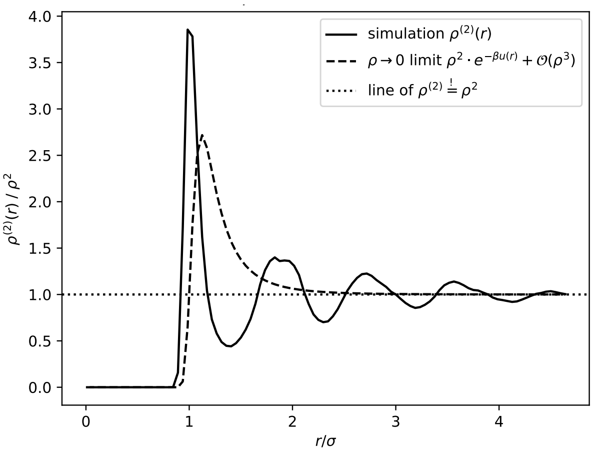

Figure 4.1: Typical $g(r)$ curves for a homogeneous simple fluid in thermal equilibrium, where the constituent molecules interacting with the isotropic as the Lennard-Jones pair-potential $u(r) = 4\varepsilon((^{\sigma}/_{r})^{12} - (^{\sigma}/_{r})^{6})$. σ can be thought of as the molecule diameter. The dashed curve is an analytical expansion of up until second order in density, while the solid curve is obtained from Metropolis-Hastings sampling of the canonical ensemble for the system at packing density $\Phi = 60\%$ and $k_\mathrm{B}T = \varepsilon$. The dotted line is the structure (or rather lack thereof) I am assuming to arrive at eq. (4.3)

Describing Spatial Correlations The latter point (2) can be expressed with the *radial distribution function* $g(r)$: it is obtained by taking the continuous version of a histogram of pair locations $(\boldsymbol{r}_1, \boldsymbol{r}_2)$, the so called *pair density*, *two-point density* or *two-body density* $\rho^{(2)}(\boldsymbol{r}_1, \boldsymbol{r}_2)$ and normalizing it with the product of densities $\rho(\boldsymbol{r}_1) \cdot \rho(\boldsymbol{r}_2)$. The latter is done to eliminate the effects of possible inhomogeneity in the density profile $\rho(\boldsymbol{r})$, isolating the (purely local) influence of grain interactions. In a homogeneous, isotropic system the two-point density only depends on the distance between its arguments and $\rho^{(2)}(\boldsymbol{r}_1, \boldsymbol{r}_2) = \rho^{(2)}(|\boldsymbol{r}_1 - \boldsymbol{r}_2|) = \rho^2 g(|\boldsymbol{r}_1 - \boldsymbol{r}_2|)$. A typical form for $g(r)$ can be found in simple fluids, as depicted in fig. 4.1: the distribution function is $g(r) \approx 0$ for r smaller than the molecule extension σ, indicating their *mutual exclusion volume*. For $r > 0$ pair-distances oscillate between being being above and below average likely, but this oscillation quickly tampers to $g(r) = 1$ (no correlation) as $r \gg \sigma$. To connect it to the previously introduced concept of a two-point cumulant: in a theory where $\rho(\boldsymbol{r})$ is a Landau-Ginzburg-like order parameter one could write

$$g(\boldsymbol{r}_2, \boldsymbol{r}_1) - 1 := \frac{\langle \rho(\boldsymbol{r}_1)\rho(\boldsymbol{r}_2)\rangle_\mathrm{c}}{\langle \rho(\boldsymbol{r}_1)\rangle \cdot \langle \rho(\boldsymbol{r}_2)\rangle} \tag{4.1}$$

Further assuming a homogeneous and isotropic system $\rho(\boldsymbol{r}) \equiv \rho$ will have the effect that $g(\boldsymbol{r}_2, \boldsymbol{r}_1)$ only depend on the distance $|\boldsymbol{r}_2 - \boldsymbol{r}_1|$. My mean-field approximation now consists of neglecting correlations altogether, and have $g(r) \equiv 1$. In an infinite system $N, V \to \infty$ this is the same as assuming the points are distributed in a *Poisson point cloud* (or *Poisson point process*), which means that grain locations are statistically independent of each other. One consequence of this is that the number of grains $N(U)$ in any given finite volume U is a Poisson distributed random variable with mean ρU (assuming homogeneous grain density ρ); hence the name.

Note, that a system of extended grains with packing density Φ distributed in a

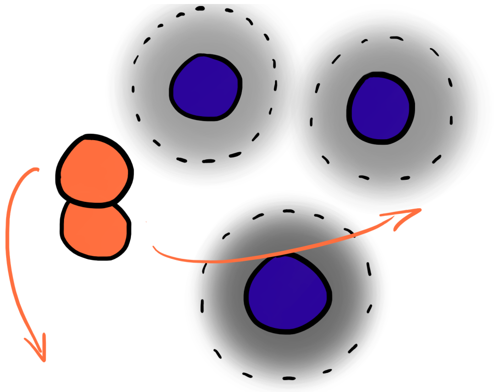

Figure 4.2: Visualization of the overlap reducing protocol approximated eq. (4.3): grains that overlap (bright orange) will in the next timestep be replaced randomly, independently from each other and uniformly in the system. The probability of landing in the shaded areas (where the grain) is estimated by the probability $1 - T(B)$ that there is a cavity at least two grain diameters across. In eq. (4.2), the correlation of grain positions is neglected (hence the name structureless random replacement) by using the Poisson point cloud expression for $1 - T(B)$

Poisson point cloud has a non-negotiable density[1] of grains with overlaps. Obviously, this value can only change when the density changes. So when I say, that we assume a Poisson point cloud, this is not meant literally: instead, I am estimating in every time step, that the probability of finding a cavity at least the size of a grain, i.e. the probability of finding a vacant spot for a grain to be overlap free, is the same as in a Poisson point cloud. Moving on: this probability is given by one minus the so called *capacity functional* (Baddeley 2007)

$$1 - T(B) = P\left(N(B) > 0\right) = e^{-2^d \Phi} \tag{4.2}$$

where B is a ball of radius σ, into which one can exactly fit a spherical grain of diameter σ without any other grains at the surface of B and beyond being able to overlap with it.

Mean-Field Iteration Equation The probability of any active grain landing on some inactive grain after replacing it is given by the fraction of volume that the inactive grain takes up. This fraction can be estimated by $(N - N_A) \cdot \Phi / N$. Thus the expectation value $N_A(t)$ of the number of active grains changes from t to $t + 1$ with

$$\underbrace{N_A(t+1) - N_A(t)}_{\substack{\text{change in} \\ \text{active grain number}}} = - \underbrace{N_A(t) \cdot e^{-2^d \Phi}}_{\substack{\text{number of grains} \\ \text{finding vacant spots} \\ \text{by eq. (4.2)}}} + \underbrace{N_A(t) \cdot (N - N_A(t)) \cdot \frac{\Phi}{N}}_{\substack{\text{number of previously inactive grains} \\ \text{that an active grain will land on}}} \tag{4.3}$$

The stationary value at $t \to \infty$ is obtained by assuming $\lim_{t\to\infty} N_A(t) =: N_A^\infty$ exists and taking the $t \to \infty$ limit on both sides

$$N_A^\infty \cdot e^{-2^d \Phi} = N_A^\infty (N - N_A^\infty) \cdot \Phi / N \tag{4.4}$$

---

[1] calculating this is an easy, but instructive exercise in the theory of point clouds, see for example Baddeley (2007) of grains involved in overlaps $\Phi_A = \Phi(1 - \exp(2^d \Phi))$ for notes

This equation for N_A^∞ is solved by either 0 (which I interpret as the absorbing phase) or $1 - N_A^\infty/N = e^{-2^d\Phi}/\Phi$ (which I interpret as the steady state value in the active phase). Since we know that the transition is continuous, solving the active phase expression $N_A^\infty(\Phi) = 0$ for the packing density should give us the critical point Φ_c. Doing so results in

$$\Phi_\mathrm{c} = e^{-2^d\Phi_\mathrm{c}} \tag{4.5}$$

See table 4.1 for a comparison with three literature values.

d	eq. (4.5) (rounded)	Milz and Schmiedeberg (2013)	Wilken et al. (2021)
2	0.301	0.336 ± 0.002	n.a.
3	0.2007	0.1505 ± 0.0005	0.20 [sic]

Table 4.1: Comparison of measured (from different random-organization like protocols) zero-strain-amplitude critical packing densities of with the estimates rendered by structureless random replacement.

Exponents Since the active phase relationship between N_A^∞ and Φ eq. (4.4) is analytic in $\Phi = \Phi_\mathrm{c}$, the order-parameter exponent β is an integer, given by the leading order in the Taylor expansion

$$\begin{aligned} N_A^\infty &= 1 - \frac{e^{-2^d}}{\Phi} \\ &= \underbrace{\left[1 - \frac{e^{-2^d\Phi}}{\Phi}\right]\Bigg|_{\Phi=\Phi_\mathrm{c}}}_{=0 \text{ by eq. (4.5)}} + \underbrace{\frac{\partial}{\partial(\Phi-\Phi_\mathrm{c})}\left(1 - \frac{e^{-2^d\Phi}}{\Phi}\right)\Bigg|_{\Phi=\Phi_\mathrm{c}} \cdot (\Phi-\Phi_\mathrm{c})}_{=(2^d+1/\Phi_\mathrm{c})>0, \text{ by eq. (4.5)}} + \mathcal{O}\left((\Phi-\Phi_\mathrm{c})^2\right) \\ &\sim |\Phi - \Phi_\mathrm{c}| \end{aligned} \tag{4.6}$$

meaning we have $\beta = 1$ for this, putatively mean-field, theory. We can also check how $N_A(t)$ behaves right at the critical point by inserting eq. (4.5) into eq. (4.3), resulting in

$$N_A(t+1) - N_A(t) = -\frac{\Phi_\mathrm{c}}{N} \cdot N_A(t)^2 \tag{4.7}$$

We can find a continuum limit of this equation as $t \gg 1$ by introducing units of time with a timestep $\mathrm{d}t$ and choosing to scale the system size inversely with $\mathrm{d}t$. To be more precise, we demand that $N\,\mathrm{d}t \equiv {}^1\!/\!_\eta$ remains constant, to the effect

$$\frac{\mathrm{d}N_A}{\mathrm{d}t} = -\eta\Phi_\mathrm{c} \cdot N_A(t)^2 \tag{4.8}$$

which by separation of variables is easily solved and has asymptotic $t \to \infty$ behaviour given by

$$N_A(t) = \frac{1}{{}^1\!/\!_{N_A(0)} + \eta\Phi_\mathrm{c}t} \sim t^{-1} \tag{4.9}$$

off which we read $\nu_\parallel = 1$. Since by design there is no spatial dependence in this model, there is no value for $\nu_\perp$. So far these mean-field exponents align with β and $\nu_\perp$ of DP and CDP (table 2.1).

Conclusion As displayed in table 4.1, eq. (4.5) is not completely off the two listed measurements. Unfortunately, without some means of tracking where the grains are, there seems to be no clear way to improve this estimate without assuming a $g(r)$ a priori by inserting it into $T(B)$, which would defeat the purpose of finding theories for the value of critical density that have predictive power.

4.2 Fokker-Planck Equation

Evolution Equation The next idea I considered was writing down a Fokker-Planck equation for the many body probability distribution $P(\boldsymbol{x}_1, \dots, \boldsymbol{x}_N)$ of a configurations of N grains that perform Brownian motion when they overlap. It may be derived from the Langevin-equation-like stochastic differential equation

$$\dot{\boldsymbol{x}}_k(t) = \mathbf{1}\{\text{grain } k \text{ has overlap}\} \cdot \boldsymbol{\zeta}_k(t) \tag{4.10}$$

where $\mathbf{1}\{\cdots\}$ is the indicator function of the event described in the curly braces and the $\boldsymbol{\zeta}_k(t)$ are mutually independent temporally uncorrelated noises dictating the velocities $\dot{\boldsymbol{x}}_k(t)$ of their grains' positions, obeying

$$\langle \boldsymbol{\zeta}_k(t) \rangle = 0 \tag{4.11}$$

$$\langle \boldsymbol{\zeta}_k(t) \otimes \boldsymbol{\zeta}_{k'}(t') \rangle = 2D \cdot \delta_{k,k'} \cdot \delta(t - t') \cdot \mathbb{1} \tag{4.12}$$

where $\otimes$ denotes the outer product, employed to avoid too many indices, and D is the diffusion constant of the random walk. The dynamics eq. (4.10) are a time-continuous formulation of zero strain-amplitude[2] random organization, translating to "grain k performs Brownian motion if and only if it overlaps any other grain". One can derive from this (Garcia-Palacios 2007, sec. 5.3) an evolution equation for the probability distribution $P(\boldsymbol{x}_1, \dots, \boldsymbol{x}_N, t)$ of N-grain configurations at time t

$$\frac{\partial P}{\partial t} = \sum_k D \nabla_k^2 \left(\mathbf{1}\{\text{grain } k \text{ has overlap}\} \cdot P \right) \tag{4.13}$$

where ∇_k is the gradient with respect to the position $\boldsymbol{x}_k$. The interpretation of this equation is simple when recalling the diffusion equation $\partial/\partial t P(\boldsymbol{x}, t) = D\nabla^2 P(\boldsymbol{x}, t)$: if the indicators $\mathbf{1}\{\cdots\}$ were not present (i.e. just equal to 1) every term $D\nabla_k^2$ would just generate diffusion of grain k. The presence of the indicator $\mathbf{1}\{\text{grain } k \text{ has overlap}\}$ now turns off diffusion for grain k if it does not meet the requirement of having an overlap.

Most Likely Dead Ends It is, however, not clear how to proceed from here in gaining any insight on the general system with N grains analytically. One reason for this is that $\mathbf{1}\{\text{grain } k \text{ has overlap}\}$ depends on all grain positions in a way that does not reduce to any handleable algebraic expression in terms of the pair overlap indicators, which are just given by the grain *form factor*

$$\mathbf{1}\{\text{grains } j \text{ and } k \text{ overlap}\} = \Theta(\sigma - |\boldsymbol{r}_j - \boldsymbol{r}_k|) \tag{4.14}$$

---

[2] Introducing the periodic straining from Corté et al. 2008 would be just a matter of adding onto $\dot{\boldsymbol{x}}_k$ the contribution to velocity $\boldsymbol{u}(\boldsymbol{r}, t)$ that a grain at position $\boldsymbol{r}$ experiences at time t due to the shearing of the surrounding fluid. This would result in a drift term in eq. (4.13)

where $\Theta(x)$ is the Heaviside step function. Instead, by inverting the statement "k has no overlap" one gets "every grain $j \neq k$ does not overlap with k", which can be expressed in terms of indicator functions as

$$1 - \mathbf{1}\{\text{grain } k \text{ has overlap}\} = \prod_{j \neq k} (1 - \mathbf{1}\{\text{grains } j \text{ and } k \text{ overlap}\}) \tag{4.15}$$

where we used that logical `AND` translates into multiplication of indicators $\mathbf{1}\{\cdots\}\mathbf{1}\{\cdots\}$ and logical `NOT` into $1 - \mathbf{1}\{\cdots\}$. Multiplying out the right hand side of eq. (4.15) results in an inclusion-exclusion principle reminiscent expression

$$\begin{aligned} &1 - \mathbf{1}\{\text{grain } k \text{ has overlap}\} \\ &\quad = \sum_{\mathcal{M} \subseteq \{1,\ldots,N\} \setminus \{k\}} (-1)^{|\mathcal{M}|} \prod_{m \in \mathcal{M}} \mathbf{1}\{\text{grains } m \text{ and } k \text{ overlap}\} \end{aligned} \tag{4.16}$$

clearly containing not only handleable two-body terms, but arbitrarily high (up to N) body terms.

To mend this, one may consider that it sounds plausible that one can neglect higher n-body terms at the densities of interest (i.e. around the density at which the dynamics can just barely eliminate all overlaps), because in a system of homogeneously distributed grains, one would expect any given grain to have fewer neighbours than in the densest packings, e.g. less than six (triangular crystal packing) for two-dimensional discs and less than twelve (face centre cubic packing) for three-dimensional spheres. However, since we are dealing with a discontinuously changing, discrete quantity, breaking the assumption of few overlaps results not in proportionate, small error as physicists are accustomed to, but in non-negligible discontinuous changes; simple example for how jarring this behaviour is can be easily seen with only $N = 3$, where, if we, for brevity, define

$$O_{mk} := \mathbf{1}\{\text{grains } m \text{ and } k \text{ overlap}\} \tag{4.17}$$

the right hand side of eq. (4.16) becomes for e.g. $k = 1$

$$\begin{aligned} 1 - \mathbf{1}\{\text{grain } k \text{ has overlap}\} &= (-1)^{|\emptyset|} + (-1)^{|\{2\}|} O_{12} + (-1)^{|\{2\}|} O_{13} + (-1)^{|\{2,3\}|} O_{12} O_{13} \\ &= 1 - O_{12} - O_{13} + O_{12} O_{13} \end{aligned} \tag{4.18}$$

If we now "assume only pair overlaps" by neglecting $O_{12}O_{13}$ then in configurations where 1 overlaps with both grain 2 and 3 the supposed approximation results in

$$\begin{aligned} 1 - \mathbf{1}\{\text{grain } k \text{ has overlap}\} &= 1 - O_{12} - O_{13} + O_{12} O_{13} \\ &\approx 1 - O_{12} - O_{13} \\ &= 1 - 1 - 1 \\ &= -1 \end{aligned} \tag{4.19}$$

which is not even a logical value. Even if this was not a concern and one could cut off eq. (4.16) in eq. (4.13), surely there would be more than one overlap per particle at the critical density and hence terms higher than second or even third order in $\Theta(\sigma - r)$ would have to be included. Thus it becomes attractive to switch approaches, with the goal of dealing only with generators involving two-body terms.

4.3 Many-Body Reaction System

4.3.1 From Instantaneous Activation to Reactions

Ideas and Inspirations To make progress with understanding eq. (4.13), I took a hint from the reaction-diffusion realization of the Manna transition, such as Master equations for grains on a lattice like Rossi, Pastor-Satorras, and Vespignani (2000) or Pastor-Satorras and Vespignani (2000), or phenomenological field theories like Wijland, Oerding, and Hilhorst (1998), Janssen and Stenull (2016) or Wiese (2016), whose reaction terms are just one- and two-body in nature: I got the idea to relax the requirement that grain activation and deactivation must be instantaneous[3]. Instead, one can introduce active grains A and inactive grains I as two different species of grain, and have only active grains move around (say by diffusion or repulsion) while inactive grains are immobile; then two reactions would be introduced, with the goal of making our reaction system resemble overlap reducing protocols like random organization and biased random organization:

1. Active grains spontaneously decay into inactivity exponentially fast with rate μ
$$A \overset{\mu}{\to} I$$
2. Pairs of grains (j,k) closer than one diameter σ react with a *higher rate* $\lambda > \mu$ to a pair of active grains
$$a_j + a_k \xrightarrow{\lambda \cdot O_{jk}} 2A$$
where the $a_k \in \{A, I\}$ and O_{jk} is the indicator of overlap between j and k from eq. (4.17).

It is worth pausing briefly to recall what we want to do differently now: we detached being active from having overlaps and instead instate dynamics that make it *very unlikely* for an active grain to not be involved in an overlap and vice versa making it *very unlikely* for an inactive grain to have an overlap[4]. Since being active/inactive now is a degree of freedom, the outcome space has now been extended from $\{(\boldsymbol{x}_1, \dots, \boldsymbol{x}_N)\}$ to $\{((a_1, , \dots, a_N, \boldsymbol{x}_1, \dots, \boldsymbol{x}_N))\}$.

The benefit that this brings is the following: the proposed reactions involve only two-body terms but will relax to the correct activation state, albeit gradually (over the time-scales μ^{-1} and λ^{-1}). This is more helpful that relying on an infinite amount of arbitrarily high n-body terms for a instantaneous fool-proof check for whether a grain is involved in overlaps or not.

We expect to recover the behaviour of continuous-time random organization (see eq. (4.13)) in the limit $\lambda \gg \mu \gg \tau_{\text{motion}}^{-1}$ compared to the timescales[5] of active grain

---

[3] as it is in eq. (4.13)

[4] Note that this did not destroy any absorbing states: if all grains are overlap free and inactive, none of the introduced processes can give rise to activity again

[5] be that D/σ^2 for diffusion constant D or perhaps v/σ for repulsion with drift-velocity v that we could introduce if we want to imitate the deterministic displacements in Milz and Schmiedeberg 2013 or Wilken et al. 2023

motion τ_{motion}; this is because that limit (however carried out in practice) may be interpreted as sending to zero the characteristic times λ^{-1} and μ^{-1} it takes for the reactions to produce the correct state of activations.

However it is, at this stage, not necessarily clear how to best describe this mathematically, especially how exactly to implement that the reaction $a_j + a_k \to 2A$ only takes place when there is an overlap between j and k. In the following I will first discuss how one would implement this for one or two grains and then lead over on how to formulate it for an arbitrary number of grains in section 4.3.2.

One Isolated Grain An approach familiar to statistical physics is the derivation of a master equation. To proceed, we start with the simplest case where it is fairly obvious what to do: an isolated grain, i.e. a grain that does not and, for the time we are interested in it, will not overlap with other grains. If we choose $\lambda, \mu \gg D\sigma^{-2}$, this is a scenario one would expect to happen frequently at lower densities, where grains can easily find regions devoid of other grains. Reactions then happen so much faster than diffusion (tuned by D) that the latter does not play a role. In this situation the probabilities $P_a(t)$ of being active ($a = A$) or inactive ($a = I$) change in time by

$$\begin{aligned} \frac{\partial P_A(t)}{\partial t} &= -\mu \cdot P_A(t) \\ \frac{\partial P_I(t)}{\partial t} &= +\mu \cdot P_A(t) \end{aligned} \tag{4.20}$$

or as an evolution equation for the probability-covector via a rate matrix[6] equation

$$\frac{\partial}{\partial t} \begin{pmatrix} P_A(t) & P_I(t) \end{pmatrix} = \begin{pmatrix} P_A(t) & P_I(t) \end{pmatrix} \begin{pmatrix} -\mu & +\mu \\ 0 & 0 \end{pmatrix} \tag{4.21}$$

with solution (found for example by splitting into eigenvectors of the rate matrix)

$$\begin{aligned} P_A(t) &= P_A(0) \cdot e^{-\mu t} \\ P_I(t) &= P_I(0) \cdot (1 - e^{-\mu t}) \end{aligned} \tag{4.22}$$

i.e. an *exponentially fast* decay from $A \to I$, where $P_a(0)$ is the probability of the isolated grain being in activation state a at time 0. So, on timescales relative to which μ^{-1} is negligible, this decay to the correct activation state (namely inactivity I) is instantaneous.

Two Isolated Grains The next more complicated case is an *isolated grain pair* (j, k) undergoing the just described reactions; negligibility of motion now among other things means that we may assume that the positions $\boldsymbol{x}_j$ and $\boldsymbol{x}_k$ of the involved grains does not change and so neither does the indicator of overlap between j and k, that by eq. (4.17) reads $O_{jk} = \mathbf{1}\{|\boldsymbol{x}_j - \boldsymbol{x}_k| < \sigma\}$. The rate with which the joint probability P_{a_j,a_k} of grain j having activation state a_j and grain k activation state a_k changes is

---

[6] note that the matrix is not hermitian, which would preserve $\sum_a |P_a|^2$ instead of probability $\sum_a P_a$; hermitianess is replaced by all rows summing to zero

then given by

$$
\begin{aligned}
\frac{\partial P_{AA}(t)}{\partial t} &= \overbrace{(-\mu P_{AA}(t) - \mu P_{AA}(t))}^{\substack{\text{independent deactivation}\\ \text{of either grain}}} + \overbrace{\lambda \cdot O_{jk} \cdot (P_{AI}(t) + P_{IA}(t) + P_{II}(t))}^{\substack{\text{activation conditioned}\\ \text{on overlap between } j \text{ and } k}} \\
\frac{\partial P_{AI}(t)}{\partial t} &= (-\mu P_{AI}(t) + \mu P_{AA}(t)) - \lambda \cdot O_{jk} \cdot P_{AI}(t) \\
\frac{\partial P_{IA}(t)}{\partial t} &= (+\mu P_{AA}(t) - \mu P_{IA}(t)) - \lambda \cdot O_{jk} \cdot P_{IA}(t) \\
\frac{\partial P_{II}(t)}{\partial t} &= (+\mu P_{AI}(t) + \mu P_{IA}(t)) - \lambda \cdot O_{jk} \cdot P_{II}(t)
\end{aligned}
\tag{4.23}
$$

where we extended the single-grain equation of $A \to I$ from eq. (4.20) by first noting that in the case of $O_{jk} = 0$, where the behaviour is independent, the rate of change of an initially uncorrelated pair reads

$$
\begin{aligned}
\frac{\partial}{\partial t}\left(P_{a_j}(t)P_{a_k}(t)\right) &= \frac{\partial P_{a_j}(t)}{\partial t}P_{a_k}(t) + P_{a_j}(t)\frac{\partial P_{a_k}(t)}{\partial t} \\
&= \mu(\delta_{a_j,I} - \delta_{a_j,A})P_{A,j}(t)P_{a_k}(t) + \mu(\delta_{a_k,I} - \delta_{a_k,A})P_{a_j}(t)P_{A,k}(t)
\end{aligned}
$$

and then, by the argument that the decay term should have the same form in general, inferring what the two-grain decay term looks like by replacing $P_{a_j}P_{a_k} \rightsquigarrow P_{a_j,a_k}$. The corresponding evolution equation to eq. (4.23) for the probability-covector via a rate matrix equation reads

$$
\frac{\partial}{\partial t}\boldsymbol{P}(t) = \boldsymbol{P}(t)\left(Q_\mu + Q_\lambda\right) \tag{4.24}
$$

where $\boldsymbol{P}(t)$ is the probability covector

$$
\boldsymbol{P}(t) = \begin{pmatrix} P_{AA}(t) & P_{AI}(t) & P_{IA}(t) & P_{II}(t) \end{pmatrix} \tag{4.25}
$$

and where Q_μ and Q_λ are rate matrices generating inactivation $A \to I$ and activation $a_j + a_k \to 2A$ respectively, reading

$$
\begin{aligned}
Q_\mu &:= \mu \cdot \begin{pmatrix} -2 & 1 & 1 & 0 \\ 0 & -1 & 0 & 1 \\ 0 & 0 & -1 & 1 \\ 0 & 0 & 0 & 0 \end{pmatrix} \\
Q_\lambda &:= \lambda \cdot O_{jk} \cdot \begin{pmatrix} 0 & 0 & 0 & 0 \\ 1 & -1 & 0 & 0 \\ 1 & 0 & -1 & 0 \\ 1 & 0 & 0 & -1 \end{pmatrix}
\end{aligned}
\tag{4.26}
$$

We plot the solutions of eq. (4.23) in fig. 4.3 for both the case of $O_{jk} = 0$ (j and k not overlapping) and $O_{jk} = 1$ (j and k overlapping): when $O_{jk} = 0$ (for simplicity starting out at $P_{II}(0) = 0$), the pair decays approximately like

$$
P_{II}(t) \overset{O_{jk}=0}{\approx} 1 - e^{-\mu t}
$$

to both being inactive with 100% probability. On the other hand, when $O_{jk} = 1$ (with simplicity starting out at $P_{AA}(0) = 0$), the pair decays approximately like

$$P_{AA}(t) \overset{O_{jk}=1}{\approx} P_{AA}^{\infty}(1 - e^{-\lambda t})$$

to the stationary value $P_{AA}^{\infty} = \lambda/(\lambda + 2\mu)$ given by the balance of decays $A \to I$ and activation $A + I \to 2A$ and $I + I \to 2A$. Note that P_{AA}^{∞} moves ever closer to 1 the larger the pair activation rate λ the is compared to the rate of decay to inactivity μ.

Equation for a Diffusing Grain We want to now try to get the grain motion back into the picture by introducing diffusion of active grains. The behaviour of the isolated grain eq. (4.21) does not change when diffusion is introduced, because decay $A \to I$ happens with rate μ no matter where exactly the grain is or how it is moving. For a grain pair eq. (4.24) it does matter though. Hence, for simplicity we are after all interested in what the equations with motion look like, when there is just one grain: if active grains diffused, but did not decay, the time evolution of $P_A(\boldsymbol{x}, t)$ would obviously just be the diffusion equation $\left({}^{\partial}\!/_{\partial t} - D\nabla^2\right) P_A(\boldsymbol{x}, t) = 0$ with active-grain diffusion constant D. So together with the decay term $-\mu P_A(\boldsymbol{x}, t)$ we get

$$\begin{aligned} \left(\frac{\partial}{\partial t} - D\nabla^2\right) P_A(\boldsymbol{x}, t) &= -\mu \cdot P_A(\boldsymbol{x}, t) \\ \frac{\partial}{\partial t} P_I(\boldsymbol{x}, t) &= +\mu \cdot P_A(\boldsymbol{x}, t) \end{aligned} \tag{4.27}$$

which one may again write in matrix, or rather in operator form

$$\frac{\partial}{\partial t}\boldsymbol{P}(t) = \boldsymbol{P}(t)\left(Q_D + Q_\mu\right) \tag{4.28}$$

with Q_μ generating reactions by coupling $P_A(\boldsymbol{x}, t)$ and $P_I(\boldsymbol{x}, t)$

$$Q_\mu : \begin{pmatrix} P_A(\boldsymbol{x}) & P_I(\boldsymbol{x}) \end{pmatrix} \longmapsto \begin{pmatrix} P_A(\boldsymbol{x}) & P_I(\boldsymbol{x}) \end{pmatrix} \begin{pmatrix} -\mu & +\mu \\ 0 & 0 \end{pmatrix} \tag{4.29}$$

and Q_D generating diffusion exclusively in the active state by acting with $D\nabla^2$ exclusively on the P_A-component

$$\begin{aligned} Q_D : \begin{pmatrix} P_A(\boldsymbol{x}) & P_I(\boldsymbol{x}) \end{pmatrix} &\longmapsto \begin{pmatrix} D\nabla^2 P_A(\boldsymbol{x}) & 0 \end{pmatrix} \\ &= D\nabla^2 \begin{pmatrix} P_A(\boldsymbol{x}) & P_I(\boldsymbol{x}) \end{pmatrix} \begin{pmatrix} 1 & 0 \\ 0 & 0 \end{pmatrix} \\ &= \left[\begin{pmatrix} D\nabla^2 & 0 \\ 0 & 0 \end{pmatrix} \begin{pmatrix} P_A(\boldsymbol{x}) \\ P_I(\boldsymbol{x}) \end{pmatrix}\right]^{\intercal} \end{aligned} \tag{4.30}$$

In Fourier space eq. (4.27) reads

$$\begin{aligned} \frac{\partial \tilde{P}_A(\boldsymbol{k}, t)}{\partial t} &= (-D\boldsymbol{k}^2 - \mu) \cdot \tilde{P}_A(\boldsymbol{k}, t) \\ \frac{\partial \tilde{P}_I(\boldsymbol{k}, t)}{\partial t} &= +\mu \cdot \tilde{P}_A(\boldsymbol{k}, t) \end{aligned} \tag{4.31}$$

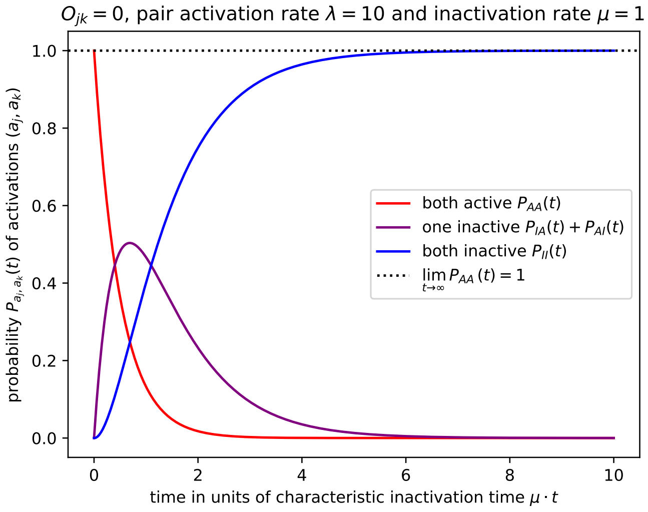

(a) Solution to eq. (4.24) when $O_{jk} = 0$ (grain j and k *do not* overlap): decay (blue curve) with characteristic time μ^{-1} to complete inactivity $P_{II}^{\infty} = 100\%$ with initial conditions $P_{AA}(0) = 100\%$ and all other $P_{a_j,a_k}(0) = 0\%$. Note that the time axis goes all the way to $\mu t = 10$

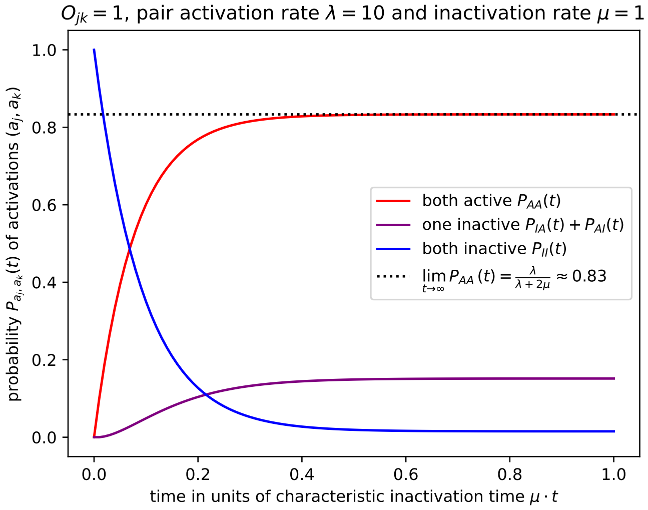

(b) Solution to eq. (4.24) when $O_{jk} = 1$ (grain j and k overlap): decay (red curve) with characteristic time λ^{-1} to asymptotic probability $P_{AA}^{\infty} = {}^{\lambda}\!/\!_{(\lambda+2\mu)}$. The initial conditions are $P_{II}(0) = 100\%$ and all other $P_{a_j,a_k}(0) = 0\%$. The asymptotic value will be the closer to 1 the further one goes to the limit of $\lambda \gg \mu$. Note that the time axis goes only until $\mu t = 1$. The stationary value P_{AA}^{∞} is determined by noting that ${}^{\partial \boldsymbol{P}}\!/\!_{\partial t} \to 0$ as $t \to \infty$ and solving it by finding all covectors $\boldsymbol{P}^{\infty}$ from the left null-space of Q, i.e. those fulfilling $0 = \boldsymbol{P}^{\infty} Q$

Figure 4.3: Solution of eq. (4.23) both with (fig. 4.3a) and without (fig. 4.3b) j and k overlapping, as indicated by O_{jk} (respectively $O_{jk} = 1$ and $O_{jk} = 0$). They show that when $\lambda \gg \mu$, the probability of the activation states being correct is reached exponentially very quickly.

where the solution is obvious for the first equation and then easily obtained for the second equation by integration

$$\begin{aligned}\tilde{P}_A(\boldsymbol{k},t) &= e^{-(D\boldsymbol{k}^2+\mu)t}\tilde{P}_A(\boldsymbol{k},0)\\ \tilde{P}_I(\boldsymbol{k},t) &= \tilde{P}_I(\boldsymbol{k},0) + \frac{\mu}{D\boldsymbol{k}^2+\mu}\left(1-e^{-(D\boldsymbol{k}^2+\mu)t}\right)\tilde{P}_A(\boldsymbol{k},0)\end{aligned}$$

As $t \to \infty$ the probability $\tilde{P}_A(\boldsymbol{k},t)$ of any active-grain mode being occupied vanishes, leading, unsurprisingly, to

$$P_I(t) := \int \mathrm{d}^d x\, P_I(\boldsymbol{x},t) \xrightarrow{t\to\infty} 100\%$$

Two Diffusing Grains We can now again extend this to two grains. Let ∇_j and ∇_k be the gradients with respect to $\boldsymbol{x}_j$ and $\boldsymbol{x}_k$ respectively. To make active grains not only decay but diffuse we extend eq. (4.24) by first introducing dependence on position $P_{a_j,a_k}(\boldsymbol{x}_j,\boldsymbol{x}_k)$, such that now we track both the activation states a_j and a_k and the positions $\boldsymbol{x}_j$ and $\boldsymbol{x}_k$ of grains j and k. Then we add the generator Q_D of active grain diffusion

$$\frac{\partial}{\partial t}\boldsymbol{P}(\boldsymbol{x}_j,\boldsymbol{x}_k,t) = \boldsymbol{P}(\boldsymbol{x}_j,\boldsymbol{x}_k,t)\left(Q_D+Q_\mu+Q_\lambda\right) \tag{4.32}$$

where Q_D is written down most compactly via its transpose $Q_D^\intercal$ (not its adjoint $Q_D^\dagger$, we just want to transpose the matrix that the derivative operators are arranged in)

$$\begin{aligned}Q_D^\intercal : \begin{pmatrix}P_{AA}(\boldsymbol{x}_j,\boldsymbol{x}_k)\\ P_{AI}(\boldsymbol{x}_j,\boldsymbol{x}_k)\\ P_{IA}(\boldsymbol{x}_j,\boldsymbol{x}_k)\\ P_{II}(\boldsymbol{x}_j,\boldsymbol{x}_k)\end{pmatrix} &\longmapsto \begin{pmatrix}(D\nabla_j^2+D\nabla_k^2)P_{AA}(\boldsymbol{x}_j,\boldsymbol{x}_k)\\ D\nabla_j^2 P_{AI}(\boldsymbol{x}_j,\boldsymbol{x}_k)\\ D\nabla_k^2 P_{IA}(\boldsymbol{x}_j,\boldsymbol{x}_k)\\ 0\end{pmatrix}\\ &= \begin{pmatrix}(D\nabla_j^2+D\nabla_k^2) & & & \\ & D\nabla_j^2 & & \\ & & D\nabla_k^2 & \\ & & & 0\end{pmatrix}\begin{pmatrix}P_{AA}(\boldsymbol{x}_j,\boldsymbol{x}_k)\\ P_{AI}(\boldsymbol{x}_j,\boldsymbol{x}_k)\\ P_{IA}(\boldsymbol{x}_j,\boldsymbol{x}_k)\\ P_{II}(\boldsymbol{x}_j,\boldsymbol{x}_k)\end{pmatrix}\end{aligned} \tag{4.33}$$

Note also that we also now need to be careful with grain indistinguishability: since we will only care on *how many* active grains there are at any given location and not *who they are*, there is no point in tracking the identity of grains. $P_{a_j,a_k}(\boldsymbol{x}_j,\boldsymbol{x}_k)$ should be the same as $P_{a_k,a_j}(\boldsymbol{x}_k,\boldsymbol{x}_j)$. and in both cases it should be the probability of the even "*some* grain of activity state a_j is located at $\boldsymbol{x}_j$ and *some* grain of activity state a_k is located at $\boldsymbol{x}_k$". This has consequences for the normalization: there is a $(1/N!)$ prefactor (with $N = 2$ here)

$$\frac{1}{2!}\left(\sum_{a_j}\int \mathrm{d}^d x_j\right)\left(\sum_{a_k}\int \mathrm{d}^d x_k\right)P_{a_j,a_k}(\boldsymbol{x}_j,\boldsymbol{x}_k) \quad = \quad 100\% \tag{4.34}$$

where the sums $\sum_a$ run over $a \in \{A, I\}$.

Towards a More Scalable Language While these discussions illustrate the basic idea of how one would implement the evolution equations for $P_{a_1,\dots,a_N}(\boldsymbol{x}_1,\dots,\boldsymbol{x}_N)$, it is clear that doing so in these manually crafted matrices is not scalable. This burden seems very unnecessary, given that the reactions involved are very simple. To now implement this idea in a *concise* way for an arbitrary number of grains, one may turn to more sophisticated frameworks for reaction system descriptions, that take into account the spatial correlation of grains. This end is served by the formalism developed in Doi (1976a), that discusses using the many-body language typically employed in many-body quantum systems (say, electrons and phonons in a crystalline solid) for classical physical stochastic systems and gains insight into the many-body aspects of diffusion controlled chemical reactions in Doi (1976b) using that technique.

Before introducing the framework to the extent I deem necessary to understand my model, I want to reformulate the generators Q_μ and Q_λ as a showcase: Let $\langle A|$ and $\langle I|$ be the basis vectors of the space in which we the probability covector $\boldsymbol{P} \simeq \langle P|$ lies. We now want to think of them as embedded in a symmetric Fock-space with vaccuum state $|0\rangle$ and creation/annihilation operators with commutation relations $\left[A, A^\dagger\right] = 1$ and $\left[I, I^\dagger\right] = 1$ (all other commutators vanishing). Starting out for simplicity with a single grain Q_μ: the probability vector $\boldsymbol{P}^\intercal$ may be written as a ket

$$|P\rangle = P_I\,|I\rangle + P_A\,|A\rangle = (P_A A^\dagger + P_I I^\dagger)\,|0\rangle \tag{4.35}$$

In this language eq. (4.20) reads

$$\begin{aligned}\frac{\partial}{\partial t}\,|P(t)\rangle &\overset{!}{=} +\mu P_A(t)\,|I\rangle - \mu P_A(t)\,|A\rangle \\ &= \mu(P_A A^\dagger - P_A I^\dagger)\,|0\rangle \\ &= \mu A^\dagger\cdot \underbrace{P_A(t)\,|0\rangle}_{=A\left|P(t)\right\rangle} - I^\dagger\cdot \underbrace{P_A(t)\,|0\rangle}_{=A\left|P(t)\right\rangle} \\ &= \underbrace{\mu(A^\dagger - I^\dagger)A}_{Q_\mu^\dagger}\,|P(t)\rangle\end{aligned} \tag{4.36}$$

where we used

$$\begin{aligned}A\,|P(t)\rangle &= A(P_A A^\dagger + P_I I^\dagger)\,|0\rangle \\ &= (P_A(\underbrace{\left[A, A^\dagger\right]}_{=1} + A^\dagger A) + P_I(\underbrace{\left[A, I^\dagger\right]}_{=0} + I^\dagger A))\,|0\rangle \\ &= P_A\,|0\rangle + \underbrace{P_A A^\dagger A\,|0\rangle}_{=0} + \underbrace{P_I I^\dagger A\,|0\rangle}_{=0} \\ &= P_A\,|0\rangle\end{aligned} \tag{4.37}$$

Just like the Markov rate matrix, the translation into the Fock-space formalism is not symmetric. Instead, one should interpret

$$\underbrace{(I^\dagger - A^\dagger)A}_{(\text{(creation 'to')} - \text{(creation 'from')})\times\text{(annihilation 'from')}} \tag{4.38}$$

Conveniently, once we have written down the generator for $A \to I$ in this way, it is valid for all grain numbers[7]:

$$\begin{aligned} Q_\mu^\dagger \left|A^n I^m\right\rangle &:= (I^\dagger - A^\dagger)A \cdot (A^\dagger)^n (I^\dagger)^m \left|0\right\rangle \\ &= \mu(I^\dagger - A^\dagger)(\underbrace{\left[A,(A^\dagger)^n\right]}_{n(A^\dagger)^{n-1}} + (A^\dagger)^n A)(I^\dagger)^m \left|0\right\rangle \\ &= n\mu(I^\dagger - A^\dagger)(A^\dagger)^{n-1}(I^\dagger)^m \left|0\right\rangle \\ &= n\mu((I^\dagger)^{m+1}(A^\dagger)^{n-1} - (A^\dagger)^n (I^\dagger)^m)\left|0\right\rangle \\ &= +n\mu \left|A^{n-1}I^{m+1}\right\rangle - n\mu \left|A^n I^m\right\rangle \end{aligned} \tag{4.39}$$

which are the correct rates: in state $\left|A^n I^m\right\rangle$, n active grains decay to with rate μ to a state $\mu \left|A^{n-1}I^{m+1}\right\rangle$ with one active grain less and an inactive grain more. The reaction $a_1 + a_2 \longmapsto 2A$ is similarly simple to write down with operators

$$Q_\lambda^\dagger = \sum_{a_1,a_2} \left(A^\dagger A^\dagger - a_1^\dagger a_2^\dagger\right) a_1 a_2 \tag{4.40}$$

4.3.2 Field Operator Language

Field Operators and Bra-Ket-Notation, Single-Species Case In contrast to our situation, the papers, for simplicity's sake, elaborate their ideas almost entirely for the case of a single particle species, but the concepts generalize easily. The central starting-point ideas of the papers are (a) the introduction of a many-particle Hilbert-space with *vaccuum state* (or *vacant state*) $\left|0\right\rangle$ and *annihilation/creation field operator pairs* $\Psi(\boldsymbol{r})$ and $\Psi^\dagger(\boldsymbol{r})$ for respectively removing or inserting particles at location $\boldsymbol{r}$ (in our case down the line it will become one for each species of particle), which obey the commutation relations

$$\left[\Psi(\boldsymbol{r}), \Psi^\dagger(\boldsymbol{r}')\right] = \delta(\boldsymbol{r} - \boldsymbol{r}') \tag{4.41}$$

(all other commutators vanishing, especially all commutators between field operators belonging to distinct particle species); the purpose being (b) interpreting the probability distribution on all particle configurations with all possible particle numbers $P = (P^{(0)}, P^{(1)}, P^{(2)}, \dots)$, which is defined on the disjoint union of all N-particle configuration spaces $\{(\boldsymbol{x}_1, \dots, \boldsymbol{x}_N)\}$

$$\Omega = \dot{\bigcup}_{N=0}^{\infty} \{(\boldsymbol{x}_1, \dots, \boldsymbol{x}_N)\} \tag{4.42}$$

(with $P^{(N)}$ being the restriction of P to $\{(\boldsymbol{x}_1, \dots, \boldsymbol{x}_N)\}$) as a Dirac-bra[8]

$$\left\langle P\right| = \sum_{N=0}^{\infty} \int \mathrm{d}P^{(N)}(\boldsymbol{x}_1, \dots, \boldsymbol{x}_N) \underbrace{\left\langle 0\right| \Psi(\boldsymbol{x}_1) \cdots \Psi(\boldsymbol{x}_N)}_{=: \left\langle \boldsymbol{x}_1, \dots, \boldsymbol{x}_N \right|} \tag{4.43}$$

---

[7] note that $\left[A,(A^\dagger)^n\right] = n(A^\dagger)^{n-1}$ is easily shown by induction via $\left[A,(A^\dagger)^n\right] = \left[A,A^\dagger\right](A^\dagger)^{n-1} + A^\dagger\left[A,(A^\dagger)^{n-1}\right]$

[8] or alternatively a Dirac-ket, like in Doi (1976a) and Doi (1976b), but I choose bras for this section of the text to keep closer to Markov-Process conventions (see eq. (4.46)) rather than those of Quantum Mechanics. We will switch between using $\left|P\right\rangle$ and $\left\langle P\right|$ as is convenient.

with (if one is willing to deal with $P(\boldsymbol{x}_1, \dots, \boldsymbol{x}_N)$ possibly being distributional)

$$\mathrm{d}P\left(\boldsymbol{x}_1, \dots, \boldsymbol{x}_N\right) = \frac{\mathrm{d}^d x_1 \cdots \mathrm{d}^d x_N}{N!} P(\boldsymbol{x}_1, \dots, \boldsymbol{x}_N) \tag{4.44}$$

(the $N!$ coming from the indifference of the dynamics to the identity of Ψ-particles, usually called *particle indistinguishability*) that will evolve in time according to an operator Q

$$\frac{\partial}{\partial t} \langle P(t)| = \langle P(t)|\, Q \tag{4.45}$$

in analogy to evolving the probability covector $\boldsymbol{P}(t)$ of a finite-state (and thus finite-dimensionally described) Markov-Process according to a *master equation* given by some rate matrix Q (examples being eq. (4.21) and eq. (4.24))

$$\frac{\partial}{\partial t} \boldsymbol{P}(t) = \boldsymbol{P}(t)\, Q \tag{4.46}$$

and also, more loosely, in analogy to the Schrödinger equation

$$i \frac{\partial}{\partial t} |\psi(t)\rangle = H\, |\psi(t)\rangle$$

appropriating the powerful Bra-Ket notation to stochastic ends; besides the latter benefit, we will demonstrate shortly that this is a convenient formulation of reaction-systems where fully resolved spatial-correlations are important (like in our present case). In fact, one can glean off the fields of quantum-many body systems and quantum field theory in the search for approaches to solving problems. An example for this was worked out by Doi (1976b) themselves, namely the expansion (in Feynman-diagrams) of the probability-generating function $G(z,t) = \left\langle z^N \right\rangle$ of the number of particles N (some time t after they were initialized as a Poisson point cloud at time 0), performing Brownian motion and undergoing the reaction $\Psi + \Psi \to \Psi$ at some finite rate when closer than some reaction distance (reminiscent of coalescing random walks on lattices).

Multiple Species Case As already foreshadowed, in our case we want to introduce two grain species, active $A(\boldsymbol{r})$ and inactive $I(\boldsymbol{r})$ grains, where, similar to the single-species eq. (4.41) we have $\left[A(\boldsymbol{r}), A^\dagger(\boldsymbol{r}')\right] = \delta(\boldsymbol{r} - \boldsymbol{r}')$ and $\left[I(\boldsymbol{r}), I^\dagger(\boldsymbol{r}')\right] = \delta(\boldsymbol{r} - \boldsymbol{r}')$ with all other commutators vanishing, which can be summarized as

$$\left[a(\boldsymbol{r}), a'^\dagger(\boldsymbol{r}')\right] = \delta_{a,a'} \delta(\boldsymbol{r} - \boldsymbol{r}') \tag{4.47}$$

with *activation states* $a, a' \in \{I, A\}$ and all other commutators vanishing. Relative to the single species case, this extends the outcome space Ω to all possible configurations of positions and activation states $\{(a_1, \dots, a_N, \boldsymbol{x}_1, \dots, \boldsymbol{x}_N)\}$ for all grain numbers N

$$\Omega = \dot{\bigcup}_{N=0}^{\infty} \{(a_1, \dots, a_N, \boldsymbol{x}_1, \dots, \boldsymbol{x}_N)\} \tag{4.48}$$

$A(\boldsymbol{r})$ and $I(\boldsymbol{r})$ should be interpreted as describing the stochastic density field of active/inactive grains as opposed to the interpretation these kinds of operators have in their far more common use as quantum many-body descriptions. Writing $\langle P|$ in terms of the probability distribution $P = (P^{(0)}, P^{(1)}, P^{(2)}, \dots)$ now is a matter of writing

$$\langle P| = \sum_{N=0}^{\infty} \int \mathrm{d}P^{(N)}\,(a_1, \dots, a_N, \boldsymbol{x}_1, \dots, \boldsymbol{x}_N)\, \underbrace{\langle 0|\, a_1(\boldsymbol{x}_1) \cdots a_N(\boldsymbol{x}_N)}_{=:\, \langle a_1,\dots,a_N,\boldsymbol{x}_1,\dots,\boldsymbol{x}_N|} \tag{4.49}$$

with

$$\begin{aligned} &\int \mathrm{d}P^{(N)}(a_1, \dots, a_N, \boldsymbol{x}_1, \dots, \boldsymbol{x}_N)\, (\cdots) = \\ &\qquad \int \frac{\mathrm{d}^d x_1 \cdots \mathrm{d}^d x_N}{N!} \sum_{a_1 \cdots a_N} P^{(N)}_{a_1,\dots,a_N}(\boldsymbol{x}_1, \dots, \boldsymbol{x}_N)\, (\cdots) \end{aligned} \tag{4.50}$$

where also here the division by $N!$ stems from indistinguishability amongst I and A grains respectively.

Random Variable Operators and Expectation Values The expectation value of a random variable $\mathcal{X} : \Omega \to \mathbb{R}$ is by definition computed with

$$\begin{aligned} \langle \mathcal{X} \rangle = \sum_{N=0}^{\infty} \sum_{a_1 \cdots a_N} \int \frac{\mathrm{d}^d x_1 \cdots \mathrm{d}^d x_N}{N!}\, &P^{(N)}_{a_1,\dots,a_N}(\boldsymbol{x}_1, \dots, \boldsymbol{x}_N) \\ &\times \mathcal{X}^{(N)}(a_1, \dots, a_N, \boldsymbol{x}_1, \dots, \boldsymbol{x}_N) \end{aligned} \tag{4.51}$$

where $\mathcal{X}^{(N)}$ is the restriction of the random variable $\mathcal{X}$ to the N-grain configuration space $\{a_1, \dots, a_N, \boldsymbol{x}_1, \dots, \boldsymbol{x}_N\}$. By eq. (4.49) and the commutation relations $[a(\boldsymbol{r}), a'(\boldsymbol{r}')] = \delta_{a,a'}\delta(\boldsymbol{r} - \boldsymbol{r}')$ from eq. (4.47) (see appendix A.2), we can write

$$\begin{aligned} P^{(N)}_{a_1,\dots,a_N}(\boldsymbol{x}_1, \dots, \boldsymbol{x}_N) &= \langle P | a_1, \dots, a_N, \boldsymbol{x}_1, \dots, \boldsymbol{x}_N \rangle \\ &= \langle P|\, a_1^{\dagger}(\boldsymbol{x}_1) \cdots a_N^{\dagger}(\boldsymbol{x}_N)\, |0\rangle \end{aligned} \tag{4.52}$$

(compare Doi 1976a, eq. 16) By shortening the notation for integration and summation over the outcome space to

$$\sum_{N=0}^{\infty} \int \frac{\mathrm{d}^d r_1 \cdots \mathrm{d}^d r_N}{N!} \sum_{a_1 \cdots a_N} \qquad \longleftrightarrow \qquad \int \mathrm{d}\omega \tag{4.53}$$

for legibility, where $\omega = (a_1, \dots, a_N, \boldsymbol{x}_1, \dots, \boldsymbol{x}_N) \in \Omega$ is an outcome with an associated ket

$$|\omega\rangle = |a_1, \dots, a_N, \boldsymbol{x}_1, \dots, \boldsymbol{x}_N\rangle \tag{4.54}$$

we see that eq. (4.51) may be written with help of a resolution of identity $\mathbb{1} = \int \mathrm{d}\omega'\, |\omega'\rangle \langle \omega'|$ (verified in appendix A.2)

$$\begin{aligned} \langle \mathcal{X} \rangle &= \int \mathrm{d}\omega\, P(\omega) \mathcal{X}(\omega) \\ &= \int \mathrm{d}\omega\, \langle P|\omega\rangle\, \mathcal{X}(\omega) \\ &= \int \mathrm{d}\omega \int \mathrm{d}\omega'\, \langle P|\omega'\rangle\, \underbrace{\langle \omega'|\omega\rangle}_{\delta(\omega-\omega')}\, \mathcal{X}(\omega) \end{aligned} \tag{4.55}$$

such that by $\delta(\omega-\omega')\mathcal{X}(\omega)=\delta(\omega-\omega')\mathcal{X}(\omega')$ it is possible to write

$$\begin{aligned}\langle\mathcal{X}\rangle &= \int \mathrm{d}\omega \int \mathrm{d}\omega' \, \langle P|\omega'\rangle \, \langle\omega'|\omega\rangle \, \mathcal{X}(\omega') \\ &= \langle P| \left(\int \mathrm{d}\omega' \, \mathcal{X}(\omega') \, |\omega'\rangle \, \langle\omega'|\right) \int \mathrm{d}\omega \, |\omega\rangle\end{aligned} \tag{4.56}$$

where one should recall that

$$\int \mathrm{d}\omega \, |\omega\rangle = \sum_{N=0}^{\infty} \int \frac{\mathrm{d}^d x_1 \cdots \mathrm{d}^d x_N}{N!} \sum_{a_1 \cdots a_N} |a_1, \dots, a_N, \boldsymbol{x}_1, \dots, \boldsymbol{x}_N\rangle \tag{4.57}$$

and it should be clarified that

$$\delta(\omega-\omega') = \delta_{N,N'} \cdot \sum_{\pi\in S_N} \prod_{k=1}^{N} \delta_{a_k, a'_{\pi(k)}} \delta(\boldsymbol{x}_k - \boldsymbol{x}'_{\pi(k)}) \tag{4.58}$$

for $\omega=(a_1,\dots,a_N,\boldsymbol{x}_1,\dots,\boldsymbol{x}_N)$ and $\omega'=(a'_1,\dots,a'_{N'},\boldsymbol{x}'_1,\dots,\boldsymbol{x}'_{N'})$. The reason for doing this is that we see that there is a canonical operator pendant X to the random variable $\mathcal{X}$, abstractly given by

$$X := \int \mathrm{d}\omega \, \mathcal{X}(\omega) \, |\omega\rangle \, \langle\omega| \tag{4.59}$$

Thus the expectation value expression eq. (4.51) condenses to

$$\langle\mathcal{X}\rangle_t = \langle P(t)| \, X \, |\mathrm{sum}\rangle \tag{4.60}$$

where, as Doi (1976a) notes, we write

$$\begin{aligned}\int \mathrm{d}\omega \, |\omega\rangle &= \sum_{N=0}^{\infty} \int \frac{\mathrm{d}^d x_1 \cdots \mathrm{d}^d x_N}{N!} \sum_{a_1 \cdots a_N} |a_1, \dots, a_N, \boldsymbol{x}_1, \dots, \boldsymbol{x}_N\rangle \\ &= \sum_{N=0}^{\infty} \int \frac{\mathrm{d}^d x_1 \cdots \mathrm{d}^d x_N}{N!} \sum_{a_1 \cdots a_N} a_1^\dagger(\boldsymbol{x}_1) \cdots a_N^\dagger(\boldsymbol{x}_N) \, |0\rangle \\ &= \sum_{N=0}^{\infty} \frac{1}{N!} \left(\int \mathrm{d}^d x_1 \sum_{a_1} a_1^\dagger(\boldsymbol{x}_1)\right) \cdots \left(\int \mathrm{d}^d x_n \sum_{a_n} a_n^\dagger(\boldsymbol{x}_n)\right) \\ &= \sum_{N=0}^{\infty} \frac{1}{N!} \left(\int \mathrm{d}^d r \sum_{a} a^\dagger(\boldsymbol{r})\right)^N \\ &= \exp\left(\int \mathrm{d}^d r \sum_{a} a^\dagger(\boldsymbol{r})\right) |0\rangle \\ &=: |\mathrm{sum}\rangle\end{aligned} \tag{4.61}$$

(compare Doi 1976a, eqs. 28 - 31). Random variables that happen to split up into the form

$$\mathcal{X}^{(N)}(a_1,\dots,a_N,\boldsymbol{x}_1,\dots,\boldsymbol{x}_N) = \sum_{k=1}^{N} \mathcal{X}^{[1]}(a_k,\boldsymbol{x}_k) + \sum_{k=1}^{N}\sum_{j=1}^{k-1} \mathcal{X}^{[2]}(a_k,a_j,\boldsymbol{x}_k,\boldsymbol{x}_j) + \cdots \tag{4.62}$$

i.e. with a clean separation into one-body terms of homogeneous[9] form $\mathcal{X}^{[1]}$, two-body terms of homogeneous form $\mathcal{X}^{[2]}$ etc., work out to

$$X = \sum_{n=0}^{\infty} \frac{1}{n!} \mathcal{X}^{[n]}(a_1, \dots, a_n, \boldsymbol{x}_1, \dots, \boldsymbol{x}_n) \cdot a_1^\dagger(\boldsymbol{r}_1) \cdots a_n^\dagger(\boldsymbol{r}_n) \cdot a_1(\boldsymbol{x}_1) \cdots a_n(\boldsymbol{x}_n) \tag{4.63}$$

a formula reminiscent of splitting up quantum many-body operators into n-body components (Doi 1976a, eq. 24).

A simple and important example for the operator form of a random variable is active/inactive grain densities $\rho_a(\boldsymbol{r})$, whose ($\boldsymbol{r}$-dependent) random variables $\mathcal{A}(\boldsymbol{r})$ and $\mathcal{I}(\boldsymbol{r})$ read respectively

$$\begin{aligned} \mathcal{A}^{(N)}(\boldsymbol{r}) &= \sum_{k=1}^{N} \delta_{A,a_k} \delta(\boldsymbol{r} - \boldsymbol{x}_k) \\ \mathcal{I}^{(N)}(\boldsymbol{r}) &= \sum_{k=1}^{N} \delta_{I,a_k} \delta(\boldsymbol{r} - \boldsymbol{x}_k) \end{aligned} \tag{4.64}$$

One can read off they contain only one-body terms $\mathcal{A}^{[1]}(a, \boldsymbol{x}; \boldsymbol{r}) = \delta_{A,a}\delta(\boldsymbol{r} - \boldsymbol{x})$ and $\mathcal{I}^{[1]}(a, \boldsymbol{x}; \boldsymbol{r}) = \delta_{I,a}\delta(\boldsymbol{r} - \boldsymbol{x})$. Hence the operator for active and inactive grain density reads $A^\dagger(\boldsymbol{r})A(\boldsymbol{r})$ and $I^\dagger(\boldsymbol{r})I(\boldsymbol{r})$ respectively[10].

Properties and interpretation of $|\text{sum}\rangle$ The name $|\text{sum}\rangle$ was probably chosen in Doi (1976a) in analogy to finite state (and hence finite-dimensionally described) Markov-processes with states labelled by an index running from $j = 1, \dots, m$. In this case, a random variable $\mathcal{X}_j$ is operatorized by

$$X \overset{\substack{\text{finite}\\\text{dimen-}\\\text{sionally}}}{=} \begin{pmatrix} \mathcal{X}_1 & & & & \\ & \mathcal{X}_2 & & & \\ & & \mathcal{X}_3 & & \\ & & & \ddots & \\ & & & & \mathcal{X}_m \end{pmatrix}$$

The vector $|\text{sum}\rangle$ for finitely many states reads

$$|\text{sum}\rangle \overset{\substack{\text{finite}\\\text{dimen-}\\\text{sionally}}}{=} \begin{pmatrix} 1 \\ 1 \\ 1 \\ \vdots \\ 1 \end{pmatrix}$$

---

[9] With *homogeneous* I mean to say that every grain k, pair (k, j) etc. add into the $\mathcal{X}^{(N)}$ in exactly the same way, as given by $\mathcal{X}^{[n]}$, guaranteeing $\mathcal{X}$ is unchanged under grain identity permutations

[10] So in contrast to the expectation value formula, this time the expression is familiar from quantum physics, where the spatial density of quanta in some mode of motion $\psi_m(\boldsymbol{r})$ is given by $\psi_m^\dagger(\boldsymbol{r})\psi_m(\boldsymbol{r})$. This makes sense, because it derives not from how to interpret P versus how to interpret ψ but from the algebra of creation/annihilation operators, which is the same in both cases

and will, when passed to a covector, sum all of their components. Let the probability covector read

$$\langle P| \overset{\substack{\text{finite}\\\text{dimen-}\\\text{sionally}}}{=} \begin{pmatrix} P_1 & P_2 & P_3 & \cdots & P_m \end{pmatrix}$$

The expectation value formula now, perhaps, is more accessible and understandable:

$$\begin{aligned}
\langle P| X \,|\mathrm{sum}\rangle &\overset{\substack{\text{finite}\\\text{dimen-}\\\text{sionally}}}{=} \begin{pmatrix} P_1 & P_2 & P_3 & \cdots & P_m \end{pmatrix} \begin{pmatrix} \mathcal{X}_1 & & & & \\ & \mathcal{X}_2 & & & \\ & & \mathcal{X}_3 & & \\ & & & \ddots & \\ & & & & \mathcal{X}_m \end{pmatrix} \begin{pmatrix} 1 \\ 1 \\ 1 \\ \vdots \\ 1 \end{pmatrix} \\
&= \begin{pmatrix} P_1\mathcal{X}_1 & P_2\mathcal{X}_2 & P_3\mathcal{X}_3 & \cdots & P_m\mathcal{X}_m \end{pmatrix} \begin{pmatrix} 1 \\ 1 \\ 1 \\ \vdots \\ 1 \end{pmatrix} \\
&= P_1\mathcal{X}_1 + \cdots + P_m\mathcal{X}_m
\end{aligned}$$

where in the case of continuum degrees of freedom, such as the configurations $(\boldsymbol{x}_1, \dots, \boldsymbol{x}_N)$ the sum has to be replaced by an a more general (measure-theoretical) integral.

That $|\mathrm{sum}\rangle$ is the means by which expectation values are computed has consequences that are surprising for anyone only used to the quantum use of operator-techniques. $|\mathrm{sum}\rangle$ has the property (shown in appendix A.3)

$$a(\boldsymbol{r})\,|\mathrm{sum}\rangle = |\mathrm{sum}\rangle \tag{4.65}$$

i.e. it can absorb (and dispense) an arbitrary amount of $a(\boldsymbol{r})$ factors. Hence, for example, even though the proper operatorization of active grain density is $A^\dagger(\boldsymbol{r})A(\boldsymbol{r})$, as soon as it comes to taking averages

$$\begin{aligned}
\rho_A(\boldsymbol{r}, t) = \langle \mathcal{A}(\boldsymbol{r})\rangle &= \langle P(t)|\, A^\dagger(\boldsymbol{r}) \underbrace{A(\boldsymbol{r})\,|\mathrm{sum}\rangle}_{=|\mathrm{sum}\rangle} \\
&= \langle P(t)|\, A^\dagger(\boldsymbol{r})\,|\mathrm{sum}\rangle
\end{aligned} \tag{4.66}$$

and, in fact, the n-point density for any combination of active and inactive grains becomes

$$\begin{aligned}
\rho^{(n)}_{a_1,\dots,a_n}(\boldsymbol{r}_1, \dots, \boldsymbol{r}_n, t) &= \langle P(t)|\, a_1^\dagger(\boldsymbol{r}_1) \cdots a_n^\dagger(\boldsymbol{r}_n) \underbrace{a_1(\boldsymbol{r}_1) \cdots a_n(\boldsymbol{r}_n)\,|\mathrm{sum}\rangle}_{=|\mathrm{sum}\rangle} \\
&= \langle P(t)|\, a_1^\dagger(\boldsymbol{r}_1) \cdots a_n^\dagger(\boldsymbol{r}_n)\,|\mathrm{sum}\rangle
\end{aligned} \tag{4.67}$$

Closing Remarks on the Formalism Basics I want to close this presentation by reiterating that this is not a map to a quantum system, but expresses a *Markov process* in operator language[11]. This methodology for describing moving grains undergoing

---

[11] Here it will allow us to express the otherwise clumsy Master-equation concisely, with every term in Q very legibly introducing one simple to imagine process. Contrast this with eq. (4.23)

reactions that only occur when they are close enough (and possibly changing the grain number) merely happens to be very similar to many-body quantum physics (which, similarly, permits the creation and destruction of quanta). Q does not have to be symmetric at all (just consider all Q defined in the present text, say eq. (4.21) featuring the decay $A \to I$), let alone self-adjoint, since it is not supposed to conserve the sum of absolute squares $\sum_i |\psi_i|^2 = 1$ (or more generally the 2-norm), but the sum of probabilities $\sum_i P_i = 1$ (or more generally $\int \mathrm{d}P = 1$). In matrix terms, the first one requires the generator to be anti-hermitian, such as $(-iH)^\dagger = -(-iH)$ in the Schrödinger-equation, while the other requires the generator's rows to sum to zero $\sum_j Q_{ij} = 0$.

That quantum and statistical descriptions should be so closely related at all may come as a surprise. If so, perhaps this circumstance becomes less surprising after considering that the quantum wave function $\psi(\omega)$ on a measurement outcome space $\Omega = \{\omega\}$ has the same arguments as a probability function $P(\omega)$ on that same outcome space. Readers familiar with density functional theory, originally conceived to study the ground state of many-electron systems (Hohenberg and Kohn 1964; Kohn and Sham 1965), may also find it interesting to learn that it has a thermodynamic pendant introduced by Mermin (1965), which is used to theoretically study not just electrons at finite temperature, but has actually been very successfully applied to the study of *classical-statistical* physics of fluids (see the lecture notes Roth (2006)[12] for example). One may also recall the field theory techniques from section 2.2 or section 3.2 to study phase transitions, which many physicists are more familiar with from quantum field theory. In this view, Doi (1976a) and Doi (1976b) fit in as another example of theories of collective behaviour and theoretical quantum physics sharing techniques.

4.3.3 Mimicking Random Organization

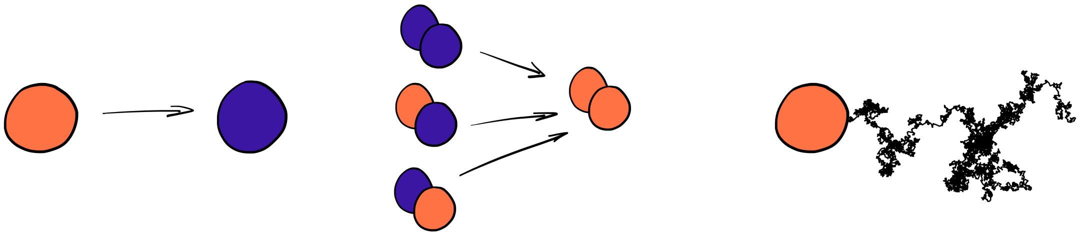

(a) decay to inactivity Q_μ (b) activation of pairs Q_λ (c) active grain diffusion Q_D

Figure 4.4: Pictorial representation of the behaviour generated by each term of a reaction-system approximating time-continuous random organization

The lessons learned in the simplified two-grain case discussed in section 4.3.1 were, that if the system is to mimick the instantaneous activation of time-continuous random organization eq. (4.13), we need both the rate of activation λ and decay μ to be much larger than the rate of motion $D\sigma^{-2}$ and we need $\lambda \gg \mu$ (see fig. 4.3). This is very unfortunate for anyone eager to apply the common perturbation techniques for

---

[12] `https://bytebucket.org/knepley/cdft-git/wiki/papers/Lecture_Notes_on_DFT__Roland_Roth.pdf`, last visited on 25.09.2025 at 14:35

small coupling constants that work so effectively for theories like quantum electrodynamics, which has the small fine-structure constant, or the diffusion-controlled reaction $\Psi + \Psi \to \Psi$ from Doi (1976b), which assumes a comparatively low reaction rate. I postpone addressing these concerns to a later, more convenient time however, with the hope of finding, for example, systematic asymptotic expansions in λ^{-1}, μ^{-1} and $({}^{\lambda}/_{\mu})^{-1}$. It is however already possible to formulate a 'wishlist' for our approximation scheme (section 4.3.5), which should help narrowing down the possibilities later.

I argued for the form of the decay (fig. 4.4a) and activation (fig. 4.4b) terms already in section 4.3.1. By furthermore deciding that during any reaction the grains will not experience instantaneous teleportation and that the reaction rate does not depend on location or time, the only possible form for the reaction generators reads

$$
\begin{aligned}
Q^\dagger_\lambda &= \frac{\lambda}{2}\int \mathrm{d}^d r_1\, \mathrm{d}^d r_2\, \underbrace{\Theta(\sigma - |\boldsymbol{r}_1 - \boldsymbol{r}_2|)}_{\text{spherical grain shape}} \sum_{a_1,a_2} \Big(A^\dagger(\boldsymbol{r}_1)A^\dagger(\boldsymbol{r}_2) - a^\dagger_1(\boldsymbol{r}_1)a^\dagger_2(\boldsymbol{r}_2)\Big)\, a_1(\boldsymbol{r}_1)a_2(\boldsymbol{r}_2) \\
Q^\dagger_\mu &= \mu \int \mathrm{d}^d r\, \big(I^\dagger(\boldsymbol{r}) - A^\dagger(\boldsymbol{r})\big)\, A(\boldsymbol{r})
\end{aligned}
\tag{4.68}
$$

where the spherical shape of the grains expresses itself in the Heaviside-function expression $\Theta(\sigma - |\boldsymbol{r}_1 - \boldsymbol{r}_2|)$. In principle one could insert any other form factor here; spheres are just arguably the simplest. Note that we could also choose to omit the reaction $2I \to 2A$ for simplicity in case we have reason to neglect inactive-inactive-overlaps. I am yet to investigate this possibility.

Finally diffusion of active grains (fig. 4.4c) is generated by the following expression (reminiscent of the second-quantized kinetic term in the Schrödinger equation)

$$
Q^\dagger_D = \int \mathrm{d}^d r\, A^\dagger(\boldsymbol{r})\, D\nabla^2 A(\boldsymbol{r}) \tag{4.69}
$$

(compare Doi 1976a, eq. 66). That this indeed generates diffusion is legibly showcased by considering the ket with just a single grain

$$
\begin{aligned}
Q^\dagger_D \,|a, \boldsymbol{x}\rangle &= \int \mathrm{d}^d r\, A^\dagger(\boldsymbol{r})\, D\nabla^2_{\boldsymbol{r}}\, \underbrace{A(\boldsymbol{r})\, a^\dagger(\boldsymbol{x})}_{\substack{[A(\boldsymbol{r}),a^\dagger(\boldsymbol{x})] \\ +a^\dagger(\boldsymbol{x})A(\boldsymbol{r})}} |0\rangle \\
&= \int \mathrm{d}^d r\, A^\dagger(\boldsymbol{r})\, D\nabla^2_{\boldsymbol{r}}\, \delta_{A,a}\delta(\boldsymbol{r} - \boldsymbol{x})\, |0\rangle \\
&\overset{\text{P.I.}}{=} \delta_{A,a} \int \mathrm{d}^d r\; \delta(\boldsymbol{r} - \boldsymbol{x})\, D\nabla^2_{\boldsymbol{r}} A^\dagger(\boldsymbol{r})\, |0\rangle \\
&= \delta_{A,a}\, D\nabla^2\, |a, \boldsymbol{x}\rangle
\end{aligned}
\tag{4.70}
$$

where we used partial integration, $\big[A(\boldsymbol{r}), a^\dagger(\boldsymbol{x})\big] = \delta_{A,a}\delta(\boldsymbol{r} - \boldsymbol{x})$ and $A(\boldsymbol{r})\,|0\rangle = 0$. This checks out, because imagine a one-grain probability distribution

$$
\big\langle P^{(1)}\big| = \sum_a \int \mathrm{d}^d x\, P(a, \boldsymbol{x})\, \langle a, \boldsymbol{x}| \tag{4.71}
$$

Then if $\left\langle P^{(1)}\right|$ is evolved with the generator of diffusion

$$\frac{\partial}{\partial t}\left\langle P^{(1)}(t)\right| = \left\langle P^{(1)}(t)\right| Q_D \tag{4.72}$$

we find that the probability distribution it translates to evolves with

$$\begin{aligned}
\frac{\partial}{\partial t}P(a,\boldsymbol{x},t) = & \\
&= \frac{\partial}{\partial t}\left\langle a,\boldsymbol{x}\middle|P^{(1)}(t)\right\rangle \\
&= \langle a,\boldsymbol{x}|\, Q_D^\dagger \left|P^{(1)}(t)\right\rangle \\
&= \langle a,\boldsymbol{x}| \sum_{a'} \int \mathrm{d}^d x'\, P(a',\boldsymbol{x}',t) \quad \underbrace{Q_D^\dagger\, |a',\boldsymbol{x}'\rangle}_{=\delta_{A,a'}\, D\nabla^2_{\boldsymbol{x}'}\, |a',\boldsymbol{x}\rangle'} \\
&= \sum_{a'} \delta_{A,a'} \int \mathrm{d}^d x'\, P(a',\boldsymbol{x}',t)\, D\nabla^2_{\boldsymbol{x}'}\, \underbrace{\langle a,\boldsymbol{x}|a',\boldsymbol{x}'\rangle}_{=\delta_{a,a'}\,\delta(\boldsymbol{x}-\boldsymbol{x}')} \\
&= \delta_{A,a}\, D\nabla^2 P(a,\boldsymbol{x},t)
\end{aligned} \tag{4.73}$$

which reads as: $P(a,\boldsymbol{x},t)$ is not changed by diffusion if it describes the probability density of the inactive component $P(I,\boldsymbol{x},t)$, but evolves with the diffusion equation when $a = A$.

4.3.4 Time Evolution of Density

We now want to derive dynamical equations for the one-body densities of either grain species $\rho_A(\boldsymbol{r},t)$ and $\rho_I(\boldsymbol{r},t)$. Doing so involves simply executing

$$\begin{aligned}
\frac{\partial \rho_a(\boldsymbol{r},t)}{\partial t} &= \frac{\partial}{\partial t}\langle P(t)|\, a^\dagger(\boldsymbol{r})\, |\mathrm{sum}\rangle \\
&= \langle P(t)|\, Q a^\dagger(\boldsymbol{r})\, |\mathrm{sum}\rangle \\
&= \langle P(t)| \left(\left[Q, a^\dagger(\boldsymbol{r})\right] + a^\dagger(\boldsymbol{r})Q\right) |\mathrm{sum}\rangle \\
&= \langle P(t)| \left[Q, a^\dagger(\boldsymbol{r})\right] |\mathrm{sum}\rangle
\end{aligned} \tag{4.74}$$

where we used conservation of probability $Q\,|\mathrm{sum}\rangle = 0$. We can by linearity separate $\left[Q, A^\dagger(\boldsymbol{r})\right] = \left[Q_D, A^\dagger(\boldsymbol{r})\right] + \left[Q_\mu, A^\dagger(\boldsymbol{r})\right] + \left[Q_\lambda, A^\dagger(\boldsymbol{r})\right]$ so computing the commutator can be done term by term.

One-Body Terms Q_D and Q_μ are relatively simple to evaluate. Because inactive grains do not propagate by design, there is no factor of I anywhere in Q_D, so its commutator with $I^\dagger(\boldsymbol{r})$ is zero

$$\left[Q_D, I^\dagger(\boldsymbol{r})\right] = 0 \tag{4.75}$$

For the case $a = A$, note that from $[A(\boldsymbol{r}), A(\boldsymbol{r}')] = 0$ and $\nabla^2_{\boldsymbol{r}'}$ not acting on the argument $\boldsymbol{r}$ follows that it is possible to pull out $\nabla^2_{\boldsymbol{r}'}A(\boldsymbol{r}')$ from the commutator:

$$\left[A(\boldsymbol{r},t), A^\dagger(\boldsymbol{r}',t)\nabla^2_{\boldsymbol{r}'}A(\boldsymbol{r}',t)\right] = \left[A(\boldsymbol{r},t), A^\dagger(\boldsymbol{r}',t)\right]\nabla^2_{\boldsymbol{r}'}A(\boldsymbol{r}',t) \tag{4.76}$$

Recalling $\left[A(\boldsymbol{r}), A^\dagger(\boldsymbol{r}')\right] = \delta(\boldsymbol{r}-\boldsymbol{r}')$ shows that the commutator with the diffusion term reads

$$\left[Q_D, A^\dagger(\boldsymbol{r})\right] = D\nabla^2 A^\dagger(\boldsymbol{r}) \tag{4.77}$$

Next, the spontaneous decay of activity $A \to I$ at rate μ is, like the diffusion term, a one-body term given by eq. (4.68)

$$Q_\mu = \int \mathrm{d}^d r' \, \mu \cdot A^\dagger(\boldsymbol{r}') \left(I(\boldsymbol{r}') - A(\boldsymbol{r}')\right) \tag{4.78}$$

The commutator is even easier to compute than for diffusion, since

$$\left[a(\boldsymbol{r}), \left(I^\dagger(\boldsymbol{r}') - A^\dagger(\boldsymbol{r}')\right) A(\boldsymbol{r}')\right] = \left[a(\boldsymbol{r}), \left(I^\dagger(\boldsymbol{r}') - A^\dagger(\boldsymbol{r}')\right)\right] A(\boldsymbol{r}')$$

because $[a(\boldsymbol{r}), A(\boldsymbol{r}')] = 0$ and

$$\left[a(\boldsymbol{r}), \left(I^\dagger(\boldsymbol{r}') - A^\dagger(\boldsymbol{r}')\right)\right] = \begin{cases} \delta(\boldsymbol{r}-\boldsymbol{r}') & a = I \\ -\delta(\boldsymbol{r}-\boldsymbol{r}') & a = A \end{cases}$$

resulting in

$$\begin{aligned} \left[Q_\mu, A^\dagger(\boldsymbol{r})\right] &= -\mu A^\dagger(\boldsymbol{r}) \\ \left[Q_\mu, I^\dagger(\boldsymbol{r})\right] &= +\mu A^\dagger(\boldsymbol{r}) \end{aligned} \tag{4.79}$$

We can inert these back into eq. (4.74) and see that the evolution equation for the active- and inactive-grain-densities are of the form

$$\begin{aligned} \frac{\partial \rho_A(\boldsymbol{r},t)}{\partial t} &= D\nabla^2 \rho_A(\boldsymbol{r},t) - \mu\rho_A(\boldsymbol{r},t) + (\cdots) \\ \frac{\partial \rho_I(\boldsymbol{r},t)}{\partial t} &= +\mu\rho_A(\boldsymbol{r},t) + (\cdots) \end{aligned} \tag{4.80}$$

Two-Body Interaction Term In contrast to the former two Q_λ contains two-body terms and hence introduces correlations between grains locations into the system. According to eq. (4.68) it reads

$$Q_\lambda = \frac{\lambda}{2} \int \mathrm{d}^d r_1 \, \mathrm{d}^d r_2 \, \Theta(\sigma - |\boldsymbol{r}_1 - \boldsymbol{r}_2|) \sum_{a_1, a_2} a_1^\dagger(\boldsymbol{r}_1) a_2^\dagger(\boldsymbol{r}_2) \left(A(\boldsymbol{r}_1)A(\boldsymbol{r}_2) - a_1(\boldsymbol{r}_1)a_2(\boldsymbol{r}_2)\right) \tag{4.81}$$

and we want to compute $\left[Q_\lambda, a^\dagger(\boldsymbol{r})\right]$. Pulling past the integrals $\int \mathrm{d}^d r_1 \, \mathrm{d}^d r_2$ and past the multiplication by the form factor $\Theta(\sigma - |\boldsymbol{r}_1 - \boldsymbol{r}_2|)$ by linearity, this reduces to computing

$$\left[a_1^\dagger(\boldsymbol{r}_1) a_2^\dagger(\boldsymbol{r}_2) \left(A(\boldsymbol{r}_1)A(\boldsymbol{r}_2) - a_1(\boldsymbol{r}_1)a_2(\boldsymbol{r}_2)\right), a^\dagger(\boldsymbol{r})\right] \tag{4.82}$$

Since all creation operators $a^\dagger(\boldsymbol{r})$ commute with each other, we can pull $a_1^\dagger(\boldsymbol{r}_1)a_2^\dagger(\boldsymbol{r}_2)$ out of the commutator

$$a_1^\dagger(\boldsymbol{r}_1) a_2^\dagger(\boldsymbol{r}_2) \left[A(\boldsymbol{r}_1)A(\boldsymbol{r}_2) - a_1(\boldsymbol{r}_1)a_2(\boldsymbol{r}_2), a^\dagger(\boldsymbol{r})\right] \tag{4.83}$$

Using the identity $[AB, C] = A[B, C] + [A, C]B$ we split the remaining commutator further

$$\begin{aligned} \big[A(\boldsymbol{r}_1)A(\boldsymbol{r}_2), a^\dagger(\boldsymbol{r})\big] &= A(\boldsymbol{r}_1)\big[A(\boldsymbol{r}_2), a^\dagger(\boldsymbol{r})\big] + \big[A(\boldsymbol{r}_1), a^\dagger(\boldsymbol{r})\big]A(\boldsymbol{r}_2) \\ &\overset{\text{eq. (4.47)}}{=} A(\boldsymbol{r}_1)\delta_{A,a}\delta(\boldsymbol{r}_2 - \boldsymbol{r}) + \delta_{A,a}\delta(\boldsymbol{r}_1 - \boldsymbol{r})A(\boldsymbol{r}_2) \\ \big[a_1(\boldsymbol{r}_1)a_2(\boldsymbol{r}_2), a^\dagger(\boldsymbol{r})\big] &= a_1(\boldsymbol{r}_1)\big[a_2(\boldsymbol{r}_2), a^\dagger(\boldsymbol{r})\big] + \big[a_1(\boldsymbol{r}_1), a^\dagger(\boldsymbol{r})\big]a_2(\boldsymbol{r}_2) \\ &\overset{\text{eq. (4.47)}}{=} a_1(\boldsymbol{r}_1)\delta_{a_2,a}\delta(\boldsymbol{r}_2 - \boldsymbol{r}) + \delta_{a_1,a}\delta(\boldsymbol{r}_1 - \boldsymbol{r})a_2(\boldsymbol{r}_2) \end{aligned} \tag{4.84}$$

The entire sought commutator hence is equal to

$$\begin{aligned} \big[Q_\lambda, a^\dagger(\boldsymbol{r})\big] = \frac{\lambda}{2}\int \mathrm{d}^d r_1\, \mathrm{d}^d r_2 \Theta(\sigma - |\boldsymbol{r}_1 - \boldsymbol{r}_2|) \sum_{a_1,a_2} a_1^\dagger(\boldsymbol{r}_1)a_2^\dagger(\boldsymbol{r}_2)\Big(\\ \underbrace{A(\boldsymbol{r}_1)\delta_{A,a}\delta(\boldsymbol{r}_2 - \boldsymbol{r}) + \delta_{A,a}\delta(\boldsymbol{r}_1 - \boldsymbol{r})A(\boldsymbol{r}_2)}_{\text{(I)}} \\ \underbrace{-a_1(\boldsymbol{r}_1)\delta_{a_2,a}\delta(\boldsymbol{r}_2 - \boldsymbol{r}) - \delta_{a_1,a}\delta(\boldsymbol{r}_1 - \boldsymbol{r})a_2(\boldsymbol{r}_2)\Big)}_{\text{(II)}} \end{aligned} \tag{4.85}$$

There is a lot of reduction to be made: both of the terms $\sim \delta_{A,a}$ will end up looking the same after the integration is executed: in either of them one of the integration variables $\boldsymbol{r}_j$ will be identified with $\boldsymbol{r}$-dependence; in either of them, the $A(\boldsymbol{r}_i)$ factor depends on the *other* integration variable $\boldsymbol{r}_j \neq \boldsymbol{r}_i$. Hence, for example the first of the two terms evaluates to

$$\delta_{a,A}\frac{\lambda}{2}\int \mathrm{d}^d r_1\, \Theta(\sigma - |\boldsymbol{r}_1 - \boldsymbol{r}|) \sum_{a_1,a_2} a_1^\dagger(\boldsymbol{r}_1)a_2^\dagger(\boldsymbol{r})A(\boldsymbol{r}_1)$$

where we may still rename variables still carrying unnecessary indices to emphasize that they only serve as dummies; both of them together amount to

$$\text{(I)} \quad = \quad \delta_{a,A}\,\lambda\int \mathrm{d}^d r'\, \Theta(\sigma - |\boldsymbol{r} - \boldsymbol{r}'|) \sum_{a_1,a_2} a_1^\dagger(\boldsymbol{r})a_2^\dagger(\boldsymbol{r}')A(\boldsymbol{r}') \tag{4.86}$$

where the dummy variables a_1 and a_2 have to be swapped for one of them in order to unify the terms. A similar treatment can be given to the remaining two terms, which also evaluate to the same operator: in either of the terms, one of the a_j dummy variables is replaced by a and its associated integrarion variable $\boldsymbol{r}_j$ by $\boldsymbol{r}$. Once again, under appropriate renaming of dummy variables (and by using that creation operators mutually commute), they sum to

$$\text{(II)} \quad = \quad -\lambda\int \mathrm{d}^d r'\, \Theta(\sigma - |\boldsymbol{r} - \boldsymbol{r}'|)a^\dagger(\boldsymbol{r})\sum_{a'} {a'}^\dagger(\boldsymbol{r}')a'(\boldsymbol{r}') \tag{4.87}$$

Note that both eq. (4.86) and eq. (4.87) are trailed by annihilation operators. While very relevant for the value of the commutator, as soon as it comes to taking averages these trailing annihilation operators will be absorbed into $|\mathrm{sum}\rangle$:

$$\begin{aligned}
(\mathrm{I}) &= \delta_{a,A}\lambda \int \mathrm{d}^d r' \, \Theta(\sigma - |\boldsymbol{r} - \boldsymbol{r}'|) \sum_{a_1,a_2} \underbrace{\langle P(t)|\, a_1^\dagger(\boldsymbol{r}) a_2^\dagger(\boldsymbol{r}') \,|\mathrm{sum}\rangle}_{=\rho^{(2)}_{a_1,a_2}(\boldsymbol{r},\boldsymbol{r}',t)} \\
(\mathrm{II}) &= -\lambda \int \mathrm{d}^d r' \, \Theta(\sigma - |\boldsymbol{r} - \boldsymbol{r}'|) \underbrace{\sum_{a'} \langle P(t)|\, a^\dagger(\boldsymbol{r}) a'^\dagger(\boldsymbol{r}') \,|\mathrm{sum}\rangle}_{=\rho^{(2)}_{a,a'}(\boldsymbol{r},\boldsymbol{r}',t)}
\end{aligned} \tag{4.88}$$

We make a case distinction between $a = A$ and $a = I$. When $a = A$, $\delta_{a,A} = 1$ and term (I) contributes to $[Q_\lambda, a^\dagger(\boldsymbol{r})]$. (I) contains the sum over all two-point density functions $\rho^{(2)}_{a_1,a_2}(\boldsymbol{r}, \boldsymbol{r}', t)$, respectively denoting the density of pairs per unit two-body configuration space volume $\mathrm{d}^d r \, \mathrm{d}^d r'$ where the grain at $\boldsymbol{r}$ has activity state $a_1 \in \{A, I\}$ and the one at $\boldsymbol{r}'$ has activity state $a_2 \in \{A, I\}$. Two of these, $\rho^{(2)}_{A,A}(\boldsymbol{r}, \boldsymbol{r}', t)$ and $\rho^{(2)}_{A,I}(\boldsymbol{r}, \boldsymbol{r}', t)$ get cancelled by their negative counterpart in (II). The result is that the Q_λ contribution to the time evolution of $\rho_A(\boldsymbol{r}, t)$ reads

$$\frac{\partial \rho_A(\boldsymbol{r}, t)}{\partial t} = (\cdots) + \lambda \int \mathrm{d}^d r' \, \Theta(\sigma - |\boldsymbol{r} - \boldsymbol{r}'|) \sum_a \rho^{(2)}_{I,a}(\boldsymbol{r}, \boldsymbol{r}', t) \tag{4.89}$$

In the second simpler case $a = I$ term (I) vanishes, since now $\delta_{a,A} = 0$. Hence the contribution of Q_λ to $\rho_I(\boldsymbol{r}, t)$ reads

$$\frac{\partial \rho_I(\boldsymbol{r}, t)}{\partial t} = (\cdots) - \lambda \int \mathrm{d}^d r' \, \Theta(\sigma - |\boldsymbol{r} - \boldsymbol{r}'|) \sum_a \rho^{(2)}_{I,a}(\boldsymbol{r}, \boldsymbol{r}', t) \tag{4.90}$$

which is precisely the negative of the contribution to $\rho_A(\boldsymbol{r}, t)$, ensuring overall conservation of grain number.

Discussion of the Evolution Equation Putting all parts together, the full equations read

$$\begin{aligned}
\left(\frac{\partial}{\partial t} - D\nabla^2\right) \rho_A(\boldsymbol{r}, t) &= -\mu \rho_A(\boldsymbol{r}, t) + \lambda \int \mathrm{d}^d r' \, \Theta(\sigma - |\boldsymbol{r} - \boldsymbol{r}'|) \sum_a \rho^{(2)}_{I,a}(\boldsymbol{r}, \boldsymbol{r}', t) \\
\frac{\partial \rho_I(\boldsymbol{r}, t)}{\partial t} &= +\mu \rho_A(\boldsymbol{r}, t) - \lambda \int \mathrm{d}^d r' \, \Theta(\sigma - |\boldsymbol{r} - \boldsymbol{r}'|) \sum_a \rho^{(2)}_{I,a}(\boldsymbol{r}, \boldsymbol{r}', t)
\end{aligned} \tag{4.91}$$

Defining *total grain density* $\rho(\boldsymbol{r}, t) = \rho_A(\boldsymbol{r}, t) + \rho_I(\boldsymbol{r}, t)$ and summing the two equations yields

$$\frac{\partial \rho(\boldsymbol{r}, t)}{\partial t} = D\nabla^2 \rho_A(\boldsymbol{r}, t) \tag{4.92}$$

which both enforces the conservation of grain number (since the integral over the laplacian of of ρ_A, which has to vanish towards infinity rapidly enough to integrate to the finite number N_A of active grains in the system, will be zero) and demonstrates that matter transport happens only by means of grain diffusion. The interpretation of the activation term can be made more apparent after splitting

$$\rho^{(2)}_{a,a'}(\boldsymbol{r}, \boldsymbol{r}') =: \rho_a(\boldsymbol{r}) \rho_{a'}(\boldsymbol{r}') \, g_{a,a'}(\boldsymbol{r}, \boldsymbol{r}') \tag{4.93}$$

where $g_{a,a'}(\boldsymbol{r},\boldsymbol{r}')$ is the two-point distribution function for an a-grain $\boldsymbol{r}$ and an a'-grain at $\boldsymbol{r}'$:

$$\frac{\partial \rho_A(\boldsymbol{r},t)}{\partial t} = \left(D\nabla^2 - \mu\right)\rho_A(\boldsymbol{r},t) + \lambda \rho_I(\boldsymbol{r},t)\int \mathrm{d}^d r'\,\Theta(\sigma - |\boldsymbol{r}-\boldsymbol{r}'|)\sum_a \rho_a(\boldsymbol{r}',t)\,g_{I,a}(\boldsymbol{r},\boldsymbol{r}',t) \tag{4.94}$$

$D\nabla^2\rho_A(\boldsymbol{r},t)$ causes diffusion of the active grain density field and $-\mu\rho_A(\boldsymbol{r},t)$ decays activity.

$$\frac{\partial \rho_A(\boldsymbol{r},t)}{\partial t} = (D\nabla^2 - \mu)\rho_A(\boldsymbol{r},t)$$

is trivially solved, most easily in Fourier-space

$$\tilde{\rho}_A(\boldsymbol{k},t) = e^{-(D\boldsymbol{k}^2+\mu)t}\,\tilde{\rho}_A(\boldsymbol{k},0)$$

or Fourier-Laplace-space

$$\int_0^\infty \mathrm{d}t\, e^{-st}\tilde{\rho}_A(\boldsymbol{k},t) = \frac{1}{s + (D\boldsymbol{k}^2 + \mu)}\cdot\tilde{\rho}_A(\boldsymbol{k},0)$$

Hence diffusion and decay together constitute the *free behaviour*, as in free of pair (or higher) interactions. $+\lambda\rho_I(\boldsymbol{r},t)\int \mathrm{d}^d r'\,\Theta(\sigma - |\boldsymbol{r}-\boldsymbol{r}'|)\sum_a \rho_a(\boldsymbol{r}',t)\,g_{I,a}(\boldsymbol{r},\boldsymbol{r}',t)$ increases activity *the more inactive grains are involved in overlaps*; overall changes in the density profile $\partial\rho(\boldsymbol{r},t)/\partial t$ are effected exclusively by active grain diffusion.

Finding the evolution of the active grain density field was a matter of executing the commutators appearing in $\left[Q, a^\dagger(\boldsymbol{r})\right]$. This recipe in principle works for computing arbitrarily high n-point densities (which are, to the very least, significantly trickier to just guess than eq. (4.94))

$$\frac{\partial}{\partial t}\langle P(t)|\, a_1^\dagger(\boldsymbol{r}_1)\cdots a_n^\dagger(\boldsymbol{r}_n)\,|\mathrm{sum}\rangle = \langle P(t)|\left[Q, a_1^\dagger(\boldsymbol{r}_1,t)\cdots a_n^\dagger(\boldsymbol{r}_n,t)\right]|\mathrm{sum}\rangle \tag{4.95}$$

As Doi (1976a) remarks, the family of n-body evolution equations is not unlike the (significantly more well known) *Bogoliubov-Born-Green-Kirkwood-Yvon* (BBGKY) hierarchy for classical fluids, as in that the n-body density equation is closed by providing an expression for the $(n+1)$-body density.

4.3.5 Critical Density Estimation

Just like random organization, the dynamics specified in section 4.3.3 that approximate it experience an absorbing state transition with infinitely many absorbing states: when the system is very dilute (and $D\sigma^{-2} < \mu$ such that Brownian motion is not too fast), there will be barely any overlaps that could cause $a_1 + a_2 \rightarrow 2A$ with a lot of space to resolve them, which the overlap-less active grains cannot traverse before they get struck by $A \rightarrow I$. Without overlaps and active grains, the state is absorbing. When the system is so dense that overlaps could not possibly be resolved, there are necessarily overlaps, hence reliably (and indefinitely) active grains and with them (indefinite) diffusion. These two regimes must be separated by a transition, that is qualitatively a lot like random organization. In the following, I will (1) present a few of my findings

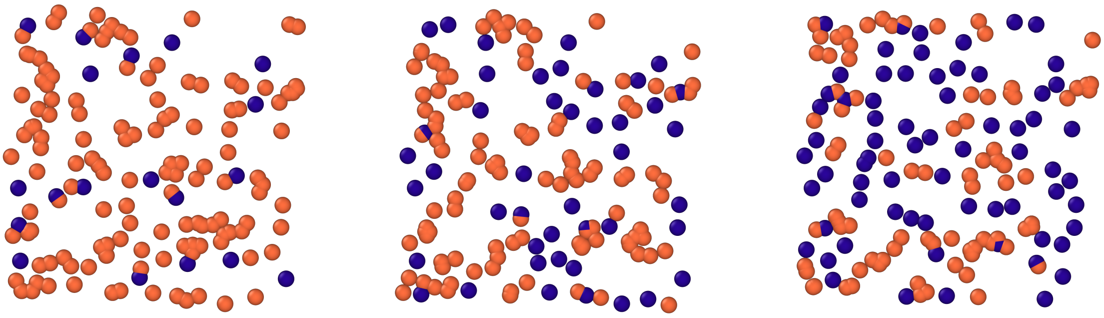

Figure 4.5: Snapshot of a small scale ($N = 150$) simulation of the dynamics defined in section 4.3.3 (at $\Phi = 40\%$, $(\lambda/\mu) = 5$ and $(\mu/D) = 100\sigma^{-2}$). From left to right, the snapshots are from the beginning, transient period and steady-state respectively. Bright, orange grains are active, dark purple ones inactive. One can see multiple grains with overlaps that are not active and many grains without overlaps that are active. However, mostly the activation state lines up with the overlaps. Images were rendered with `Ovito` (`https://www.ovito.org/`, last visited 25.11.2025)

on how the reaction system behaves as the limits $\lambda \gg \mu \gg D\sigma^{-2}$ are approached and (2) report three ultimately not unsuccessful but instructive attempts at finding an approximation.

For simplicity, I will discuss only the case of a homogeneous system $\rho(\boldsymbol{r}, t) \equiv \rho$, in which case eq. (4.94) simplifies to

$$\frac{\mathrm{d}\rho_A}{\mathrm{d}t} = -\mu\rho_A + \lambda\rho_I \sum_a \rho_a \int \mathrm{d}^d r\, \Theta(\sigma - r)\, g_{I,a}(r) \tag{4.96}$$

To better understand the system I also performed small scale simulations of the dynamics defined in section 4.3.3. A brief description of what exactly I did can be found in appendix B.

Rate Dependence of Critical Density The critical density changes with μ and λ. To start with the most obvious effect: because deactivation is not instantaneous (instead gradually generated by $A \to I$ with rate μ) an active grain has a certain 'coyote time'[13] μ^{-1} during which it can still diffuse despite 'hanging in the air' without overlaps. In that time the diameter of the volume that can still potentially be diffusively explored by the grain's center is $2\sqrt{2D\mu^{-1}}$. Add onto half of that the grain's diameter to get a *larger radius of activation* (fig. 4.7) that may be thought of as an effectively larger active grain diameter σ_A^{eff}

$$\sigma_A^{\mathrm{eff}} = \sigma + \sqrt{\frac{2D}{\mu}} \tag{4.97}$$

that converges to σ as $(\mu/D) \to \infty$. Similarly, during an activation $A + I \to 2A$, the active grain will penetrate a distance $(2D\lambda^{-1})^{1/2}$ before the I-grain first notices its new

---

[13] Used here metaphorically, see `https://en.wiktionary.org/wiki/coyote_time` (last visited on 20.11.2025): a grace period in platform game design for jumping mid-air off ledges

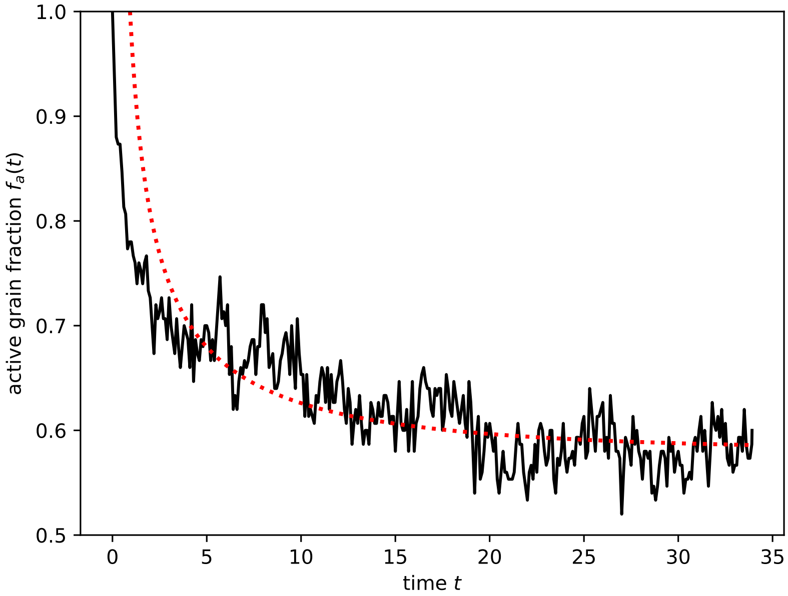

Figure 4.6: Active grain fraction $f_a(t)$ as measured from a small ($N = 150$) simulation in $d = 2$ of the dynamics defined in section 4.3.3 at $\Phi = 40\%$ (which is most probably in the active phase, since Φ far above the critical packing density of random organization given by Wilken et al. 2021, whose protocol is more similar to the instantaneous-activation limit of the present reaction system) with $(\lambda/\mu) = 5$ and $(\mu/D) = 100\sigma^{-2}$. Time is in units of μ^{-1}. One can observe a decay to some steady state value; fitting the data to $f_a(t) = f_a^\infty + (1 - f_a^\infty)e^{-t/\tau}t^{-\delta}$ (compare Corté et al. 2008, eq. 1) in a log-log-plot yields $f_a^\infty = 0.5981 \pm 0.010$, though the error should not be taken very literally, given the rest of the fit is not very good: $\tau = 17 \pm 15$ and $\delta = 0.72 \pm 0.13$; the mismatch for short times is also very visible.

overlap, effectively reducing I-grain diameter by

$$\sigma_I^{\mathrm{eff}} = \sigma - \sqrt{\frac{2D}{\lambda}} \tag{4.98}$$

also with $\sigma_I^{\mathrm{eff}} \to \sigma$ as the rate of activation is taken to $\lambda \to \infty$. Averaging the two arguably renders an effective interaction distance

$$\sigma^{\mathrm{eff}} = \sigma + \frac{1}{2}\left(\sqrt{\frac{2D}{\mu}} - \sqrt{\frac{2D}{\lambda}}\right) \tag{4.99}$$

and hence an effective packing density by $\Phi \sim \sigma^d$

$$\frac{\Phi^{\mathrm{eff}}}{\Phi} = \left(1 + \frac{1}{\sqrt{2}}\left(\sqrt{\frac{D\sigma^{-2}}{\mu}} - \sqrt{\frac{D\sigma^{-2}}{\lambda}}\right)\right)^d \tag{4.100}$$

Recall furthermore that any grain with overlap flip-flops between being active and inactve, being activated with rate $z\lambda$, where z is the number of overlap partners, and

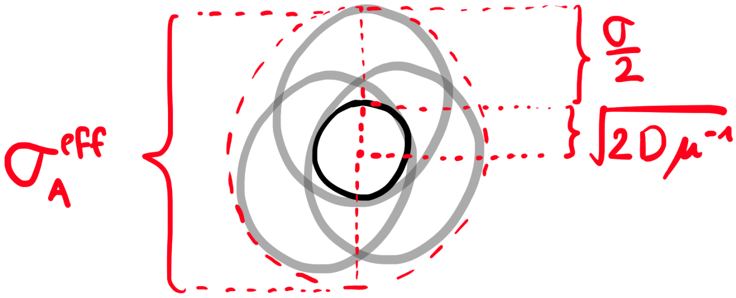

Figure 4.7: Illustration of the effective active grain diameter eq. (4.97). The black central cirle is of diameter $\sqrt{2D\mu^{-1}}$ and is the area diffusively explored by the grain before it decays to inactivity. The bigger, grey circles have diameter σ and stand for possible locations the grain could have after its random walk of duration μ^{-1}. The red doted circumference has diameter σ_A^{eff}.

deactivated with rate μ. Hence the expected fraction f_A of time that a grain with z overlap partners spends activated is given by how short the mean time μ^{-1} until decay (spent active) is compared to the mean time $(z\lambda)^{-1}$ until activation (spent inactive)

$$f_A = \frac{\mu^{-1}}{\mu^{-1} + (z\lambda)^{-1}} = \frac{z}{z + \mu/\lambda} \tag{4.101}$$

This means that, even deep into the active phase, diffusion is slower than D would let one believe, since only f_A of the time a grain overlaps is spent actually diffusing: given z overlaps, one may choose D_z^{eff} such that $(2D_z^{\text{eff}} \cdot t)^{1/2} = (2D \cdot f_A \cdot t)^{1/2}$ then average D_z^{eff} with the distribution $P\,(z \text{ overlaps})$ for overlap count z

$$\frac{\mathrm{D}^{\text{eff}}}{D} = \sum_z P\,(z \text{ overlaps}) \cdot \frac{z}{z + \mu/\lambda} \tag{4.102}$$

Note that $\mathrm{D}^{\text{eff}} \to D$ in the limit $(\lambda/\mu) \to \infty$.

It is important to clarify, that all of these intuitions apply only to a steady state with non-vanishing activity near critical point, where the system is close to being as dilute as possible while still maintaining activity (as opposed to a high density, overcrowded situation where essentially all grains have overlaps).

Approximation Attempt 1: Uncorrelated Positions Before discussing what more complicated approximations could look like, we first want to see what happens when we neglect all spatial correlation by assuming all $g_{I,a}(r) \equiv 0$. Since we work in a homogeneous system $D\nabla^2$ terms vanish and eq. (4.96) reduces to

$$\frac{\mathrm{d}\rho_A}{\mathrm{d}t} = -\mu\rho_A + \lambda\rho_I \underbrace{(\rho_A + \rho_I)B_d\sigma^d}_{=2^d\Phi} \tag{4.103}$$

where B_d is the volume of a d-dimensional unit sphere. Multiplying the entire equation with $B_d(\sigma/2)$ to work with active- and inactive grain density Φ_A and $\Phi_I = \Phi - \Phi_A$ respectively yields

$$\begin{aligned}\frac{\mathrm{d}\Phi_A}{\mathrm{d}t} &= -\mu\rho_A + \lambda(\Phi - \Phi_A)2^d\Phi \\ &= (\lambda\, 2^d\Phi - \mu)\Phi_A + \lambda\, 2^d\Phi^2\end{aligned} \tag{4.104}$$

where one can define $\eta = \lambda 2^d\Phi - \mu$ and $\kappa = \lambda 2^d\Phi^2/\eta$ followed by separating the variables to find the solution

$$\left|\frac{\Phi_A(t) + \kappa}{\Phi_A(0) + \kappa}\right| = e^{\eta t} \tag{4.105}$$

which displays a transition of behaviour when Φ crosses $\Phi_c = 2^{-d}\mu/\lambda$: when $\eta < 0$, then $\kappa < 0$ and the supposed active grain density decays to the steady state value $\Phi_A(t) \to -\kappa = |\kappa|$. As $\Phi \uparrow \Phi_c$ we get $|\kappa| \sim (1/|\Phi_c - \Phi|) \to \infty$ which links up with the regime $\Phi > \Phi_c$ where $\eta > 0$ and Φ_A grows indefinitely with $e^{|\eta|t}$. Obviously this is completely off the behaviour of the exact model. And not only that, when going to the limit $\lambda \gg \mu$ where we expected to get time continuous-random organization, we get a trivial critical density $\Phi_c = 2^{-d}\mu/\lambda \to 0$ for any dimension d, which is also wrong.

Approximation Attempt 2: No I-I-overlaps and no I-A-correlation With view to the limit $\lambda \gg \mu$, just assuming $g_{I,I}(r) \equiv 1$ looks like the most blatantly bad assumption in approximation attempt 1. The most simplistic remedy would be to skip right to the expected limit of $g_{I,I}(r) = 0$ at $r < \sigma$ while keeping $g_{I,A}(r) \equiv 1$, resulting in eq. (4.96) becoming

$$\frac{\mathrm{d}\rho_A}{\mathrm{d}t} = -\mu\rho_A + \lambda\rho_I \underbrace{(\rho_A \cdot 1 + \rho_I \cdot 0)B_d\sigma^d}_{=2^d\Phi_A} \tag{4.106}$$

where we again will multiply the equation by $B_d(\sigma/2)$ to state it in terms of packing densities

$$\begin{aligned}\frac{\mathrm{d}\Phi_A}{\mathrm{d}t} &= -\mu\Phi_A + \lambda(\Phi - \Phi_A)2^d\Phi_A \\ &= (\lambda 2^d\Phi - \mu)\Phi_A - \lambda 2^d\, \Phi_A^2\end{aligned} \tag{4.107}$$

In this one can recognize the homogeneous mean-field theory of DP and CDP from eq. (2.41) or eq. (3.1), the solution of which has already been discussed in section 2.2.3. Takeaways from the latter for the present discussion are

- There is a transition that happens when $\lambda 2^d\Phi\mu = 0$ at $\Phi_c = 2^{-d}\mu/\lambda$

- There is active/percolating phase for $\Phi > \Phi_\mathrm{c}$ where the steady state active grain density is
$$\Phi_A^\infty = \lim_{t\to\infty} \Phi_A(t) = \Phi - 2^{-d}(\mu/\lambda)$$
and hence $\Phi_A^\infty \sim |\Phi - \Phi_\mathrm{c}|$ from the active phase, giving the mean-field order parameter exponent $\beta = 1$

- At $\Phi = \Phi_\mathrm{c}$ the active grain density asymptotically goes like $\sim t^{-1}$, giving it another mean-field exponent $\nu_\| = 1$

- An absorbing phase for $\Phi < \Phi_\mathrm{c}$, where Φ_A decays to zero with characteristic time $\tau = (\lambda 2^d \Phi - \mu)^{-1}$

However, while the qualitative behaviour is not totally off, it breaks in the limit $(\lambda/\mu) \to \infty$ to time-continuous random organization. Amongst other things $\tau \to 0$ (which already demonstrates that it has nothing to do with the relaxation time of random organization) and, even more damningly, the critical packing density becomes trivial again $\Phi_\mathrm{c} \to 0$.

I suggest the following interpretation: uncorrelated positions means ignoring correlations stemming, ultimately, from relative positioning of typical grain pairs, leaving the transition of activity to inactivity entirely up to the balance of λ and μ. In the limit $\lambda \gg \mu$, this must lead to Φ_c equalling to zero: assuming $g_{I,A}(r)$ and $g_{I,I}$ are not depleting within $r < \sigma$ as time progresses to $t \to \infty$ is tantamount to claiming there will always be *some* overlap and hence always *some* activity unless there are no grains at all. This makes evident, that the stationary $g_{I,a}(r)$ need to be depleted within $r < \sigma$ (in a way will depend at least on Φ and the rates λ, μ).

Pause: when is critical density even non-trivial? Suppose a system has reached its stationary state in the active phase $\Phi > \Phi_\mathrm{c}$, where the rate of change of $\rho_A(t)$ vanishes. This turns eq. (4.96) into a steady-state equation

$$\mu\rho_A = \lambda\rho_I \sum_a \rho_a \int \mathrm{d}^d r\, \Theta(\sigma - r)\, g_{I,a}(r) \tag{4.108}$$

which reads conveniently as decay $A \overset{\mu}{\to} I$ and proliferation $a_1 + a_2 \to 2A$ striking a balance. Notice that we only need to understand the behaviour for $r \leq \sigma$. Anticipating that we want to let $(\lambda/\mu) \to \infty$ eventually, we can divide both sides by μ and find that for any sort of successful approximation we need $({}^\lambda/_\mu) \int \mathrm{d}^d r\, \Theta(\sigma - r)\, g_{I,a}(r)$ or $\int \mathrm{d}^d r\, \Theta(\sigma - r)\, ({}^\lambda/_\mu) g_{I,a}(r)$ to converge to some finite number as $(\lambda/\mu) \to \infty$. The result of this limit[14] will be some function $G_{I,a}(\rho)$ of density (the last remaining independent[15] control parameter)

$$\rho_A = (\rho - \rho_A) \sum_a \rho_a G_{I,a}(\rho) \tag{4.109}$$

---

[14] I want to remind at this point, that in the limit $\lambda \gg \mu \gg D\sigma^{-2}$ any overlapping grains should be active, and hence $g_{I,a}(r) = 0$ for all $r < \sigma$. This interestingly means, that the information on Φ_c lies in the manner in which $g_{a,a'}(r)$ responds to λ and μ changing relative to $D\sigma^{-2}$, despite the former two being entirely auxiliary in purpose.

[15] By rescaling time we can eliminate one of the rates, say by non-dimensionalizing time with $D\sigma^{-2}$

Imagine now we can expand the density dependences of $G_{I,a}(\rho)$ in a well-behaved power series $\sum_{n=0}^{\infty} Y_{I,a}^{(n)} \rho^n$ of ρ

$$\rho_A = (\rho - \rho_A) \sum_{n=0}^{\infty} \left((\rho - \rho_A) Y_{I,I}^{(n)} + \rho_A Y_{I,A}^{(n)} \right) \rho^n \tag{4.110}$$

At the critical point active grain density vanishes and

$$0 = \rho^2 \sum_{n=0}^{\infty} Y_{I,a}^{(n)} \rho^n \tag{4.111}$$

We see that if only one of the terms is non-vanishing, then the equation becomes $0 = \rho^{n+2}$, i.e. again trivial critical density. We conclude that at least two terms in the power series expansion, if existent, would have to be non-vanishing and we can rule out a homogeneous dependence ρ^p of $\sum_a \rho_a G_{I,a}(\rho)$ on density.

It is generally true though, that we need the limit of $\sum_a \rho_a G_{I,a}(\rho)$ as $\rho_A \to 0$ to be an expression in terms of ρ with a non-trivial roots $\rho^* \neq 0$ which would be our value for the critical number density ρ_c (related to critical packing density by $\Phi_\mathrm{c} = B_d({}^{\sigma}\!/_2)^d \rho_\mathrm{c}$).

Involving Motion In hindsight it is not surprising that either of the previous attempts resulted in a trivial critical density: the limit towards time-continuous random organization is not just $\lambda \gg \mu$, it is $\lambda \gg \mu \gg D\sigma^2$. Without involving motion, quantified by D, into our equations (like attempts 1 and 2 did), we have little basis for expecting any sensible relation to space, the very thing that the grains are packed in: by neglecting any positional information, also neglect the role of motion, as quantified by the rate $D\sigma^{-2}$. Its value should affect how the $g_{a,a'}(r)$ look, since it relates the characteristic timespans λ^{-1} and μ^{-1} over which reactions occur to the volume of a patch of space diffusively explored by an active grain $\sim (2D\mu^{-1})^{d/2}$.

Because the diffusion term $D\nabla^2\rho_A$ vanishes in a homogeneous system, the only way in which grain diffusion expresses itself in the steady state equation eq. (4.108) is through the shape of the I-a pair distribution functions $g_{I,a}(r)$. From very small-scale simulations of the dynamics I performed to get a better intuition for the reaction system (see fig. 4.8 and fig. 4.9a), one can make the educated guess that $g_{I,I}(r) \approx 0$ compared to $g_{I,a}(r)$ (see fig. 4.8b). We also see verification (fig. 4.8a) that the diffusion-related length scales defined in eq. (4.97) and eq. (4.98) are indeed characteristic length scales for the behaviour of $g_{I,A}(r)$ around the activation-distance $r = \sigma$.

The probably crudest imitation one could give of $g_{I,A}(r) = g_{A,I}(r)$ as seen fig. 4.9b is some $r < \sigma$ plateau value $g_{I,A}^0$, followed by a linear rise (beginning at about $r = \sigma - (2D\lambda^{-1})^{1/2}$) to the expected $r \to \infty$ $g_{I,A}(r)$-plateau value of

$$g_{I,A}^{\infty} := \frac{1}{4} \tag{4.112}$$

(reached at about $r = \sigma + (2D\mu^{-1})^{1/2}$). The crudest approximation for the $|\boldsymbol{r}_2 - \boldsymbol{r}_1| < \sigma$ plateau of $g_{I,A}(\boldsymbol{r}_1, \boldsymbol{r}_2)$ should be product of the respective likelihoods for an overlapping pair of grains at $\boldsymbol{r}_1$ and $\boldsymbol{r}_2$, that the $\boldsymbol{r}_1$-grain is inactive (which has probability $1 - f_A$) and that the $\boldsymbol{r}_2$-grain is active (which has probability f_A)

$$g_{I,A}(r < \sigma_I^{\mathrm{eff}}) \approx g_{I,A}^0 := f_A(1 - f_A) = \frac{\mu/\lambda}{z + \mu/\lambda} \cdot \frac{z}{z + \mu/\lambda} \tag{4.113}$$

where z is the mean number of overlaps of the $\boldsymbol{r}_2$-grain (by spatial homogeneity the same for all grains). However, this cannot be enough, since, as just discussed, the resulting expression *needs at least* two powers of density to not yield trivial critical density. This is not to mention, that in the limit $\mu \gg D\sigma^{-2}$, which we need to take first, the sloped section of $g_{I,A}(r)$ vanishes, leaving only the plateau $g^0_{I,A}$.

Hence, I conclude that, before suggesting even more involved empirically motivated shapes for $g_{I,A}(r)$, it is probably best to try and obtain a more systematic approximation attempt that involves multiple powers of ρ. Judging by experiences from fluid theory, I expect to obtain by neglecting the existence of n-fold overlaps. Unfortunately, without anything at hand that resembles the Boltzmann-Gibbs distribution, this expansion has to be built from the ground up and will hence be the subject of future research.

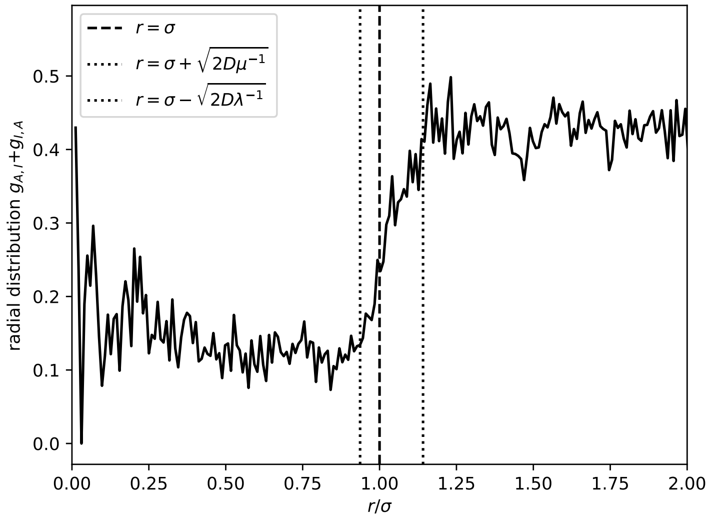

(a) $g_{A,I}(r) + g_{I,A}(r)$

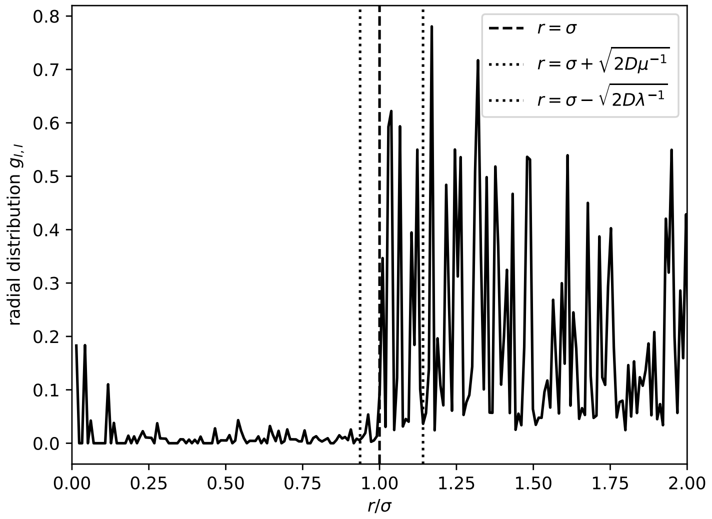

(b) $g_{I,I}(r)$

Figure 4.8: Measured A-I (fig. 4.8a) and I-I (fig. 4.8b) radial distribution functions as measured from a small two-dimensional simulation ($N = 150$) in the steady state of the dynamics defined in section 4.3.3 at $\Phi = 40\%$ with $(\lambda/\mu) = 5$ and $(\mu/D) = 100\sigma^{-2}$. In (a) one can see that $(2D\mu^{-1})^{1/2}$ and $(2D\lambda^{-1})^{1/2}$ are characteristic length scales of spatial I-A-correlation, more specifically for the width of the transition from closer than the reaction distance $r \ll \sigma$ to outside of reaction range $r \gg \sigma$. Note that it does not plateau to 1 for large r; this is actually correct, since $g(r)$ plateaus to 1 and splits into $g(r) = \sum_{a,a'} g_{a,a'}(r)$. In (b) one can see that $g_{I,I}(r)$ is depleted at. In either image there seem to be significantly larger $g_{I,a}(r)$ values towards $r \to 0$. While a rise of $g_{I,a}(r)$ towards $r = 0$ cannot be entirely ruled out, there is also no clear evidence for it here, because fluctuations of the histograms underlying these curves are significantly amplified by multiplication with $r^{-(d-1)}$ close to $r = 0$.

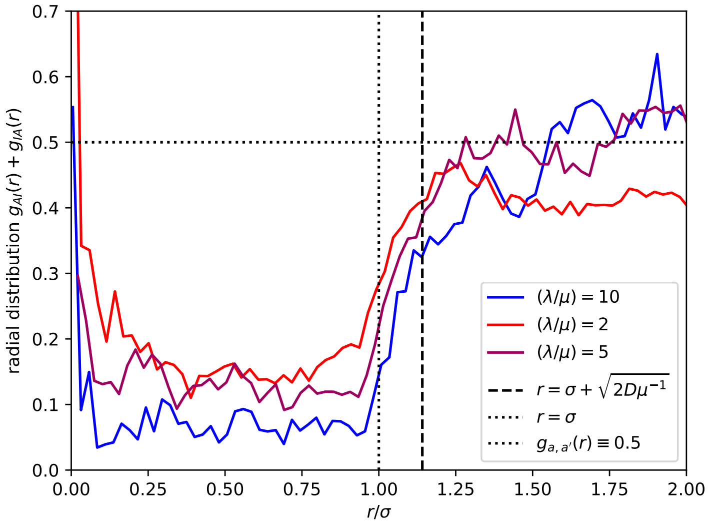

(a) $r \in [0, 2\sigma]$ showing the depletion of $g_{I,A}(r) + g_{A,I}(r)$ within $r < \sigma$ with rising (λ/μ)

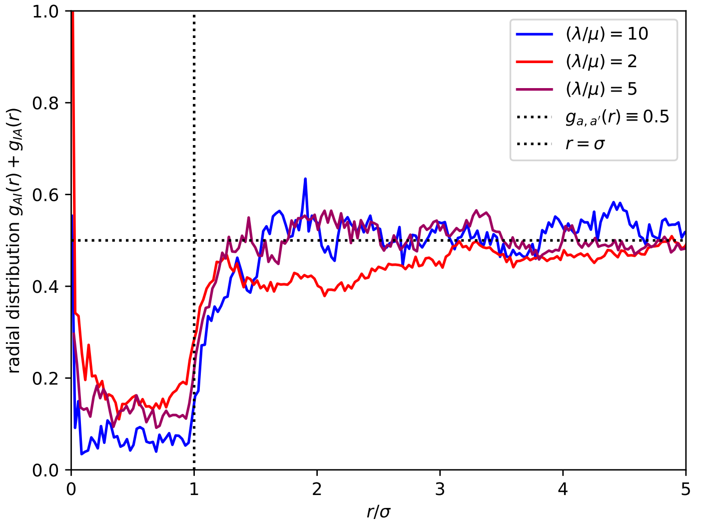

(b) $r \in [0, 5\sigma]$ showing the plateauing of $g_{I,A}(r) + g_{A,I}(r)$ to 0.5

Figure 4.9: Radial distribution $g_{I,A}(r) + g_{A,I}(r)$ of A-I grain pairs measured from a very small scale ($N = 50$) two-dimensional simulation of the dynamics defined in section 4.3.3 at different reaction rate ratios $(\lambda/\mu) = 2, 5, 10$.

5 Summary and Outlook

Literature work In summary, I have given a rudimentary presentation of the theory of continuous phase transitions (chapter 2). I started by introducing the concept of an order-parameter in the context of field theories for critical points (like the Curie point and DP) as well as simulations (like random organization). I proceeded to explain, that phase transitions exhibit scaling-behaviour at criticality, which which depends only on very general physical properties (like symmetries), and divides continuous transitions on only a handful of universality classes. In the pursuit of understanding the literature on random organization, I researched the field theory approach to phase transitions as pioneered by Wilson (1971b) and applied to non-equilibrium transitions by works like Janssen (1976). This included getting an idea on how these field theories are justified and how they relate to the commonly encountered space- and time-resolved Langevin equations, in which an appropriate noise term is added onto a mean-field theory in order to arrive at a description of the universality class of interest.

As presented in chapter 3, I concluded from my literature work that analytical study of the Manna transition is dominated by abstract field theories of the entire universality class, geared towards the renormalization (semi-)group procedure, including only few relevant couplings. The determination of (highly model dependent) critical thresholds on the other hand is being attacked with simulation studies, like the introductory Corté et al. (2008) or Milz and Schmiedeberg (2013) and Wilken et al. (2021). The latter two placed random organization on a spectrum of overlap reducing protocols that has common protocols for the production of athermally jammed states on the other end.

Finally, I dove into the literature of applying the many-body operator formalism, typically used in many-body quantum physics, to classical physical systems like chemical reactions whose outcome is highly dependent on the spatial correlation; pioneering works on this are Martin, Siggia, and Rose (1973) and Doi (1976a). These two also turn out to be seminal contributions to the study of dynamical phase transitions with field theory techniques.

Own investigations I presented my trial and error process towards finding analytical models of random organization that might be used to calculate the critical packing density analytically. The first challenge was to find a proper language for describing the random organization system.

To this end I made a very crude discrete time calculation (presented in section 4.1) in which, for tractability, I had to neglect the spatial correlations of grains (making it a mean-field theory). The thus obtained critical densities for $d = 2$ and $d = 3$ were not extremely accurate, but surprisingly close to the critical densities of the random organization protocols of Milz and Schmiedeberg (2013) and Wilken et al. (2021) (see table 4.1).

There was however no clear way to improve these calculations, that did not involve assuming some radial distribution a priori, which would have been self-defeating. Hence I turned to many-body descriptions. I quickly found that time-continuous models are both easier to write down and closer to physicists' core skill sets. The first of these was eq. (4.13), a Fokker-Planck equation in all grain positions $(\boldsymbol{x}_1, \dots, \boldsymbol{x}_N)$, that checks for every grain if it has any overlaps with an appropriate indicator function; by multiplying the probability distribution $P(\boldsymbol{x}_1, \dots, \boldsymbol{x}_N)$ by said indicator, diffusion of grain k is then conditioned on k having overlaps. While a direct translation of random organization to continuous time, this approach has the downside that it comes with arbitrarily high n-body terms in the generator alone; I could not identify a way to salvage this directly.

However, I next pursued the idea of relaxing the requirement that a particle has to be registered as active or inactive immediately after respectively gaining an overlap or loosing all overlaps. Inspired by theories that had reaction-diffusion models of the reaction pair $A + I \to 2A$ and $A \to I$ beyond mean field as their frame of reference (like Wijland, Oerding, and Hilhorst (1998)), sought out frameworks for implementing these in a concise manner (section 4.3.1) and found Doi (1976a) and Doi (1976b), which implements among other things diffusion controlled reactions beyond mean-field calculations in the operator language typical of many-body quantum theory. I explained the formalism and formulated a random organization mimicking model (section 4.3.3), that had the aforementioned reactions and a diffusion term exclusively for active grains. I derived from it the time evolution equation of the active-grain and inactive-grain density fields (eq. (4.94)) as well as outlined the algorithm by which one may in principle derive a hierarchy of n-body densities akin to the BBGKY hierarchy (eq. (4.67)). The evolution equations of the density fields involved the radial distributions $g_{a,a'}(r)$ (where $a, a' \in \{I, A\}$ are the two grain species / activation states) which respectively are analogous to the radial distribution function, with the difference that they quantify distance distributions conditioned on one grain being in activation state a and the other in activation state a'. I analysed the model by inserting (unsuccessfully) three very simple assumptions for the $g_{a,a'}(r)$; how they failed points the way to better approximations, with non-trivial critical density: (1) assuming uncorrelated grain locations in any way leads to predicting a critical trivial density and (2) $g_{I,A}(r)$, the radial distribution of pairs where one partner is active an the other inactive, cannot depend on a single power ρ^p of density, but must depend at least on two.

Outlook It should be noted that, despite the good (albeit hand-waving) arguments for random organization to be in the conserved directed percolation class, the lack of a unifying frame-work for far from equilibrium universal phenomena can make it ambiguous what constitutes a universality class. RG fixed point analysis would make this clear, but for it to apply one would have to first establish a rigorous link between any given model and the field theory. Furthermore, the error bars on critical exponents measured from simulation and experiment can be debatable and hence the sorting of models in one universality class or another on less solid foundations than meets the eye. This also applies to sorting random orgainzation into the Manna versus DP class. In section 3.2.2 I discussed the great similarities between DP and Manna models (absorbing state transition, similar field theories). I also discussed an important difference: proliferation of activity in random organization is limited by having to draw from the (overall conserved) pool of grains in the system, which constrains and hence correlates activations at any given time step (not the case in directed percolation problems). However, as stated at the end of section 3.2.2, *given* a packing structure, a DP problem may help to understand how activity propagates.

The remainder of the outlook concerns itself with the many-body reaction model (defined in section 4.3.3). I have not reached a final conclusion on how well the reaction system is suited to finding the random organization density analytically. The experimentation with the formalism towards the end of the thesis left interesting loose ends:

- It is an option to just insert empirically determined expressions for $g_{a,a'}(r)$. Of course, it is neither guaranteed to be easy nor is it desirable: a priori structure defeats the purpose of a predictive theory. However, to begin to asses the self-consistency of this description, it would be interesting to check this

- As is characteristic for purely non-equilibrium statistical physics problems, our lack of an explicit expression for the stationary probability distribution (given by the implicit condition $\langle P_\infty | Q = 0$ for steady states) means that, for a full characterization of the system under study, not only do we have to approximate our observables of interest from our probability distribution, a challenge that makes equilibrium statistical physics very rich in itself, but we additionally need to approximate P_∞. I do not mean to say, that I rule out such an expression with certainty, just that I do not expect one. From my view, it remains to be seen how accessible P_∞ is. Besides, a successful approximative scheme might very well not be in need of the full distribution anyway; there may be asymptotic expansions in λ^{-1} and μ^{-1}, for example.

- The link of random organization to athermal jamming is of physical interest to the latter. Note that one could introduce repulsions between active particles like in Milz and Schmiedeberg (2013) and Wilken et al. (2021), by just adding onto the rate operator Q a term generating drift between grain pairs, for example

  $$Q_v = \frac{v}{2}\int \mathrm{d}^d r_1\, \mathrm{d}^d r_2\, \Theta(\sigma - |\boldsymbol{r}_1 - \boldsymbol{r}_2|) A^\dagger(\boldsymbol{r}_1) A^\dagger(\boldsymbol{r}_2)\, (\hat{\boldsymbol{r}}_{21}\nabla_1 + \hat{\boldsymbol{r}}_{12}\nabla_2)\, A(\boldsymbol{r}_1) A(\boldsymbol{r}_2) \tag{5.1}$$

  where $\hat{\boldsymbol{r}}_{21} = (\boldsymbol{r}_2 - \boldsymbol{r}_1)/|\boldsymbol{r}_2 - \boldsymbol{r}_1|$, ∇_k is the gradient with respect to $\boldsymbol{r}_k$ and v is the drift velocity. This changes the time-evolution *and steady state* of the two-point density $\rho^{(2)}_{a,a'}(\boldsymbol{r}, \boldsymbol{r}')$, changing the predicted critical density Φ_c (moving it at least towards the athermal jamming Φ_J). Hence, if the random organization calculations bear fruit, approaching time-continuous biased random organization is on the table.

Despite the abstractness and even without the link to jamming, studying of models such as random organization is methodically interesting: the tools necessary to attack them and the ideas central to solving them can point the way for obtaining other results in the theoretical study of phenomena emergent from complexity.

A Longer Operator Formalism Computations

A.1 Commutator with Creation Operator

Lemma 1. *Commutators between strings of annihilation operators in the left argument and a creation operator in the right argument (which by taking adjoints can also be transferred to having an annihilation operator in the left and a string of creation operators in the right argument) evaluate to*

$$\left[a_1(\boldsymbol{r}_1)\cdots a_n(\boldsymbol{r}_n), {a'}^{\dagger}(\boldsymbol{r}')\right] = \sum_{k=1}^{n} \delta_{a_k,a'}\delta(\boldsymbol{r}_k - \boldsymbol{r}') \prod_{\substack{l=1\\ l\neq k}}^{n} a_l(\boldsymbol{r}_l) \tag{A.1}$$

i.e. the sum over all possibilities to replace, in the string of annihilation operators in the left-argument, exactly one annihilation operator $a_k(\boldsymbol{r}_k)$ by the product of the Kronecker-Delta $\delta_{a_k,a'}$ and the Dirac-Delta $\delta(\boldsymbol{r}_k - \boldsymbol{r}')$

Proof. Starting from the base case of the commutation relations eq. (4.47), which read

$$\left[a(\boldsymbol{r}), {a'}^{\dagger}(\boldsymbol{r}')\right] = \delta_{a,a'}\delta(\boldsymbol{r} - \boldsymbol{r}')$$

and is the trivial case of there only being one operator to replace by $\delta_{a,a'}\delta(\boldsymbol{r} - \boldsymbol{r}')$, we can see inductively by $[XY, Z] = X[Y, Z] + [X, Z]Y$ that

$$\begin{aligned}
&\left[a_1(\boldsymbol{r}_1)\cdots a_{n+1}(\boldsymbol{r}_{n+1}), {a'}^{\dagger}(\boldsymbol{r}')\right]\\
&\quad = \underbrace{\underbrace{\left[a_1(\boldsymbol{r}_1)\cdots a_n(\boldsymbol{r}_n), {a'}^{\dagger}(\boldsymbol{r}')\right]}_{\sum_{k=1}^{n} \delta_{a_k,a'}\delta(\boldsymbol{r}_k - \boldsymbol{r}')\prod_{\substack{l=1\\ l\neq k}}^{n} a_l(\boldsymbol{r}_l)} a_{n+1}(\boldsymbol{r}_{n+1})}_{\substack{\text{replacement of all factors except for}\\ a_{n+1}(\boldsymbol{r}_{n+1}) \text{ by } \delta_{a_k,a'}\delta(\boldsymbol{r}_k - \boldsymbol{r}')}} + \underbrace{a_1(\boldsymbol{r}_1)\cdots a_n(\boldsymbol{r}_n)\underbrace{\left[a_{n+1}(\boldsymbol{r}_{n+1}), {a'}^{\dagger}(\boldsymbol{r}')\right]}_{\delta_{a_{n+1},a'}\delta(\boldsymbol{r}_{n+1} - \boldsymbol{r}')}}_{\text{replacement of } a_{n+1}(\boldsymbol{r}_{n+1}) \text{ by } \delta_{a_{n+1},a'}\delta(\boldsymbol{r}_{n+1} - \boldsymbol{r}')}\\
&\quad = \sum_{k=1}^{n+1} \delta_{a_k,a'}\delta(\boldsymbol{r}_k - \boldsymbol{r}') \prod_{\substack{l=1\\ l\neq k}}^{n+1} a_l(\boldsymbol{r}_l)
\end{aligned} \tag{A.2}$$

□

A.2 Manipulating Kets with Operators

As can be read off (the adjoint version of) eq. (A.1), applying an annihilation operator $a(\boldsymbol{r})$ to a configuration ket $\left|a'_1, \dots, a'_{n'}, \boldsymbol{r}'_1, \dots, \boldsymbol{r}'_{n'}\right\rangle$ works out to

$$\begin{aligned}
&a(\boldsymbol{r})\left|a'_1, \dots, a'_{n'}, \boldsymbol{r}'_1, \dots, \boldsymbol{r}'_{n'}\right\rangle \\
&\quad= a(\boldsymbol{r}){a'_1}^{\dagger}(\boldsymbol{r}'_1) \cdots {a'_{n'}}^{\dagger}(\boldsymbol{r}'_{n'}) \left|0\right\rangle \\
&\quad= \underbrace{\left[a(\boldsymbol{r}), {a'_1}^{\dagger}(\boldsymbol{r}'_1) \cdots {a'_{n'}}^{\dagger}(\boldsymbol{r}'_{n'})\right]}_{\sum_{k=1}^{n} \delta_{a,a'_k} \delta(\boldsymbol{r}-\boldsymbol{r}'_k) \prod_{\substack{l=1^n \\ l\neq k}} {a'_l}^{\dagger}(\boldsymbol{r}'_l)} \left|0\right\rangle + {a'_1}^{\dagger}(\boldsymbol{r}_1) \cdots {a'_{n'}}^{\dagger}(\boldsymbol{r}_{n'}) \underbrace{a(\boldsymbol{r}) \left|0\right\rangle}_{=0} \\
&\quad= \sum_{k\in\{1,\dots,n'\}} \delta_{a,a'_k} \delta(\boldsymbol{r} - \boldsymbol{r}'_k) \left|\{(a'_l, \boldsymbol{r}'_l)\}_{l\in\{1,\dots,n\}\setminus\{k\}}\right\rangle
\end{aligned} \tag{A.3}$$

(used, for example, used in eq. 25 from Doi 1976a). In this sense, applying the annihilation operator $a(\boldsymbol{r})$ to a configuration ket reduces the number of grains by one if there was a grain exactly at $\boldsymbol{r}$ (vanishing the ket otherwise). Applying two annihilation operators accordingly results in

$$\begin{aligned}
&a_1(\boldsymbol{r}_1)a_2(\boldsymbol{r}_2)\left|a'_1, \dots, a'_{n'}, \boldsymbol{r}'_1, \dots, \boldsymbol{r}'_{n'}\right\rangle \\
&\quad= a_2(\boldsymbol{r}_2) \sum_{k_1\in\{1,\dots,n'\}} \delta_{a_1,a'_{k_1}} \delta(\boldsymbol{r}_1 - \boldsymbol{r}'_{k_1}) \left|\{(a'_l, \boldsymbol{r}'_l)\}_{l\in\{1,\dots,n'\}\setminus\{k_1\}}\right\rangle \\
&\quad= \sum_{k_1\in\{1,\dots,n'\}} \sum_{k_2\in\{1,\dots,n'\}\setminus\{k_1\}} \delta_{a_1,a'_{k_1}} \delta(\boldsymbol{r}_1 - \boldsymbol{r}'_{k_1}) \cdot \delta_{a_2,a'_{k_2}} \delta(\boldsymbol{r}_2 - \boldsymbol{r}'_{k_2}) \\
&\qquad\qquad \times \left|\{(a'_l, \boldsymbol{r}'_l)\}_{l\in\{1,\dots,n'\}\setminus\{k_1,k_2\}}\right\rangle \\
&\quad= \sum_{\substack{(k_1,k_2)\in \\ C_2(\{1,\dots,n'\})}} \prod_{m=1}^{2} \delta_{a_m,a'_{k_m}} \delta(\boldsymbol{r}_m - \boldsymbol{r}'_{k_m}) \cdot \left|\{(a'_l, \boldsymbol{r}'_l)\}_{l\in\{1,\dots,n'\}\setminus\{k_1,k_2\}}\right\rangle
\end{aligned} \tag{A.4}$$

where with $C_n(M)$ I mean the set of all possible ordered choices[1] of n distinct elements from the set M (with $C_n(\{1, \dots, n\}) \simeq S_n$ the set of permutations, and $C_n(M) = \emptyset$ if $|M| < n$ since then there are not even n options in M to choose from); we interpret ordered choices from $C_n(M)$ conveniently as tuples $(k_1, \dots, k_n)$ when summing over them. This inductively generalizes to:

Lemma 2. *Applying n annihilation operators to a configuration ket with n' particles results in*

$$\begin{aligned}
&a_1(\boldsymbol{r}_1) \cdots a_n(\boldsymbol{r}_n)\left|a'_1, \dots, a'_{n'}, \boldsymbol{r}'_1, \dots, \boldsymbol{r}'_{n'}\right\rangle \\
&\quad= \sum_{\substack{(k_1,\dots,k_n)\in \\ C_n(\{1,\dots,n'\})}} \left(\prod_{m=1}^{n} \delta_{a_m,a'_{k_m}} \delta(\boldsymbol{r}_m - \boldsymbol{r}'_{k_m})\right) \left|\{(a'_l, \boldsymbol{r}'_l)\}_{l\in\{1,\dots,n'\}\setminus\{k_1,\dots,k_n\}}\right\rangle
\end{aligned} \tag{A.5}$$

with special case when $n = n'$, where selection of

$$a_1(\boldsymbol{r}_1) \cdots a_n(\boldsymbol{r}_n)\left|a'_1, \dots, a'_n, \boldsymbol{r}'_1, \dots, \boldsymbol{r}'_n\right\rangle = \sum_{\pi\in S_n} \prod_{k=1}^{n} \delta_{a_k,a'_{\pi(k)}} \delta(\boldsymbol{r}_k - \boldsymbol{r}'_{\pi(k)}) \left|0\right\rangle \tag{A.6}$$

---

[1] which is most elegantly understood as all injective maps $\{1, \dots, n\} \to M$

Corollary 1. *The inner product of two configuration kets evaluates to*

$$\left\langle a_1,\dots,a_n,\boldsymbol{r}_1,\dots,\boldsymbol{r}_n \middle| a'_1,\dots,a'_{n'},\boldsymbol{r}'_1,\dots,\boldsymbol{r}'_{n'} \right\rangle = \delta_{n,n'} \sum_{\pi\in S_n} \prod_{k=1}^{n} \delta_{a_k,a'_{\pi(k)}} \delta(\boldsymbol{r}_k - \boldsymbol{r}'_{\pi(k)}) \tag{A.7}$$

(see Doi (1976a, eq. 16) for a similar identity in the simpler case of a single particle species)

Corollary 2. *Applying the operator* $a_1^\dagger(\boldsymbol{r}_1)\cdots a_n^\dagger(\boldsymbol{r}_n)a_1(\boldsymbol{r}_1)\cdots a_n(\boldsymbol{r}_n)$ *to any configuration ket* $\left|a'_1,\dots,a'_N,\boldsymbol{r}'_1,\dots,\boldsymbol{r}'_N\right\rangle$ *results in*[2]

$$\begin{aligned} & a_1^\dagger(\boldsymbol{r}_1)\cdots a_n^\dagger(\boldsymbol{r}_n)a_1(\boldsymbol{r}_1)\cdots a_n(\boldsymbol{r}_n)\left|a'_1,\dots,a'_N,\boldsymbol{r}'_1,\dots,\boldsymbol{r}'_N\right\rangle \\ &= a_1^\dagger(\boldsymbol{r}_1)\cdots a_n^\dagger(\boldsymbol{r}_n) \sum_{\substack{(k_1,\dots,k_n)\in\\ C_n(\{1,\dots,N\})}} \prod_{m=1}^{n} \delta_{a_m,a'_{k_m}} \delta(\boldsymbol{r}_m - \boldsymbol{r}'_{k_m}) \left|\{(a'_l,\boldsymbol{r}'_l)\}_{l\in\{1,\dots,n'\}\setminus\{k_1,\dots,k_n\}}\right\rangle \\ &= \sum_{\substack{(k_1,\dots,k_n)\in\\ C_n(\{1,\dots,N\})}} \prod_{m=1}^{n} \delta_{a_m,a'_{k_m}} \delta(\boldsymbol{r}_m - \boldsymbol{r}'_{k_m}) \left|a'_1,\dots,a'_N,\boldsymbol{r}'_1,\dots,\boldsymbol{r}'_N\right\rangle \end{aligned} \tag{A.8}$$

which turns out to be precisely the multiplication by the random variable of the n-point density

$$\rho^{(n)}_{a_1,\dots,a_n}(\boldsymbol{r}_1,\dots,\boldsymbol{r}_n) = \left\langle \sum_{\substack{(k_1,\dots,k_n)\in\\ C_n(\{1,\dots,N\})}} \prod_{m=1}^{n} \delta_{a_m,a'_{k_m}} \delta(\boldsymbol{r}_m - \boldsymbol{r}'_{k_m}) \right\rangle \tag{A.9}$$

as defined for N-particle configurations.

Corollary 3. *Using the notation* $|\omega\rangle$ *for* $\omega\in\Omega$*, where* Ω *is the outcome space, introduced by eq.* (4.54) *and the measure* $\mathrm{d}\omega$ *introduced by eq.* (4.53)*, we have the resolution identity*

$$\mathbb{1} = \int \mathrm{d}\omega\, |\omega\rangle\langle\omega| \tag{A.10}$$

Proof. For any $\omega' = \left|a'_1,\dots,a'_{N'},\boldsymbol{x}'_1,\dots,\boldsymbol{x}'_{N'}\right\rangle$ we get

$$\begin{aligned} \int \mathrm{d}\omega\, |\omega\rangle\langle\omega|\omega'\rangle &= \sum_{N=0}^{\infty} \int \frac{\mathrm{d}^d x_1\cdots\mathrm{d}^d x_N}{N!} \sum_{a_1\cdots a_N} \left|a_1,\dots,a_N,\boldsymbol{x}_1,\dots,\boldsymbol{x}_N\right\rangle \\ &\qquad \times \underbrace{\left\langle a_1,\dots,a_N,\boldsymbol{x}_1,\dots,\boldsymbol{x}_N \middle| a'_1,\dots,a'_{N'},\boldsymbol{x}'_1,\dots,\boldsymbol{x}'_{N'}\right\rangle}_{\delta_{N,N'}\sum_{\pi\in S_{N'}}\prod_{k=1}^{N'}\delta_{a_k,a'_{\pi(k)}}\delta(\boldsymbol{x}_k-\boldsymbol{x}'_{\pi(k)})} \\ &= \frac{1}{N'!}\sum_{\pi\in S_{N'}} \underbrace{\left|a'_{\pi(1)},\dots,a'_{\pi(N')},\boldsymbol{x}'_{\pi(1)},\dots,\boldsymbol{x}'_{\pi(N')}\right\rangle}_{\substack{=\left|a'_1,\dots,a'_{N'},\boldsymbol{x}'_1,\dots,\boldsymbol{x}'_{N'}\right\rangle \text{ (i.e.: ket unchanged} \\ \text{under permutation of particle identities)}}} \\ &= \frac{|S_{N'}|}{N'!}\cdot\left|a'_1,\dots,a'_{N'},\boldsymbol{x}'_1,\dots,\boldsymbol{x}'_{N'}\right\rangle \\ &= \left|a'_1,\dots,a'_{N'},\boldsymbol{x}'_1,\dots,\boldsymbol{x}'_{N'}\right\rangle \end{aligned} \tag{A.11}$$

---

[2] When $C_n(\{1,\dots,N\}) = \emptyset$ due to $n > N$, the convention of empty sums vanishing $\sum_{k\in\emptyset}(\cdots) = 0$ applies.

where we used $|S_N| = N!$; Since we decompose any bra/ket as integrals of these configuration bras/kets, $\int \mathrm{d}\omega\, |\omega\rangle\langle\omega|$ indeed acts like identity on all of them. □

Corollary 4. *With appendix 1, one can immediately see that*

$$\begin{aligned}\langle P|a_1,\dots,a_N,\boldsymbol{r}_1,\dots,\boldsymbol{r}_N\rangle &= \sum_{N'=0}^{\infty}\int \frac{\mathrm{d}^d r'_1\cdots \mathrm{d}^d r'_{N'}}{N'!}\sum_{a'_1\cdots a'_{N'}} P^{(N')}(a'_1,\dots,a'_{N'},\boldsymbol{r}'_1,\dots,\boldsymbol{r}'_{N'})\\ &\qquad\times\underbrace{\left\langle a'_1,\dots,a'_{N'},\boldsymbol{r}'_1,\dots,\boldsymbol{r}'_{N'}\middle|a_1,\dots,a_N,\boldsymbol{r}_1,\dots,\boldsymbol{r}_N\right\rangle}_{\delta_{N,N'}\sum_{\pi\in S_n}\prod_{k=1}^{N}\delta_{a_k,a'_{\pi(k)}}\delta(\boldsymbol{r}_k-\boldsymbol{r}'_{\pi(k)})}\\ &= P^{(N)}_{a_1,\dots,a_N}(\boldsymbol{r}_1,\dots,\boldsymbol{r}_N)\end{aligned} \tag{A.12}$$

where we used that

$$P^{(N)}_{a_{\pi(1)},\dots,a_{\pi(N)}}(\boldsymbol{r}_{\pi(1)},\dots,\boldsymbol{r}_{\pi(N)}) = P^{(N)}_{a_1,\dots,a_N}(\boldsymbol{r}_1,\dots,\boldsymbol{r}_N)$$

for any permutation $\pi \in S_N$ of the particle identities.

A.3 Properties of $|\text{sum}\rangle$

Averages in the Doi formalism are computed by sandwiching operators X corresponding to random variables $\mathcal{X}$ in between the probability distribution $\langle P|$ and a special vector $|\text{sum}\rangle$ given by

$$|\text{sum}\rangle = \exp\left(\int \mathrm{d}^d r \sum_a a^\dagger(\boldsymbol{r})\right)|0\rangle \tag{A.13}$$

This definition is very similar to coherent states in quantum physics and corresponds to a vector containing only ones in finite-dimensional Markov chains (see section 4.3.2). We now want to show that

Proposition 1. *$|sum\rangle$ absorbs any creation operator applied to it*

$$a(\boldsymbol{r})\,|\text{sum}\rangle = |\text{sum}\rangle \tag{A.14}$$

Proof. We can show it without loss of generality for only one creation operator type, say active grains $A(\boldsymbol{r})$. We first define

$$S^\dagger := \int \mathrm{d}^d r \sum_a a^\dagger(\boldsymbol{r}) \tag{A.15}$$

and note that

$$\begin{aligned}\left[A(\boldsymbol{r}),S^\dagger\right] &= \int \mathrm{d}^d r\,\Big(\underbrace{\left[A(\boldsymbol{r}),A^\dagger(\boldsymbol{r}')\right]}_{=\delta(\boldsymbol{r}-\boldsymbol{r}')}+\underbrace{\left[A(\boldsymbol{r}),I^\dagger(\boldsymbol{r}')\right]}_{=0}\Big)\\ &= \int \mathrm{d}^d r\,\delta(\boldsymbol{r}-\boldsymbol{r}')\\ &= 1\end{aligned} \tag{A.16}$$

such that one can see $\left[A(\boldsymbol{r}), (S^\dagger)^n\right] = n(S^\dagger)^{n-1}$ inductively

$$\begin{aligned}\left[A(\boldsymbol{r}), (S^\dagger)^n\right] &= S^\dagger \underbrace{\left[A(\boldsymbol{r}), (S^\dagger)^{n-1}\right]}_{\substack{=(n-1)(S^\dagger)^{n-2} \text{ by} \\ \text{ind. assumption}}} + \underbrace{\left[A(\boldsymbol{r}), S^\dagger\right]}_{=1}(S^\dagger)^{n-1} \\ &= n(S^\dagger)^{n-1}\end{aligned} \tag{A.17}$$

We expand

$$\begin{aligned}A(\boldsymbol{r})\,|\text{sum}\rangle &= A(\boldsymbol{r}) \exp\left(S^\dagger\right)|0\rangle \\ &= \sum_{n=0}^{\infty} \frac{1}{n!} A(\boldsymbol{r})(S^\dagger)^n\,|0\rangle \\ &= \sum_{n=0}^{\infty} \frac{1}{n!}\left(\left[A(\boldsymbol{r}), (S^\dagger)^n\right] + (S^\dagger)^n A(\boldsymbol{r})\right)|0\rangle \\ &= \sum_{n=1}^{\infty} \underbrace{\frac{1}{n!} \cdot n}_{=\frac{1}{(n-1)!}}(S^\dagger)^{n-1}\,|0\rangle \\ &= \sum_{n=0}^{\infty} \frac{1}{n!}(S^\dagger)^n\,|0\rangle \\ &= |\text{sum}\rangle\end{aligned} \tag{A.18}$$

□

B Reaction System Simulation

The simulations were written in `Python 3.13.3` with `numpy 2.3.4`. All analysis additionally used `scipy 1.16.3` for curve fitting and `matplotlib 3.10.7` for plotting. The purpose of writing these simulations was to observe the system in action and gather ideas. They were used to challenge and ultimately support or discourage a few speculations I had.

Simulation The small scale simulations of the dynamics specified section 4.3.3 that I mentioned throughout section 4.3.5 was, implemented as follows: N grains, which each have the attributes position $\boldsymbol{x}_k \in [0, L]^d$ and activation state $a_k \in \{A, I\}$, are initially set to `active` and their positions randomly, independently and uniformly distributed throughout the box $[0, L]^d$.

The grain diameter σ is computed from the packing fraction Φ via $\Phi = NB_d\sigma^d/L^d$, where B_d is the volume of the d-dimensional unit ball. Activation rate λ, inactivation rate μ and diffusion constant D can also be set.

With periodic boundary conditions in place, I then repeatedly perform the following update, terminating either when a certain maximum number of iterations is surpassed or an absorbing state is reached:

1. Determine all reactions that could possibly happen next. This always includes $A \to I$ for every grain; on top of that, any overlapping pair i and j is registered as a potential next reaction $a_i + a_j \to 2A$

2. For every reaction R registered in step 1, a duration τ_R is drawn from an exponential distribution $\sim e^{-\alpha_R t}$ where r is the reaction rate ($\alpha_R = \lambda$ when R is $a_j + a_k \to 2A$ and $\alpha_R = \mu$ when R is $A \to I$)

3. Only the reaction R with the shortest duration τ_R is realized

4. In the duration τ_R all active grains would have diffused. To account for this, every active grain is shifted by a random step drawn from an isotropic multidimensional normal distribution with variance $2D\tau_R$

5. Repeat from step 1 unless any of the stopping criteria (maximum number of iterations is surpassed or an absorbing state is reached) is fulfilled.

For later analysis the activation states and positions of all grains in the systems are regularly dumped to a file in the `.xyz` format (see `https://en.wikipedia.org/wiki/XYZ_file_format`, last visited 20.11.2025).

Measurements While it is clear how to determine the active grain plotted in fig. 4.6, $g_{a,a'}(r)$ warrants explaining. They were obtained with the following steps

1. Determine from an $f_a(t)$ a 'burn-in time' T after which the system is in the steady state
2. Sample n configurations from the steady state. For all pairs where one grain has activation state a and the other activation sate a', sort all distances from all samples into a histogram $H_{a,a'}(k)$ with bin width $\mathrm{d}r$ and bin centres $\{r_k\}$
3. Average the histogram $h_{a,a'}(k) = H_{a,a'}(k)/n$
4. Divide the averaged histogram $h_{a,a'}(k)$ by $\rho^2 S_d r_k^{d-1}\,\mathrm{d}r$, where S_d stands for the (hyper-)surface area of a d-dimensional unit shell and $\rho = N/L^d$ to obtain the estimate for $g_{a,a'}(r_k)$

Bibliography

Adzhemyan, Loran Ts. et al. (2023). “Field-theoretic analysis of directed percolation: Three-loop approximation”. en. In: *Physical Review E* 107.6, p. 064138. ISSN: 2470-0045, 2470-0053. DOI: `10.1103/PhysRevE.107.064138`.

Baddeley, Adrian J. (2007). “Spatial Point Processes and their Applications”. In: School of Mathematics and Statistics, University of Western Australia.

Bardeen, J., L. N. Cooper, and J. R. Schrieffer (1957). “Theory of Superconductivity”. In: *Phys. Rev.* 108 (5), pp. 1175–1204. DOI: `10.1103/PhysRev.108.1175`.

Bernal, J. D. and J. Mason (Dec. 1960). “Packing of Spheres: Co-ordination of Randomly Packed Spheres”. en. In: *Nature* 188.4754, 910–911. ISSN: 0028-0836, 1476-4687. DOI: `10.1038/188910a0`.

Broadbent, Simon and J. M. Hammersley (1957). “Percolation processes”. In: *Mathematical Proceedings of the Cambridge Philosophical Society* 53, pp. 629 –641.

Brown, Harvey R., Wayne Myrvold, and Jos Uffink (2009). “Boltzmann’s H-theorem, its discontents, and the birth of statistical mechanics”. In: *Studies in History and Philosophy of Science Part B: Studies in History and Philosophy of Modern Physics* 40.2, pp. 174–191. ISSN: 1355-2198. DOI: `https://doi.org/10.1016/j.shpsb.2009.03.003`.

Cardy, J L and R L Sugar (1980). “Directed percolation and Reggeon field theory”. In: *Journal of Physics A: Mathematical and General* 13.12, p. L423. DOI: `10.1088/0305-4470/13/12/002`.

Chatterjee, Sayani, Arghya Das, and Punyabrata Pradhan (June 2018). “Hydrodynamics, density fluctuations, and universality in conserved stochastic sandpiles”. en. In: *Physical Review E* 97.6, p. 062142. ISSN: 2470-0045, 2470-0053. DOI: `10.1103/PhysRevE.97.062142`.

Cheung, Anson (Jan. 2023). *Phase Transitions and Collective Phenomena*. Lecture Notes. University of Cambridge.

Corté, Laurent et al. (May 2008). “Random organization in periodically driven systems”. en. In: *Nature Physics* 4.5, 420–424. DOI: `10.1038/nphys891`.

Coupette, Fabian (2023). “Percolation: Connecting the Dots”. en. In: DOI: `10.6094/UNIFR/236560`.

Dantas, Wellington Gomes et al. (Sept. 2006). “Generalized Manna sandpile model with height restrictions”. In: *Brazilian Journal of Physics* 36.3a, pp. 750–754. DOI: `10.1590/s0103-97332006000500031`.

Doi, Masao (1976a). “Second quantization representation for classical many-particle system”. In: *Journal of Physics A: Mathematical and General* 9.9, p. 1465. DOI: `10.1088/0305-4470/9/9/008`.

Doi, Masao (1976b). “Stochastic theory of diffusion-controlled reaction”. In: *Journal of Physics A: Mathematical and General* 9.9, 1479–1495. ISSN: 0305-4470, 1361-6447. DOI: `10.1088/0305-4470/9/9/009`.

Doussal, Pierre Le and Kay Jörg Wiese (Mar. 2015). “An exact mapping of the stochastic field theory for Manna sandpiles to interfaces in random media”. In: *Physical Review Letters* 114.11, p. 110601. ISSN: 0031-9007, 1079-7114. DOI: `10.1103/PhysRevLett.114.110601`.

Ehrenfest, Paul and Tatyana Ehrenfest (1911). “Begriffliche Grundlagen der statistischen Auffasung in der Mechanik”. In: *Encyklopädie der mathematischen Wissenschaften* Band IV, 2. Teil, 3–90.

Garcia-Palacios, J. L. (2007). *Introduction to the theory of stochastic processes and Brownian motion problems*. arXiv: `cond-mat/0701242 [cond-mat.stat-mech]`.

Grassberger, P. (Dec. 1982). “On phase transitions in Schlögl’s second model”. en. In: *Zeitschrift für Physik B Condensed Matter* 47.4, 365–374. ISSN: 0722-3277, 1434-6036. DOI: `10.1007/BF01313803`.

Grassberger, P. and K. Sundermeyer (1978). “Reggeon field theory and markov processes”. en. In: *Physics Letters B* 77.2, 220–222. ISSN: 03702693. DOI: `10.1016/0370-2693(78)90626-3`.

Hinrichsen, Haye (Nov. 2000). “Non-equilibrium critical phenomena and phase transitions into absorbing states”. In: *Advances in Physics* 49.7, 815–958. ISSN: 1460-6976. DOI: `10.1080/00018730050198152`.

Hohenberg, P. and W. Kohn (Nov. 1964). “Inhomogeneous Electron Gas”. en. In: *Physical Review* 136.3B, B864–B871. ISSN: 0031-899X. DOI: `10.1103/PhysRev.136.B864`.

Jaeger, Gregg (May 1998). “The Ehrenfest Classification of Phase Transitions: Introduction and Evolution”. In: *Archive for History of Exact Sciences* 53.1, 51–81. ISSN: 0003-9519, 1432-0657. DOI: `10.1007/s004070050021`.

Janssen, H. K. (1981). “On the nonequilibrium phase transition in reaction-diffusion systems with an absorbing stationary state”. en. In: *Zeitschrift für Physik B Condensed Matter* 42.2, 151–154. ISSN: 0340-224X, 1434-6036. DOI: `10.1007/BF01319549`.

Janssen, H. K., Ue Kutbay, and K. Oerding (Mar. 1999). “Equation of state for directed percolation”. In: *Journal of Physics A: Mathematical and General* 32.10, 1809–1817. ISSN: 0305-4470, 1361-6447. DOI: `10.1088/0305-4470/32/10/003`.

Janssen, Hans-Karl (Dec. 1976). “On a Lagrangean for classical field dynamics and renormalization group calculations of dynamical critical properties”. en. In: *Zeitschrift für Physik B Condensed Matter and Quanta* 23.4, 377–380. ISSN: 0340-224X, 1434-6036. DOI: `10.1007/BF01316547`.

Janssen, Hans-Karl and Olaf Stenull (2016). “Directed percolation with a conserved field and the depinning transition”. In: *Phys. Rev. E* 94 (4), p. 042138. DOI: `10.1103/PhysRevE.94.042138`.

Janssen, Hans-Karl and Uwe C. Täuber (Jan. 2005). “The field theory approach to percolation processes”. In: *Annals of Physics* 315.1, 147–192. ISSN: 0003-4916. DOI: `10.1016/j.aop.2004.09.011`.

Jensen, Iwan (1999). “Low-density series expansions for directed percolation: I. A new efficient algorithm with applications to the square lattice”. In: *Journal of Physics A: Mathematical and General* 32.28, 5233–5249. ISSN: 0305-4470, 1361-6447. DOI: `10.1088/0305-4470/32/28/304`.

Kadanoff, Leo P. (June 1966). "Scaling laws for ising models near T c". en. In: *Physics Physique Fizika* 2.6, 263–272. ISSN: 0554-128X. DOI: `10.1103/PhysicsPhysiqueFizika.2.263`.

Kohn, W. and L. J. Sham (Nov. 1965). "Self-Consistent Equations Including Exchange and Correlation Effects". en. In: *Physical Review* 140.4A, A1133–A1138. ISSN: 0031-899X. DOI: `10.1103/PhysRev.140.A1133`.

Lorenz, Edward N. (1995). *The Essence of Chaos*. eng. London: UCL Press. ISBN: 9786610054848.

Lubeck, S. (Dec. 2004). "Universal scaling behavior of non-equilibrium phase transitions". In: *International Journal of Modern Physics B* 18.31n32, 3977–4118. ISSN: 0217-9792, 1793-6578. DOI: `10.1142/S0217979204027748`.

Manna, S.S. (1991). "Critical exponents of the sand pile models in two dimensions". In: *Physica A: Statistical Mechanics and its Applications* 179.2, pp. 249–268. ISSN: 0378-4371. DOI: `https://doi.org/10.1016/0378-4371(91)90063-I`.

Martin, P. C., E. D. Siggia, and H. A. Rose (1973). "Statistical Dynamics of Classical Systems". en. In: *Physical Review A* 8.1, 423–437. ISSN: 0556-2791. DOI: `10.1103/PhysRevA.8.423`.

Mermin, N. David (Mar. 1965). "Thermal Properties of the Inhomogeneous Electron Gas". en. In: *Physical Review* 137.5A, A1441–A1443. ISSN: 0031-899X. DOI: `10.1103/PhysRev.137.A1441`.

Milz, Lars and Michael Schmiedeberg (Dec. 2013). "Connecting the random organization transition and jamming within a unifying model system". en. In: *Physical Review E* 88.6, p. 062308. ISSN: 1539-3755, 1550-2376. DOI: `10.1103/PhysRevE.88.062308`.

Obukhov, S.P. (Apr. 1980). "The problem of directed percolation". en. In: *Physica A: Statistical Mechanics and its Applications* 101.1, 145–155. ISSN: 03784371. DOI: `10.1016/0378-4371(80)90105-3`.

Onsager, Lars (1944). "Crystal Statistics. I. A Two-Dimensional Model with an Order-Disorder Transition". In: *Phys. Rev.* 65 (3-4), pp. 117–149. DOI: `10.1103/PhysRev.65.117`.

O'Hern, Corey S. et al. (2003). "Jamming at zero temperature and zero applied stress: The epitome of disorder". en. In: *Physical Review E* 68.1, p. 011306. ISSN: 1063-651X, 1095-3787. DOI: `10.1103/PhysRevE.68.011306`.

Pastor-Satorras, Romualdo and Alessandro Vespignani (Nov. 2000). "Field theory of absorbing phase transitions with a nondiffusive conserved field". In: *Physical Review E* 62.5, R5875–R5878. ISSN: 1095-3787. DOI: `10.1103/physreve.62.r5875`.

Pine, D. J. et al. (Dec. 2005). "Chaos and threshold for irreversibility in sheared suspensions". en. In: *Nature* 438.7070, 997–1000. ISSN: 0028-0836, 1476-4687. DOI: `10.1038/nature04380`.

Reichl, Linda E. (2016). *A modern course in statistical physics*. eng. Fourth revised and updated edition. Weinheim, Germany: Wiley-Vch, Verlag GmbH und Co. KGaA. ISBN: 978-3-527-41349-2. DOI: `10.1002/9783527690497`.

Rossi, Michela, Romualdo Pastor-Satorras, and Alessandro Vespignani (Aug. 2000). "Universality Class of Absorbing Phase Transitions with a Conserved Field". en. In: *Physical Review Letters* 85.9, 1803–1806. ISSN: 0031-9007, 1079-7114. DOI: `10.1103/PhysRevLett.85.1803`.

Roth, Roland (Nov. 2006). *Introduction to Density Functional Theory of Classical Systems: Theoy and Applications*. English. Lecture Notes.

Taylor, G. I. (Jan. 1923). en. In: *Philosophical Transactions of the Royal Society of London. Series A, Containing Papers of a Mathematical or Physical Character* 223.605–615, 289–343. ISSN: 0264-3952, 2053-9258. DOI: `10.1098/rsta.1923.0008`.

The Royal Swedish Academy of Sciences (June 2003). *The Nobel Prize in Physics 2003: Advanced Information*. `https://www.nobelprize.org/uploads/2013/06/advanced-physicsprize2003.pdf`. Accessed: 26.10.2025.

Tong, David (2017). *Statistical Field Theory*. Lecture Notes. University of Cambridge.

Wiese, Kay Jörg (Apr. 2016). "Coherent-state path integral versus coarse-grained effective stochastic equation of motion: From reaction diffusion to stochastic sandpiles". In: *Physical Review E* 93.4. ISSN: 2470-0053. DOI: `10.1103/physreve.93.042117`.

— (Jan. 2020). *Master Class: Advanced Statistical Field Theory*. Accessed: 18.06.2025.

— (2024). "Hyperuniformity in the Manna Model, Conserved Directed Percolation and Depinning". In: *Phys. Rev. Lett.* 133 (6), p. 067103. DOI: `10.1103/PhysRevLett.133.067103`.

Wijland, F. van (Oct. 2002). "Universality class of nonequilibrium phase transitions with infinitely many-absorbing-states". In: *Physical Review Letters* 89.19, p. 190602. ISSN: 0031-9007, 1079-7114. DOI: `10.1103/PhysRevLett.89.190602`.

Wijland, F. van, K. Oerding, and H.J. Hilhorst (Mar. 1998). "Wilson renormalization of a reaction–diffusion process". In: *Physica A: Statistical Mechanics and its Applications* 251.1–2, 179–201. ISSN: 0378-4371. DOI: `10.1016/s0378-4371(97)00603-1`.

Wilken, Sam et al. (July 2021). "Random Close Packing as a Dynamical Phase Transition". en. In: *Physical Review Letters* 127.3, p. 038002. DOI: `10.1103/PhysRevLett.127.038002`.

Wilken, Sam et al. (2023). "Dynamical Approach to the Jamming Problem". In: *Phys. Rev. Lett.* 131 (23), p. 238202. DOI: `10.1103/PhysRevLett.131.238202`.

Wilson, K (Aug. 1974). "The renormalization group and the epsilon expansion". In: *Physics Reports* 12.2, 75–199. ISSN: 03701573. DOI: `10.1016/0370-1573(74)90023-4`.

Wilson, Kenneth G. (Nov. 1971a). "Renormalization Group and Critical Phenomena. I. Renormalization Group and the Kadanoff Scaling Picture". en. In: *Physical Review B* 4.9, 3174–3183. ISSN: 0556-2805. DOI: `10.1103/PhysRevB.4.3174`.

— (Nov. 1971b). "Renormalization Group and Critical Phenomena. II. Phase-Space Cell Analysis of Critical Behavior". en. In: *Physical Review B* 4.9, 3184–3205. ISSN: 0556-2805. DOI: `10.1103/PhysRevB.4.3184`.

Ódor, Géza (Aug. 2004). "Universality classes in nonequilibrium lattice systems". In: *Reviews of Modern Physics* 76.3, 663–724. ISSN: 1539-0756. DOI: `10.1103/revmodphys.76.663`.

Declaration of Authorship

I hereby declare that the presented thesis is the result of my own independent work. All sources used, whether directly or indirectly, have been properly acknowledged in the given Bibliography. This thesis has not been submitted to any other examination board and has not been published before.

Erlangen, 26.11.2025

Mishael Derla